Chemical and Biochemical Studies of
Ubiquitin Conjugation Machinery

by

Renuka K. Pandya

B.A. Biology
Cornell University, 2004

SUBMITTED TO THE DEPARTMENT OF BIOLOGY
IN PARTIAL FULFILLMENT OF THE REQUIREMENTS FOR THE DEGREE OF

DOCTORATE OF PHILOSOPHY IN BIOLOGY

AT THE

MASSACHUSETTS INSTITUTE OF TECHNOLOGY

JUNE 2010

Signature of Author…………………………………………………………………………
Renuka K. Pandya
Department of Biology
May 24, 2010

Certified by…………………………………………………………………………………
Hidde L. Ploegh
Member, Whitehead Institute
Professor of Biology
Thesis Supervisor

Accepted by……………………………………………………………………...............
Tania A. Baker
Professor of Biology
Co-Chair, Biology Graduate Committee

Chemical and Biochemical Studies of Ubiquitin Conjugation Machinery

by

Renuka K. Pandya

Submitted to the Department of Biology
on May 24, 2010 in Partial Fulfillment of the Requirements for the Degree of Doctorate of
Philosophy in Biology at the Massachusetts Institute of Technology

Abstract

The post-translational modification of proteins is a major mechanism employed in eukaryotic cells to expand the functional diversity of the proteome. Covalent modification of amino acid side chains confers new or altered functionality to the modified protein by creating new recognition surfaces on the protein for the interaction of nucleic acids or other proteins, modulating enzymatic activity, or altering cellular localization or half-life. The post-translational modification of proteins with ubiquitin (Ub) is an important mechanism of regulating protein function. Ub is a 76-residue protein that is primarily attached to lysine residues in target proteins through an enzymatic cascade catalyzed by E1, E2, and E3 enzymes. Ub conjugation is important for fundamental cellular processes, including transcription, DNA repair, endocytosis, apoptosis, and signal transduction. Ub conjugation is reversible. Proteases termed deubiquitinating enzymes (DUBs) function to remove Ub from target proteins.

Genome sequencing efforts have uncovered the existence of many predicted enzymes with unknown function. Many enzymes have been assigned function based on sequence homology to proteins with known function without confirmation of enzymatic activity. A powerful chemical approach to determine enzyme function from a complex mixture of proteins is activity-based protein profiling. This method makes use of chemical probes that are active site-directed for the assignment of function to proteins. We describe here the design and generation of an expanded set of Ub-based chemical probes with which we identified and recovered E1, E2, and E3 Ub ligases from cell lysates. Furthermore, we describe the biochemical and structural characterization of the catalytic domain of one E3 Ub ligase we recovered, HUWE1, and the identification of a structural element within the catalytic domain of HUWE1 that modulates its activity. Finally, we discuss a protein engineering method that we are applying to the HUWE1 catalytic domain to understand how the conformational flexibility of this domain is important to its function.

Thesis Supervisor: Hidde L. Ploegh
Title: Member, Whitehead Institute; Professor of Biology

TABLE OF CONTENTS

Acknowledgements

Many people have shaped my time as a graduate student at MIT. I thank my advisor, Hidde Ploegh, for encouraging me to reach far, think big, and put my best foot forward. He entrusted me to pursue my interests with enthusiasm tempered by skepticism from the day I spoke with him. My committee members, Mike Yaffe and Tania Baker, have also been instrumental in fostering my learning throughout the years, and I appreciate their valuable input during both committee meetings and informal conversations. I thank Thomas Schwartz and Wade Harper for serving on my thesis defense committee.

A special thanks to Thomas Schwartz and James Partridge, with whom I was fortunate to collaborate. I learned a great deal from just a short walk across the street to the Schwartz lab.

The Ploegh lab is full of bright individuals who have contributed to my thesis through numerous conversations, by sharing advice, by looking at data, or through friendship. Thanks to Kerry Love, with whom I worked for two years, for both scientific conversations and laughter, and to Robert Miller, for his good cheer, and for making many things possible on short notice. Thanks also to Shahram Misaghi, Greg Korbel, Ferenc Reinhardt, Eric Spooner, Tom DiCesare, Christian Schlieker, Jadyn Damon, Nick Yoder, Max Popp, John Antos, and Clarissa Lee.

I'm lucky to have some wonderful graduate school friends, Jane Kim and Wendy Lam. Thank you for your friendship, support, camaraderie, and commiseration.

I thank my family: my big brother Naveen Sastry, whom I'll always look up to, and my parents, K.V. and Sesha Sastry. Their love and support is constant and tangible.

Finally, I thank my husband, Ankur Pandya. I can't imagine where I'd be without you and the joy you bring me every day. Thank you for believing in me.

For my parents

CHAPTER 1: INTRODUCTION

Introduction

Post-translational modification of proteins is one of two major mechanisms employed by eukaryotic cells to expand the functional diversity of the proteome. This mechanism, along with RNA splicing, increases the number of protein variants in the cell by one to two orders of magnitude over those encoded in the genome (Walsh, Garneau-Tsodikova et al. 2005; Walsh 2006). Covalent modification of amino acid side chains increases their heterogeneity and imparts new or altered functionality to the modified protein by creating new recognition surfaces on the protein for the interaction of nucleic acids or other proteins, modulating enzymatic activity, or altering cellular localization or half-life. Post-translational modifications are utilized in all three major evolutionary lineages of life; however, the range of modifications and frequency of occurrence in eukaryotes far exceeds that in prokaryotes and archaea. Here, we discuss the covalent modification of proteins with ubiquitin (Ub), an 8-kDa protein that is highly conserved in eukaryotes. Ub is attached to protein targets through a sequential cascade of enzymatic reactions catalyzed by E1 activating, E2 conjugating, and E3 ligase enzymes. The human genome encodes over 300 enzymes dedicated to Ub conjugation, and approximately 100 Ub proteases, termed deubiquitinating enzymes, which function to remove Ub from modified proteins (Nijman, Luna-Vargas et al. 2005; Li, Bengtson et al. 2008) (Figure 1). Ub conjugation is necessary for fundamental cellular processes, including cell cycle progression, transcriptional regulation, DNA repair, apoptosis, protein trafficking, endocytosis, and signal transduction, and thus represents an important form of post-translational modification in the cell (Pickart 2001; Kerscher, Felberbaum et al. 2006; Bernassola, Karin et al. 2008).

Figure 1.
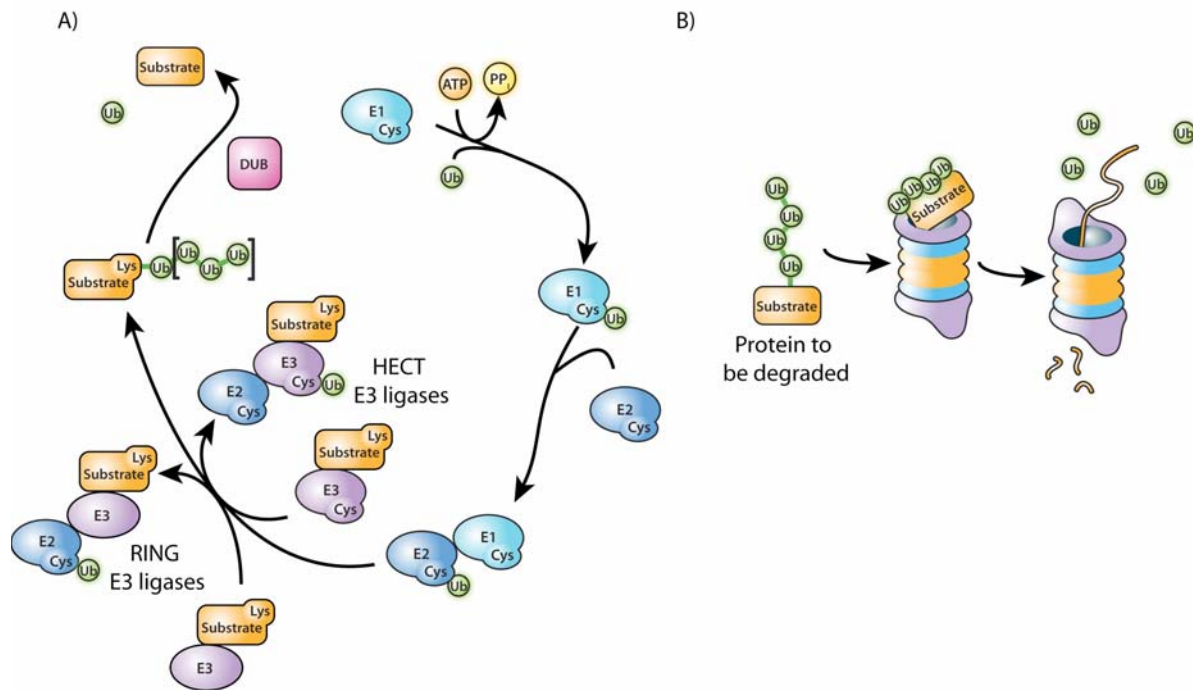
Figure 1 The ubiquitin-proteasome pathway.

(**A**) Ubiquitin is a 76-amino acid protein that is activated and conjugated to target proteins by an enzymatic cascade of reactions catalyzed by E1, E2, and E3 enzymes. E1 activates Ub by adenylating Ub's C-terminal glycine in an ATP-dependent step and subsequently transfers Ub to its active site-cysteine. The E1~Ub thioester complex associates with E2, transferring Ub to the E2 catalytic cysteine in a transthiolation reaction. E3s facilitate the final step of Ub conjugation through one of two mechanisms. The RING (and related U-box) E3s bring the E2~Ub thioester complex in proximity to substrate, whereas the HECT E3s form an E3~Ub intermediate on a catalytic cysteine. Ub is generally attached in an isopeptide linkage via its C-terminus and the ε-amino group of a lysine residue in the target, which may be a substrate protein or Ub itself. Deubiquitinating enzymes (DUBs) reverse Ub conjugation, generating free Ub monomers and substrate.
(**B**) Substrates conjugated with a polyubiquitin chain containing at least four ubiquitin molecules linked through Lys48 are targeted to the 26S proteasome for degradation. Figure adapted from (Hochstrasser 2009).

Ubiquitin is the founding member of a family of small protein modifiers. Members of

this family share two structural features: a globular domain containing a characteristic three-

dimensional structure, termed the β-grasp fold, and a flexible C-terminal tail ending in a glycine

residue (Dye and Schulman 2007). The C-terminal glycine of Ub is typically attached to the ε-amino group of a lysine in isopeptide linkage to target proteins; less frequently, Ub can be conjugated to the amino terminus of target proteins, including Ub itself (Kuo, den Besten et al. 2004; Kirisako, Kamei et al. 2006; Tokunaga, Sakata et al. 2009), Cys (Cadwell and Coscoy 2005; Ravid and Hochstrasser 2007), or Ser/Thr residues (Tait, de Vries et al. 2007; Wang, Herr et al. 2009). An additional level of complexity arises in ubiquitin conjugation because ubiquitin itself contains seven lysine residues, which function as acceptor sites for building polyubiquitin chains. Proteins can therefore be modified at a single lysine with one ubiquitin molecule (monoubiquitination), at several lysine residues with ubiquitin monomers (multi-monoubiquitination), or through chains of lysine-linked polyubiquitin (polyubiquitination). The modification of proteins with a single ubiquitin molecule, for example, can serve as a signal for endocytosis and functions in DNA repair (Hicke 2001; Matsushita, Kitao et al. 2005).

Polyubiquitin chains with specific linkages possess different three-dimensional conformations and distinct topologies. Structural studies of Lys63-linked, Lys48-linked, and linear chains indicate that they adopt different conformations that are differentially read out by ubiquitin binding domains in partner proteins to confer specific functional consequences (Cook, Jeffrey et al. 1994; Eddins, Carlile et al. 2006; Ryabov and Fushman 2006; Dikic, Wakatsuki et al. 2009; Komander, Reyes-Turcu et al. 2009). For example, polyubiquitin chains consisting of four or more Lys48-linked ubiquitin residues bind to the 26S proteasome receptor subunit S5a, thus targeting the ubiquitinated protein for proteasomal degradation (Thrower, Hoffman et al. 2000). In contrast, Lys63-linked polyubiquitin chains function to activate certain proteins for DNA repair, signal transduction, and endocytosis (Pickart and Fushman 2004; Chen and Sun 2009), although there is some evidence that Lys63-linked polyubiquitin chains also function to

target proteins for proteasomal degradation (Saeki, Kudo et al. 2009). Emerging roles for K11-linked chains in ERAD (Xu, Duong et al. 2009) and cell cycle progression (Jin, Williamson et al. 2008), and evidence for the existence of polyubiquitin chains containing all seven different linkages in cells (Peng, Schwartz et al. 2003; Xu, Duong et al. 2009) speak to the complexity of polyubiquitination signals and the diversity of functional outcomes it generates.

Ubiquitin-like modifiers

A growing family of proteins termed ubiquitin-like modifiers (Ubls) shares structural similarity with ubiquitin (Table 1). Nine Ubls, including ISG15, Nedd8, and SUMO, have demonstrated capability of covalently modifying protein targets, and more are likely to possess this ability (Hochstrasser 2009). Conjugation of most ubiquitin-like modifiers follows a similar mechanistic framework to ubiquitin and requires catalysis by dedicated E1, E2, and E3 enzymes. Like ubiquitin, these modifiers serve to alter protein function and function in a wide array of cellular processes. The first Ubl identified was ISG15, a type I interferon-induced gene, encoding a 15-kDa protein composed of two ubiquitin-like domains (Narasimhan, Wang et al. 2005). ISG15 is activated by its E1 enzyme Uba7 and conjugated via its specific E2 UBE2L6 and one of several E3s (Kim, Giannakopoulos et al. 2004; Zhao, Beaudenon et al. 2004; Nakasato, Ikeda et al. 2006; Wong, Pung et al. 2006; Zou and Zhang 2006; Durfee, Kelley et al. 2008). Nedd8 is activated by its own E1, the heterodimeric NAE1-UBA3 complex, and transferred to target proteins by one of two Nedd8 E2s and at least one E3, Dcn1 (Liakopoulos, Doenges et al. 1998; Osaka, Kawasaki et al. 1998; Gong and Yeh 1999; Kurz, Ozlu et al. 2005; Huang, Ayrault et al. 2009). Nedd8 is primarily conjugated to the cullin RING E3 ligases, the largest subfamily of E3s, and potently stimulates their activity (Duda, Borg et al. 2008; Saha and

Deshaies 2008). Cullin RING E3s function in cell cycle progression, signal tranduction, DNA replication, and viral modulation (Petroski and Deshaies 2005). Three human SUMO modifiers (SUMO1, SUMO2, and SUMO3) are activated by a dedicated SUMO E1 (the heterodimeric Aos1-UBA2 complex) and transferred to targets by one SUMO-specific E2 and one of several E3 enzymes. SUMO modifies proteins involved in DNA replication and repair and serves as a binding site for proteins containing SUMO-interacting motifs (SIMs) (Johnson 2004; Kerscher 2007).

Table 1.

Table 1. Known UBLs and their activating and conjugating enzymes

UBL*	Identity with ubiquitin (%)	Function
Ubiquitin	100	Protein turnover, localization, binding to other proteins
Rub1p (NEDD8)	55	Activation of cullin-based E3s
ISG15	32 and 37[†]	Type 1 interferon response; antiviral function
FAT10	32 and 40[†]	Type 1 interferon pathway; antiviral function
Smt3 (SUMO1, SUMO2, SUMO3)	18	Protein localization and activity; signal for target ubiquitination
Atg8	ND	Autophagosome formation
Atg12	ND	Autophagosome formation
Urm1	ND	Response to oxidative stress
UFM1	ND	Unknown

ND, not detectable by standard BLAST searches. *UBLs are listed as the yeast (*Saccharomyces cerevisiae*) symbol if the UBL is present in yeast, otherwise vertebrate symbols are listed. Known vertebrate orthologues with symbols that differ from yeast proteins are listed in parentheses. †The identities listed are for each of the two ubiquitin-related domains.
Figure adapted from Hochstrasser, M. Nature 458 (7237): 422-29 and Schulman, BA. Nat Rev Mol Cell Biol. 10(5):319-31.

Ubl conjugation pathways appear to originate from multiple rounds of duplication and divergence of enzymes and protein modifiers originating from prokaryotic biosynthetic pathways (Hochstrasser 2009). Ubiquitin E1 enzyme shares sequence similarity with the bacterial proteins molybdopterin biosynthetic enzyme B (MoeB) and thiamine biosynthesis protein F (ThiF), proteins that are involved in the molybdopterin and thiamin cofactor biosynthesis, respectively. The synthesis of these cofactors requires incorporation of a sulphur atom into their precursor proteins. This sulphur atom is donated from the sulphur-containing proteins molybdopterin-

converting factor subunit 1 (MoaD) and thiamine biosynthesis protein S (ThiS), small proteins

that possess the β-grasp fold and C-terminal diglycine motif characteristic of ubiquitin and

ubiquitin-like modifiers (Rudolph, Wuebbens et al. 2001; Wang, Xi et al. 2001). In a manner

reminiscent of the eukaryotic E1 activating enzyme, MoeB and ThiF catalyze the adenylation of

MoaD and ThiS's C-terminal glycine residue, respectively, activating it for subsequent

conversion of the acyl-adenylate intermediate into a thiocarboxylate that serves as the source of

sulphur for downstream reactions (Huang, Walden et al. 2004; Duda, Walden et al. 2005).

Prokaryotic homologues of MoeB and ThiF enzymes suggest that E1-like enzymes may function

in other biosynthetic or post-translational modification systems.

In spite of the presence of proteasomes in prokaryotes and archaea, Ub and Ubls were

unknown in these evolutionary lineages until recently. A prokaryotic ubiquitin-like protein

(Pup) was identified in *Mycobacterium tuberculosis* that is conjugated to substrates as a signal

for proteasome-mediated degradation (Pearce, Mintseris et al. 2008). Pup is a 64-amino acid

protein that does not share sequence or structural homology with ubiquitin – it is mainly

unstructured with the exception of an α-helix near its C terminus. Notably, the C terminus of

Pup terminates in the residues Gly-Gly-Gln. In the mycobacterial pupylation pathway, the C-

terminal glutamine residue is deamidated by deamidase of Pup (Dop) to generate a glutamic

acid, which is conjugated via its side chain carboxylate group to the ε-amino group of substrate

lysine residues (Sutter, Damberger et al.). The mechanism of Pup conjugation is currently

unknown. The only protein known to be required for pupylation is proteasome accessory protein

A (PafA), a protein with no homology to known E1, E2, or E3 enzymes (Pearce, Mintseris et al.

2008).

The identification of the small ubiquitin-like proteins SAMP1 and SAMP2 shows that the

third evolutionary lineage of life, archaea, also utilize a ubiquitin-like conjugation system (Humbard, Miranda et al.). SAMP1 and SAMP2 were identified in a search for proteins containing a β-grasp fold and C-terminal di-glycine motif in the deduced genome of the archaeon *Haloferax volcanii.* Of the five proteins with these characteristics, only SAMP1 and SAMP2 were found to be capable of protein conjugation. SAMP1 and SAMP2 are attached via their C-terminal glycine to the ε-lysine group of at least nine substrates (Humbard, Miranda et al.). Interestingly, identification of SAMPylated proteins by tandem mass spectrometry revealed that several of the modified proteins share homology with enzymes in Ubl-conjugation and/or sulphur activation pathways. Two of the SAMPylated proteins, HVO_0558 and HVO_0559, are homologues of Uba4, the E1 activating enzyme for the ubiquitin-like modifier Urm1 (Humbard, Miranda et al.). HVO_0558 resembles Uba4's N-terminal domain, and HVO_0559 resembles Uba4's C-terminal domain. It is unknown whether these proteins activate SAMPs for conjugation, and whether there exist SAMP E2 or E3 enzymes.

Ubiquitin Activation and Conjugation Enzymes and Ligases

Ubiquitin is conjugated to target proteins through a sequential series of reactions catalyzed by E1 activating enzyme, E2 conjugating enzyme, and E3 ligase (Pickart 2001). E1 enzyme binds Ub and Mg^{2+}-ATP and catalyzes the adenylation of Ub's C-terminal gycine residue. Activated Ub undergoes nucleophilic attack by the E1 catalytic cysteine, forming an E1~Ub thioester (the tilde [~] is used here to refer to a covalent linkage). Ub is then transferred to the E2 catalytic cysteine in a thioesterification reaction. E3 ligases facilitate the final step of Ub conjugation by associating with both the E2~Ub thioester complex and substrate and promoting the transfer of Ub from the E2 to a substrate lysine residue. The mechanism of this

final step of ubiquitin transfer depends on the type of E3 ligase catalyzing the reaction. The majority of E3s belong to the RING (*R*eally *I*nteresting *N*ew *G*ene) class, which function as adaptor proteins to bring the Ub-loaded E2 enzyme in proximity to substrate. In contrast, the HECT (*h*omologous to *E*6AP *C-t*erminus) domain-containing E3s form a Ub~thioester intermediate on a catalytic cysteine prior to transferring Ub to substrate. A third class of E3s are neither RING nor HECT-type. We will focus discussion on the RING and HECT E3s.

Ubiquitin/Ubiquitin-like activating enzyme (E1)

Crystal structures of ThiF-ATP, ThiF-ThiS, and several MoeB-MoaD complexes reveal that the first step of Ub/Ubl activation is highly conserved (Lake, Wuebbens et al. 2001; Duda, Walden et al. 2005; Lehmann, Begley et al. 2006). MoeB and ThiF are homodimers with two symmetric catalytic centers. MoeB and ThiF enzymes contain a four-stranded β-sheet that binds a hydrophobic patch on MoaD or ThiS, respectively, that corresponds to the Ile44-centered hydrophobic patch on ubiquitin. The C-terminus of ThiS or MoaD extends toward bound Mg^{2+}-ATP. A catalytic Arg residue that functions in ATP binding is provided by the opposite MoeB or ThiS monomer and a conserved Asp residue coordinates Mg^{2+}. For the purpose of this discussion, we will focus on canonical E1 enzymes, defined as the E1 enzymes for ubiquitin (Ube1 and Uba6), SUMO (Aos1-UBA2), NEDD8 (APPBP1-UBA3), and ISG15 (Uba7), because of their shared structural and mechanistic features (Dye and Schulman 2007). These canonical eukaryotic E1 enzymes are similar to MoeB and ThiF in that they contain a homodimeric or heterodimeric adenylation domain that recognizes the correct Ub/Ubl and catalyzes the adenylation of its C-terminal glycine. Of these two domains, only one binds Mg^{2+}-ATP and Ubl; the second adenylation domain provides structural stability. Canonical E1

enzymes possess, in addition, two domains that function in Ub/Ubl transfer: a ubiquitin fusion domain (UFD) that associates with E2 enzyme, and a catalytic cysteine domain, containing the active site cysteine residue that forms a thioester linkage with the Ub/Ubl C-terminus. One unique feature among the canonical Ub/Ubl activation pathways is that the number of Ub/Ubl E1s differ. For example, the ubiquitin pathway contains two E1 enzymes, Ube1 and UBA6. The discovery of Uba6, expressed in vertebrates and sea urchins, challenged a long-held assumption that Ube1 is the only E1 for the Ub pathway (Chiu, Sun et al. 2007; Jin, Li et al. 2007; Pelzer, Kassner et al. 2007). Uba6 can activate Ub and the Ubl, FAT10, and the two E1s show selectivity for the E2s that they charge with Ub. In contrast, in the SUMO pathway, a single SUMO E1 enzyme activates SUMO-1, SUMO-2, and SUMO-3 (Desterro, Rodriguez et al. 1999; Gong, Li et al. 1999). An important question is to understand how E1 enzymes selectively interact with the correct Ubl, and how the E1~Ub/Ubl complex mediates E2 selectivity.

The mechanism of catalysis by E1 enzyme involves two half-reactions: an adenylation reaction that harnesses the energy of ATP hydrolysis to generate a high-energy Ub/Ubl~AMP intermediate, and a thioesterification reaction (Figure 2). E1 activates Ub/Ubl by catalyzing the adenylation of Ub/Ubl's C-terminus, forming an acyl phosphate bond. The Ub/Ubl~AMP intermediate undergoes nucleophilic attack by E1's catalytic cysteine, preserving the energy in the activated Ub/Ubl C-terminus to form an E1~Ub/Ubl thioester intermediate. The E1 enzyme then binds a second set of Ub/Ubl and ATP molecules and catalyzes the adenylation of the second Ub/Ubl's C-terminus. The ternary E1 complex, composed of one non-covalently bound Ub/Ubl~AMP (referred to as Ub/Ubl[A]) and one covalently bound Ub/Ubl~thioester intermediate (referred to as Ub/Ubl[T]), then recruits an E2 conjugating enzyme, permitting Ub/Ubl transfer to the E2 catalytic cysteine. One reason for the requirement of doubly-loaded

E1 enzyme for Ub/Ubl transfer may be that coupling of the second adenylation reaction with

Ub/Ubl transfer to the E2 promotes the latter reaction energetically or conformationally

(Schulman and Harper 2009).

Figure 2.

$$E1_{SH} + ATP + Ubl \xrightleftharpoons{Mg^{2+}} E1_{SH}^{\cdot AMP \sim Ubl} + PP_i \quad (1)$$

$$E1_{SH}^{\cdot AMP \sim Ubl} \rightleftharpoons E1_{S \sim Ubl} + AMP \quad (2)$$

$$E1_{S \sim Ubl} + ATP + Ubl \xrightleftharpoons{Mg^{2+}} E1_{S \sim Ubl}^{\cdot AMP \sim Ubl} + PP_i \quad (3)$$

$$E1_{S \sim Ubl}^{\cdot AMP \sim Ubl} + E2_{SH} \rightleftharpoons E1_{SH}^{\cdot AMP \sim Ubl} + E2_{S \sim Ubl} \quad (4)$$
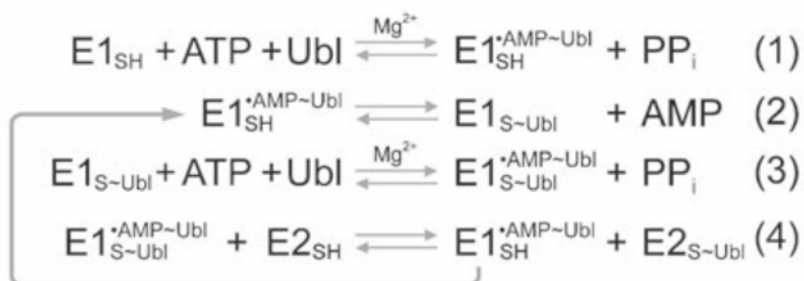
Figure 2 E1 activating enzyme mechanism.
(**1**) The E1 enzyme binds ATP, Mg^{2+}, and Ub/Ubl, and adenylates the Ub/Ubl C-terminal glycine.
(**2**) The E1 catalytic cysteine attacks the Ub~AMP, forming an E1~Ub thioester complex and releasing AMP.
(**3**) The E1 catalyzes the adenylation of a second Ub/Ubl, resulting in an E1 doubly loaded with Ub/Ubl: one noncovalently bound at its adenylation site, and the other covalently bound at its active site cysteine.
(**4**) The doubly Ub/Ubl-loaded E1 associates with E2 and transfers its thioester-bound Ub/Ubl to the E2 catalytic cysteine. Figure from (Dye and Schulman 2007).

The structures of several E1 enzymes, either alone or in complex with Ub/Ubl, ATP,

and/or E2 enzyme, have provided insight into the mechanisms of Ub/Ubl activation and the E1-

E2 Ub/Ubl transfer reaction (Figure 3a, b). Olsen *et al*. generated two SUMO C-terminal

electrophilic inhibitors and used these inhibitors to trap the SUMO E1 as if bound to its reaction

intermediates. Olsen synthesized SUMO with one of two non-hydrolysable synthetic analogs of

AMP (AMSN and AVSN) attached to SUMO's C-terminus. SUMO~AMSN mimics the natural

SUMO~AMP, the intermediate formed after the adenylation half-reaction. SUMO~AVSN

contains, in addition to the adenylate moiety, an electrophilic center, and thus covalently binds

the E1 active site cysteine to form a stable E1~SUMO~AVSN complex. This complex mimics the enzyme after catalyzing the thioesterification of SUMO's C-terminus but before the adenylate group has left. The E1~SUMO~AVSN and E1-SUMO~AMSN structures display remarkably different conformations. Prior to catalyzing the adenylation half-reaction, SUMO E1 adopts an "open" conformation, allowing it to bind ATP and SUMO. Formation of the SUMO~AMP intermediate triggers a substantial structural rearrangement of the E1 enzyme: in the E1~SUMO~AVSN structure, the catalytic cysteine domain undergoes a relative 130º rotation to a "closed" formation, placing the catalytic cysteine in what was formerly the adenylation domain. Further structural remodeling in the closed complex allow the catalytic cysteine to gain access to the SUMO~AMP intermediate (Olsen, Capili et al.) (Figure 3a).

Insight into the thioesterification half-reaction has also accumulated from structural studies. The adenylation domain of E1s for ubiquitin, SUMO, and NEDD8 are structurally similar to those of MoeB and ThiF. Structures of the E1 enzymes for Ub, SUMO, and NEDD8 with Ub/Ubl non-covalently bound to the adenylation site revealed that the catalytic cysteine residue is separated by ~35 Å from the Ub/Ubl C-terminus, suggesting that E1 in complex with Ub/Ubl~AMP intermediate adopts an alternate conformation to promote the thioesterification reaction (Walden, Podgorski et al. 2003; Lois and Lima 2005; Lee and Schindelin 2008). Additionally, docking the structure of a complex between NEDD8 E1's UFD and E2 enzyme onto a structure of a complex with APPBP1-UBA3 bound to NEDD8-AMP shows that the E1 and E2 catalytic cysteines face in opposite directions (Huang, Hunt et al. 2007). A model for the thioesterification reaction came from the structure of a trapped NEDD8 activation complex, in which APPBP1-UBA3 is bound to two NEDD8 molecules, one non-covalently at its adenylation site (NEDD8[A]), the second in thioester linkage to the catalytic cysteine (NEDD8[T]), and a

catalytic cysteine-to-alanine mutant of E2 Ubc12 (Huang, Hunt et al. 2007) (Figure 3b, right). In this structure, the E2-binding UFD is rotated 120° relative to unloaded and singly Ubl(A) loaded E1 structures, unmasking a cryptic Ubc12-binding site on the UBA3 adenylation domain and placing the Ubc12 catalytic cysteine within 20 Å of the UBA3's catalytic cysteine. Thus, the authors describe a model for E1-E2 transthiolation: the doubly-NEDD8-loaded E1 undergoes conformational rearrangements that switch it into a state facilitating E2 recruitment and Ub transfer. Following the transfer of Ubl(T) to the E2, the E1 enzyme is switched back to a state allowing release of the E2 (Huang, Hunt et al. 2007).
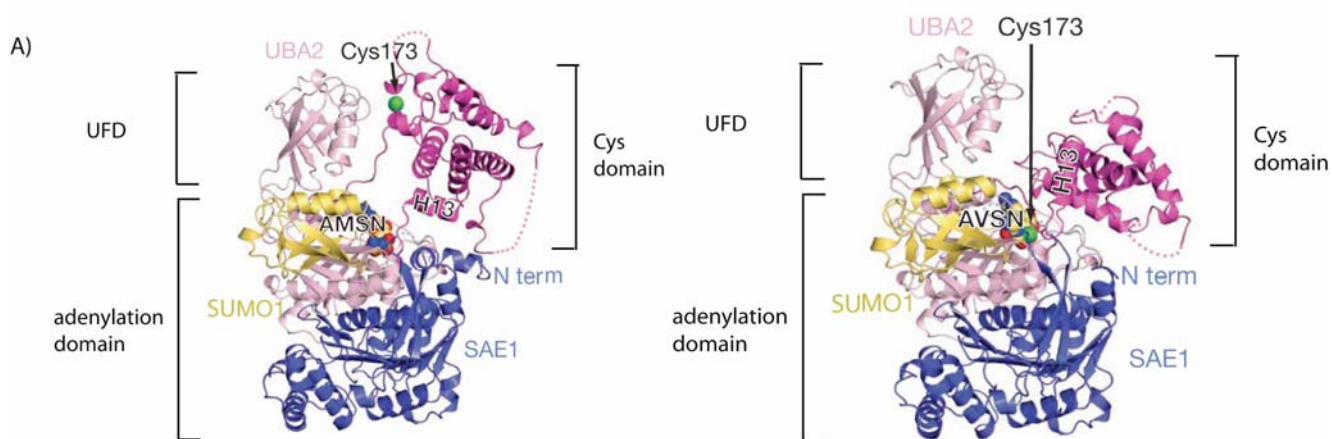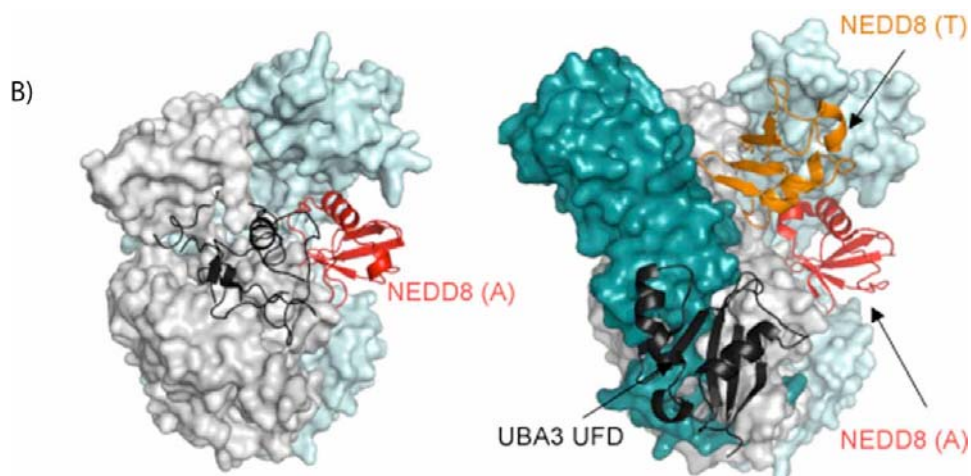
Figure 3.

Figure 3 Structures of Ubl E1 activation enzymes reveal insight into the Ubl adenylation and thioesterification reactions.

(**A**) Insight into the SUMO1 adenylation reaction catalyzed by the SUMO E1 is provided by the crystal structures of SUMO E1-SUMO1~AMSN adenylate analogue (**left**; PDB entry 3KYC) and the SUMO E1~SUMO~AVSN tetrahedral intermediate analogue (**right**; PDB entry 3KYD). Atoms from the catalytic cysteine, AMSN, and AVSN, are shown as spheres, and E1 domains and SUMO are labeled. The adenylate analogue structure (**left**) is in the "open" conformation, and numerous structural changes convert the structure to the "closed" conformation observed for the tetrahedral intermediate analogue (**right**), including a 130° rotation of the Cys domain and the melting of several elements that were structured in the open conformation. Figure from Olsen, Capili et al.
(**B**) Insight into the thioesterification reaction from the crystal structures of singly loaded E1 complex (APPBP1-UBA3-NEDD8-ATP, PDB entry IR4N, **left**) and a trapped activation complex, in which APPBP1-UBA3 is bound to two NEDD8 molecules – NEDD8(A) (yellow) and NEDD8 covalently bound to the active site cysteine (NEDD8(T); orange); Ubc12, and ATP-Mg^{2+} (PDB entry 2NVU, **right**). Rotation of the E1 UFD is revealed from the structure of the trapped activation complex.   The surfaces of APPBP1 and UBA3 are colored in light blue and gray, respectively, and the E2 Ubc12 is colored in turquoise on the right. The UBA3 UFD domain is showed in ribbon representation colored black. Figure adapted from (Riedinger 2009).

Ubiquitin/ubiquitin-like conjugating enzyme (E2)

E2 conjugating enzymes function centrally in the Ub conjugation cascade: they interact with the E1~Ub intermediate upstream and E3 ligases downstream (Figure 4).

Figure 4.

$$E2_{S\sim Ubl} + HECT\ E3_{SH} \rightleftharpoons E2_{SH} + HECT\ E3_{S\sim Ubl} \qquad (1)$$

$$HECT\ E3_{S\sim Ubl} + Target_{NH2} \longrightarrow HECT\ E3_{SH} + Target_{NH\sim Ubl} \qquad (2)$$

$$E2_{S\sim Ubl} + Target_{NH2} \xrightarrow{RING,\ NHNR\ E3} E2_{SH} + Target_{NH\sim Ubl} \qquad (3)$$
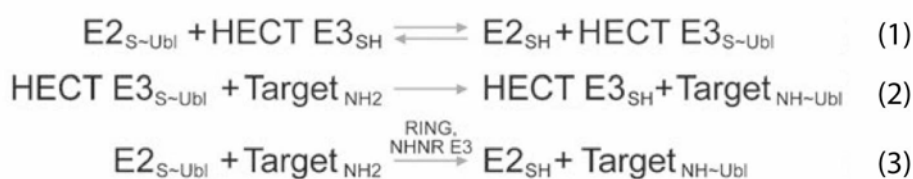
Figure 4 E2 conjugating enzyme mechanism.

(**1**) E2 enzyme charged with Ub (E2~Ub) interacts with a HECT E3 to transfer Ub from the E2 catalytic cysteine to the HECT E3 catalytic cysteine.
(**2**) HECT E3s contain a catalytic cysteine residue that forms an E3~Ub thioester intermediate prior to transferring Ub to a lysine residue in the target protein.
(**3**) E2~Ub can also interact with RING and other E3s to promote Ub conjugation. The RING and other E3s function as adaptor proteins to bring E2~Ub complex in proximity to substrate. Figure adapted from (Dye and Schulman 2007).

The SUMO and ISG15 pathways utilize a single E2 enzyme each (Ubc9 and UbcH8, respectively); the NEDD8 pathway employs two E2 enzymes (UBE2M and UBE2F); and, in contrast, over 30 E2s function in the ubiquitin pathway (Pickart and Eddins 2004). Ub- and Ubl-E2 conjugating enzymes possess a ~150-residue core, globular UBC domain, composed of four α-helices, a four-stranded β-sheet, and a short 3_{10} helix that contains the catalytic cysteine (Ye and Rape 2009). A small number of ubiquitin E2 variant (UEV) proteins contain the UBC domain but lack the active site-Cys residue, and associate with activate E2 enzymes (Hofmann and Pickart 1999; Deng, Wang et al. 2000; Moraes, Edwards et al. 2001; VanDemark, Hofmann

et al. 2001). The UBC domain is sufficient for catalysis, although some E2s contain additional

N- or C-terminal extensions in addition to the core UBC domain which may contribute to

specificity of E1 binding (Huang, Miller et al. 2004). These extensions may also regulate

intrinsic E2 activity or E3 recruitment (Pickart and Fushman 2004).

Structural and biochemical studies of E1-E2 and E2-E3 complexes show that the E1 and

E3 enzymes bind to overlapping sites on the E2 (Huang, Kinnucan et al. 1999; Zheng, Wang et

al. 2000; Huang, Paydar et al. 2005; Reverter and Lima 2005; Zhang, Windheim et al. 2005). E2

enzymes therefore cannot be re-loaded with Ub while bound to the E3, and instead cycle

between E1 and E3 to transfer multiple ubiquitin molecules or to build a polyubiquitin chain.   A

crystal structure of a complex between the UFD of NEDD8's E1, NAE1-UBA3, and the E2

Ubc12 core domain showed that the N-terminal α-helix (H1) and the loop between the first and

second β strands ($\beta 1\beta 2$ loop) of Ubc12 bind to a W-shaped surface created by four of the five β

strands and the $\alpha 13$ helix of the UFD domain (Huang, Paydar et al. 2005). Mutation of the H1

helix impairs E2~Ub thioester formation (Sullivan and Vierstra 1991; Pitluk, McDonough et al.

1995), and a bioinformatics study has shown a high degree of conservation in the N-terminal H1

for E2s of a particular Ubl (Sullivan and Vierstra 1991; Pitluk, McDonough et al. 1995; Winn,

Religa et al. 2004). Competitive binding experiments with three different human E2-E3 pairs

showed that E1 and E3 bind mutually exclusively to E2s (Eletr, Huang et al. 2005).

The labile nature of the E2~Ub thioester makes the structural study of this complex

challenging. Thus, NMR has been instrumental in providing insight into the interaction between

E2 and Ub. The C-terminus of ubiquitin (residues 71 through 76) stretches through a shallow

groove reaching the E2 active site cysteine (Miura, Klaus et al. 1999; Hamilton, Ellison et al.

2001; Brzovic, Lissounov et al. 2006). This ubiquitin-interaction region is independent of the known E1 and E3-binding surfaces (Pickart and Eddins 2004; Dye and Schulman 2007).

After the E2 interacts with E1~Ub and is charged with Ub, the E2~Ub thioester complex associates with an E3 enzyme to catalyze substrate ubiquitination. Crystal structures of E2/E3 pairs, in particular the complexes between the E2 UBE2L3 and the HECT domain of E6AP, UBE2L3 in complex with a 46-kDa portion of the RING E3 c-Cbl, and the U-box domain E3 CHIP/Ubc13-Uev1a complex, and the NMR complex of the RING E3 CNOT4 bound to UbcH5B, show that E2 binds both classes of E3s in a remarkably similar manner (Huang, Kinnucan et al. 1999; Zheng, Wang et al. 2000; Dominguez, Bonvin et al. 2004; Zhang, Windheim et al. 2005). The tips of the L1 and L2 loops and the H1 helix of the E2 contribute to binding E3 (Figure 5a). Sequence variation in these regions among different E2 enzymes contributes to E2-E3 specificity (Ye and Rape 2009). E2s may also interact with additional regions in the E3 outside of its RING or HECT domain: for example, Cdc34 uses its acidic tail to bind its E3, SCF (Kolman, Toth et al. 1992; Silver, Gwozd et al. 1992), and UBE2G2 is recruited to the E3 gp78 by binding to the G2BR peptide, outside of its RING domain (Chen, Mariano et al. 2006; Das, Mariano et al. 2009; Li, Tu et al. 2009).

The interaction between E2 and E3 enzymes is relatively weak, typically ranging from ~1 μM to the 100 μM range (Ye and Rape 2009). The Ub transfer cascade is driven forward by the selective interaction of different forms of the E2 enzyme with E1 and E3 enzymes. E1s bind preferentially to unloaded E2s, and release E2~Ub thioester; E3s bind preferentially to E2~Ub thioester, and release free E2 (Dye and Schulman 2007; Deshaies and Joazeiro 2009; Ye and Rape 2009). The vast majority of E2s in cells are charged at steady state, and the interaction of

charged E2s with E3 enzymes is thought to be rate-limiting for target ubiquitination (Jin, Li et al. 2007; Schulman and Harper 2009)

In addition to interaction with E1, E3, and Ub, certain E2 enzymes interact with substrate and play a prominent role in catalyzing substrate ubiquitination. Insights into substrate-E2 interaction have been provided from studies of complexes between the SUMO E2, Ubc9, and its substrate RanGAP1 (Sampson, Wang et al. 2001; Johnson 2004; Yunus and Lima 2006). In a structure of Ubc9 in complex with RanGAP1, substantial hydrophobic contacts between E2 and substrate contribute to binding (Bernier-Villamor, Sampson et al. 2002). In addition, residues of Ubc9 directly contact the SUMO consensus target sequence ΦKxD/E, where Φ is any hydrophobic residue and K is the lysine residue to be modified. In the ubiquitination pathway, the E2/UEV complex Ubc13/Mms2 assembles Lys63-linked polyubiquitin chains. In this example, Ub is the substrate. A structure of Ubc13/Mms2 covalently bound to one Ub molecule at the Ubc13 active site shows that noncovalent interactions between Mms2 and Ub from an adjacent complex position the acceptor Ub's Lys63 in the active site near the Ubc13~Ub linkage (VanDemark, Hofmann et al. 2001; McKenna, Moraes et al. 2003; Eddins, Carlile et al. 2006).

Figure 5.
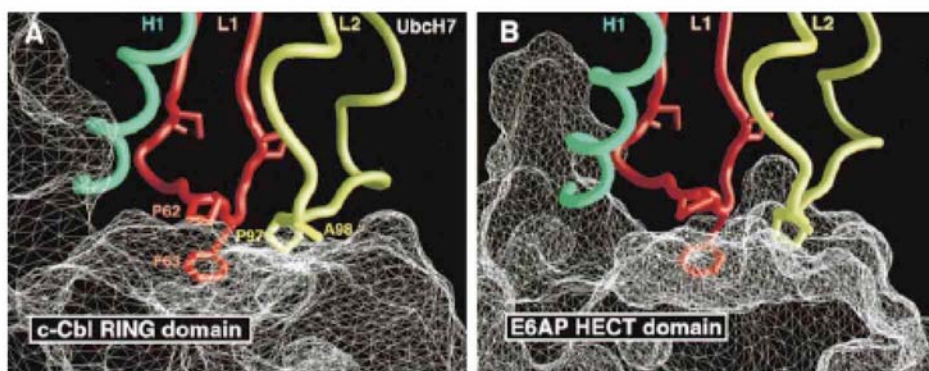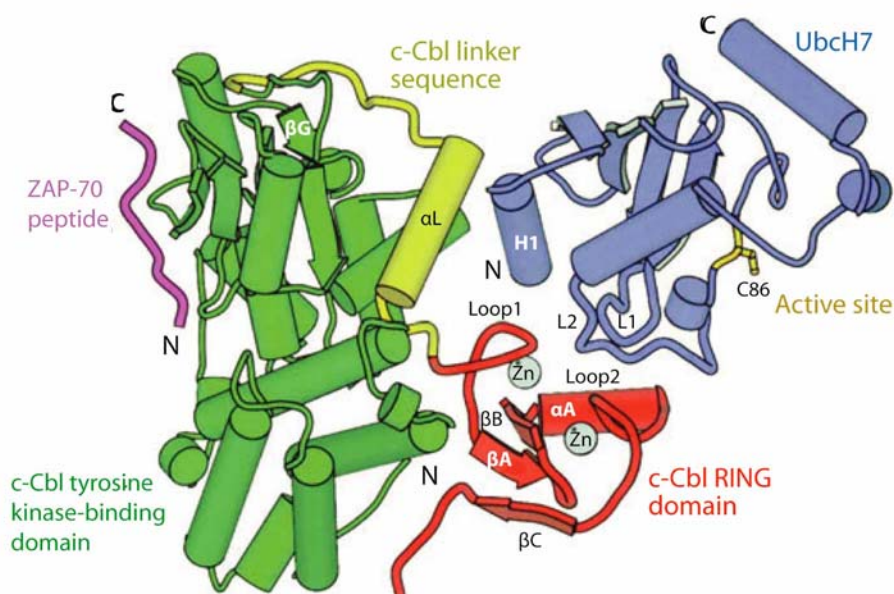
Figure 5. Interactions of E2 conjugating enzymes and E3 ligases.

(**A**) A close-up of the interaction between the E2, UbcH7, with the c-Cbl RING domain (panel **a**, **left**, from the crystal structure of c-Cbl in complex with the E2 UbcH7 and a phospho-peptide ZAP-70, PDB entry 1FBV) and the HECT E3, E6AP (panel **b**, **right**, from the crystal structure of a complex between UbcH7 and the E6AP HECT, PDB entry 1C4Z) shows that the helix H1 and loops L1 and L2 of UbcH7 interact with both RING and HECT E3s. The E3 surface is shown as a white net. UbcH7 residue Phe63 inserts its side chain into a groove formed by the E3 surface. Figure from (Zheng, Wang et al. 2000).

(**B**) Structure of the RING E3 c-Cbl in complex with the E2 UbcH7 and a phospho-peptide ZAP-70 (PDB entry 1FBV). The RING domain interacts with the E2 using both its RING domain and its linker helix. Figure from (Zheng, Wang et al. 2000).

Ubiquitin ligases (E3)

E3 Ub ligases catalyze the final step of Ub transfer to substrate. With over 300 members encoded in the human genome, E3 ligases comprise the largest class of Ub/Ubl conjugation enzymes (Li, Bengtson et al. 2008). They are divided into three classes based on their mechanism of function: (*1*) RING and RING-like, (*2*) HECT, and neither RING nor HECT classes. We focus our discussion on the RING and HECT classes here.

RING E3 ligases

RING domains contain a cross-brace structure of eight conserved cysteine or histidine residues coordinating two zinc ions (Joazeiro, Wing et al. 1999; Lorick, Jensen et al. 1999; Seol, Feldman et al. 1999). Variations in the number of zinc ions distinguish related domains. The U-box domain lacks zinc ions. Charged and polar residues, instead of the cysteine and histidine residues, form salt bridges and hydrogen bonds that stabilize a similar cross-brace structure. The RING-H2 domain contains three zinc-binding sites.

The RING domain of the E3 ligase recruits E2~Ub thioester complex. The region of interaction between RING E3s and E2 enzymes was elucidated through structural studies of RING-E2 complexes (Dye and Schulman 2007; Deshaies and Joazeiro 2009). A concave surface formed from the zinc-binding loops of the RING domain and a helix that connects the first and second Zn^{2+} coordination sites creates a concave surface to which E2s bind, using their H1 helix, loop 1, and loop 2, as described above (Zheng, Wang et al. 2000; Zhang, Windheim et al. 2005).

Hydrophobic interactions between a conserved proline-phenylalanine pair (P62 and F63 in UBE2L3) and the RING domain secure the interaction (Huang, Kinnucan et al. 1999; Zheng, Wang et al. 2000) (Figure 5b). As mentioned above, additional regions outside of the RING domain can also mediate E2-RING interactions, and the interaction between E2 and E3s is typically weak (in the micromolar range). Furthermore, the ability of a particular E2-E3 pair to bind does not always correlate with Ub ligase activity: for example, the BRCA1/BARD1 RING E3 ligase interacts with UBE2L3, but this pair is not functional in catalyzing E3 autoubiquitination (Christensen, Brzovic et al. 2007). A similar observation was made for the RING E3 heterodimer Ring1b/Bmr1 (Buchwald, van der Stoop et al. 2006), the U-box E3 CHIP (Zhang, Windheim et al. 2005), and the UbcH7-c-Cbl E2-RING pair (Huang, de Jong et al. 2009).

The role of RING E3 during catalysis is to bring the E2~Ub thioester in proximity of a lysine residue for modification. RING domains may also play a more active role, however, than as just molecular scaffolds. Evidence indicates that merely binding of E2 and RING E3s is not sufficient for catalysis (Deshaies and Joazeiro 2009; Huang, de Jong et al. 2009), and it is possible that the RING domain induces a conformational change in E2~Ub to promote Ub discharge. A conserved Asn residue located near the E2 enzyme active site aids in RING-dependent or E3-independent transfer of Ub to a substrate lysine. This Asn residue functions to stabilize the oxyanion intermediate that forms during nucleophilic attack of the substrate lysine residue on the E2~Ub thioester (Wu, Hanlon et al. 2003). RING E3s may function to allosterically activate the E2 by promoting a conformation change that positions the Asn residue in the oxyanion hole to stabilize the charged intermediate (Wu, Hanlon et al. 2003; Ozkan, Yu et al. 2005).

RING and RING-related domains often function in the context of multi-domain proteins or multi-subunit complexes. In both cases, the substrate-binding and E2-binding functionalities are separated, with the substrate binding function mediated by various protein-protein interaction modules (Dye and Schulman 2007). The multisubunit cullin-RING ligases (CRL), the largest superfamily of E3s, are an example. In these complexes, a RING domain associates with one of seven different cullins via the cullin's C-terminus. The N-terminal portion of cullin recruits substrate-recruiting adaptor proteins. CRL activity is subject to both positive and negative regulation. Covalent attachment of NEDD8 to a Lys residue in the cullin C-terminal domain enhances activity, while binding of the inhibitor CAND1 prevents CRL assembly (Petroski and Deshaies 2005; Duda, Borg et al. 2008). Modeling the complete complex by superimposing its subcomponents from known structures has raised the question of how catalysis occurs: ~50 Å separates the E2 active site Cys and the ends of substrate phosphopeptides (Dye and Schulman 2007). This situation recalls that of E1 enzyme: the distance between the adenylation site and active site Cys, and the distance between the Cys residues of E1 and E2, are not obviously juxtaposed for Ub transfer. A crystal structure of a Neddylated Cul5 C-terminal domain with bound RING protein Rbx1 (NEDD8~Cul5^{ctd}-Rbx1) shows that NEDD8 activates CRL activity by inducing a massive conformation shift in the cullin WHB and Rbx1 subdomains, removing the CAND1 binding site and switching the CRL from a "closed" state to an "open," active state (Duda, Borg et al. 2008). Kinetic experiments also showed that neddylation stimulates CRL activity through increased recruitment of E2~Ub, bridging the substrate to E2~Ub gap, and stabilizing the oxyanion transition state (Saha and Deshaies 2008).

HECT E3 ligases

In contrast to the large number of RING domain E3s, the human genome encodes 28 HECT E3s (Huibregtse, Scheffner et al. 1995). This class of enzymes is distinguished from RING E3s by its catalytic mechanism. HECT E3s form an E3~Ub intermediate on a conserved catalytic cysteine contained within the HECT domain prior to catalyzing isopeptide bond formation. The HECT (*h*omologous to *E*6AP *C-t*erminus) domain is a ~350 residue C-terminal domain catalytic defined by that of the founding member of the family, E6AP (Huibregtse, Scheffner et al. 1994). The catalytic and substrate-binding functions of HECT E3s are typically separated in different domains, with substrate binding mediated by N-terminal protein-protein interaction modules. HECT domains are classified into three subfamilies on the basis of their N-terminal regions: HERC E3s containing RCC1-like domains (RLDs), C2-WW-HECT E3s with tryptophan-tryptophan (WW) domains, and SI(ngle)-HECT E3s lacking either RLDs or WW domains (Scheffner and Staub 2007). The architecture of the HECT domain is composed of two lobes: the N-lobe, housing the E2-binding region, and the C-lobe, containing the catalytic cysteine. A peptide hinge connects the two lobes. In the crystal structure of a complex between E6AP and UbcH7, the catalytic cysteines of E2 and E3 are separated by 41 Å (Huang, Kinnucan et al. 1999) (Figure 6, left). Subsequent structures have shown that the orientation of the two lobes varies due to rotation of the C-lobe about a polypeptide linker connecting the N- and C-lobes (Verdecia, Joazeiro et al. 2003; Ogunjimi, Briant et al. 2005; Kamadurai, Souphron et al. 2009) (Figure 6). In the structure of WWP1 HECT domain, a ~100º rotation of the N-lobe about the peptide hinge reduces the distance between the E3 and E2 catalytic Cys to16 Å (Verdecia, Joazeiro et al. 2003). Furthermore, non-covalent interactions between the HECT C-lobe and Ub from the bound E2~Ub complex promote transfer of Ub from E2 to E3 (Kamadurai, Souphron et

al. 2009) (Figure 6, right). These crystal structures raise the question as to why the HECT

domain adopts a conformation in which the C-lobe is clearly too far from the E2~Ub to become

charged with Ub. One possibility is that the conformational flexibility of the HECT domain

speaks to its mechanism of catalyzing polyubiquitination chains, discussed further in the section

"Ub chain assembly" below.

Figure 6.
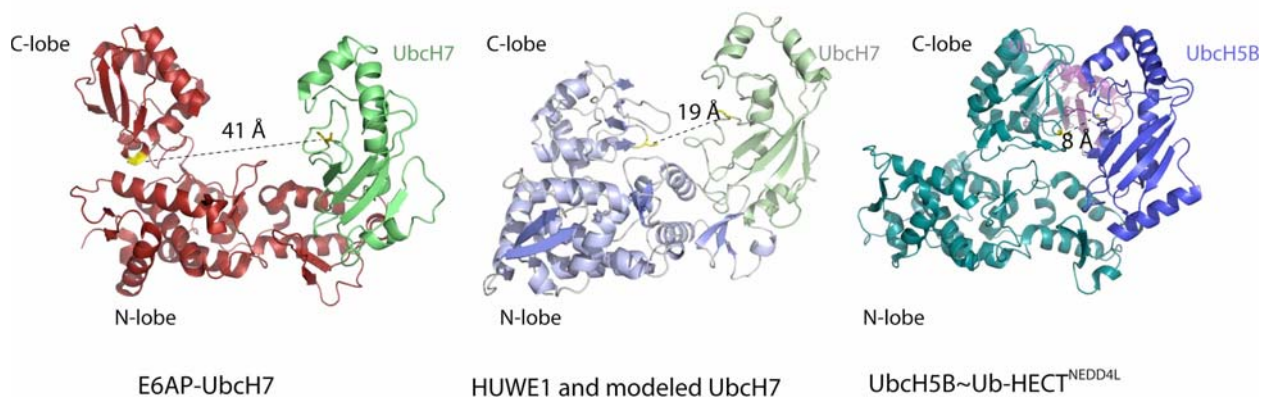
Figure 6 Structures of E3 HECT domains.

Crystal structures of HECT E3-E2 interactions. In the structure of a complex containing E6AP
and UbcH7 (**left**, PDB entry 1C4Z), 41 Å separates E2 and E3 catalytic cysteines. Rotation of
the C-lobe about the peptide hinge connecting N- and C-lobes shortens the E2-E3 catalytic
cysteine distance to 19 Å in HUWE1 (**middle**, PDB entry 3H1D) modeled with UbcH7. In the
structure of a complex of the NEDD4L HECT domain with UbcH5B containing Ub covalently
bound to the E2 active site (UbcH5B~Ub-HECT^NEDD4L, **right**, PDB entry 3JVZ) the catalytic
cysteines of E2 and E3 are separated by 8 Å, and the C-lobe of NEDD4L HECT interacts
noncovalently with Ub to facilitate the transthiolation reaction.

Polyubiquitin chain assembly

Despite evidence for the existence of polyubiquitin chains of each of the seven possible

different linkages in vivo (Peng, Schwartz et al. 2003; Xu, Duong et al. 2009), and for the

distinct functional outcomes of different polyubiquitin linkages (Dikic, Wakatsuki et al. 2009),
much remains unknown regarding the mechanisms of polyubiquitin chain synthesis. There are
several questions regarding the synthesis of a polyubiquitinated chain on a substrate. For
example, how does the E3 accommodate an increasingly long ubiquitin polymer near its active
site? How is the proper lysine residue of ubiquitin positioned to generate a polyubiquitin chain
with a specific topology? Furthermore, a polyubiquitin chain containing at least four ubiquitin
monomers is required for efficient binding to the proteasome ubiquitin receptor, S5a, and
substrates often acquire ubiquitin polymers containing over a dozen ubiquitin monomers
(Varshavsky 2005). Given the typically weak affinity between E3s and their substrates, how is a
long polyubiquitin chain added to the substrate before it dissociates from the E3?

The choice of target lysine residues for ubiquitination is largely thought to be governed
by steric considerations: access of the lysine residue to the E2~Ub or E3~Ub thioester. There are
several exceptions to this in which primary sequence motifs are recognized as consensus sites for
modification. One, noted above, is the SUMOylation of the consensus sequence ΦKxD/E,
where Φ is any hydrophobic residue and K is the lysine residue to be modified. A second
exception is the TEK box that occurs adjacent to ubiquitination sites in APC/C substrates (Jin,
Williamson et al. 2008).

Polyubiquitin chain formation can be separated into two processes: chain initiation and
chain elongation. During chain initiation, a lysine residue is targeted for attachment of the first
molecule of ubiquitin, a choice presumably governed by steric considerations. In the second
phase, additional ubiquitin molecules are added to the initiating monomer to extend the
polyubiquitin chain. These two processes are often distinguished kinetically, in that the chain
initiation is the slow step and chain extension occurs rapidly. The two steps may also be

performed by different E2s, which function together to assemble the polyubiquitin chain (Deshaies and Joazeiro 2009). For example, the yeast APC/C E3 ligase employs Ubc4 to monoubiquitinate substrate and Ubc1 to polymerize a Lys48-linked Ub chain (Rodrigo-Brenni and Morgan 2007). A similar observation comes from studies of the BRCA1/BARD1 E3 ligase. Of the six E2s with which BRCA1/BARD1 interacts, four promote monoubiquitination of BRCA1, and the remaining two extend the ubiquitin polymer on the monoubiquitinated substrate (Christensen, Brzovic et al. 2007). Some E2s can catalyze both Ub chain initiation and chain elongation, as in the case of the yeast E2 Cdc34. Cdc34 functions in conjunction with the E3 SCF to catalyze monoubiquitination of substrate, Sic1, in a slow step. Cdc34 then rapidly extends a Lys48 polyubiquitin chain on monoubiquitinated Sic1 (Petroski and Deshaies 2005; Saha and Deshaies 2008).

The standard model for polyubiquitin chain formation is the sequential addition model. According to this model, a ubiquitin monomer conjugated to substrate provides the lysine residue for nucleophilic attack on an E2~Ub thioester (in the case of RING E3s) or E3~Ub thioester (in the case of HECT E3s). In the course of repeated cycles, Ub monomers are added, one at a time, to the most distal ubiquitin in the polymer. As mentioned above, one central question pertaining to this model is how long ubiquitin chains are added to substrate before it dissociates from the E3. Furthermore, as the ubiquitin chain grows, the distal end of the chain providing the attacking lysine becomes further removed from the E2 or E3 active site. Nonetheless, a theoretical methodology developed by Pierce *et al.* predicted that the SCF E3s functions with the E2 Cdc34 to sequentially assemble a polyubiquitin chain on the engineered phosphopeptide substrate CYCE. Kinetic experiments conducted in millisecond time resolution demonstrate sequential polyubiquitin chain assembly (Pierce, Kleiger et al. 2009).

Verdecia *et al*. proposed an alternative model following crystallization of the HECT domain of the E3 WWP1. This model is based on the observation that HECT E3s can adopt a range of relative orientations due to rotation of the C-lobe about the peptide hinge connecting the N- and C-lobes, and that conformational flexibility of the domain is essential for its activity. In the indexation model, the E3 enzyme adds ubiquitin monomers sequentially to the distal end of a polyubiquitin chain anchored at its active site Cys. The growing Ub chain is accommodated by a progressive opening of the hinge connecting the two HECT lobes, until the chain is transferred *en bloc* to a substrate lysine residue (Verdecia, Joazeiro et al. 2003). One prediction of this model is that a thioester-linked polyubiquitin chain linked to an enzyme active site should be detected, an observation that has been reported for the HECT E3 E6AP (Wang and Pickart 2005). Wang *et al.* find that synthesis of Lys48-linked diubiquitin by E6AP occurs through formation of a thioester-linked diubiquitin on E6AP's active site. Li *et al.* detect thioester-linked polyubiquitin chains on the E2 Ube2g2 *in vitro* (Li, Tu et al. 2007). Ube2g2 functions with the E3 gp78 to assemble a Lys48-linked polyubiquitin chain anchored at the Ube2g2 active site before its transfer to the C-terminus of its substrate, HERP. The Lys48 residue of one ubiquitin thioesterified to Ube2g2 attacks a second Ube2g2~Ub complex to form Lys48-linked diubiquitin, and repeated cycles assemble the Ub polymer. This mechanism requires proximity of two Ube2g2~Ub complexes ; indeed, gp78 oligomerizes via two oligomerization sites, and the gp78 oligomer associates with multiple Ube2g2 molecules (Li, Tu et al. 2009). It is unclear whether this mechanism of Ub chain assembly occurs *in vivo*. The orthologous yeast E2, Ubc7, forms thioesterified polyubiquitin chains only when unstable, in which case the polyubiquitinated Ubc7 is targeted for degradation (Ravid and Hochstrasser 2007).

A final model of polyubiquitin chain formation to examine evokes the provision of a noncovalent ubiquitin binding site on the E2, E3, or other protein that anchors the polyubiquitin chain during its assembly (Hochstrasser 2006). In this model, noncovalently bound ubiquitin is positioned such that the appropriate Lys residue is available for nucleophilic attack on either the E2~Ub thioester or E3~Ub thioester. The assembled polyubiquitin chain is transferred to an enzyme active site prior to its *en bloc* attachment to a substrate lysine (Hochstrasser 2006). An experimental piece of evidence to support this model comes from the crystal structure of the Ubc13-Mms2 heterodimer, described above, in which the noncovalent binding of Ub to the Mms2 acceptor site positions its Lys63 toward the active site Ubc13~Ub. Furthermore, the HECT domains of three C2-WW-HECT E3s were recently found to contain an intrinsic ubiquitin-binding site (Ogunjimi, Wiesner et al. ; French, Kretzmann et al. 2009; Kamadurai, Souphron et al. 2009). The N-lobe of Rsp5 binds Ub and was proposed to function in controlling the linkage and length of polyubiquitin chains assembled by Rsp5 HECT domain in *in vitro* autoubiquitination assays (French, Kretzmann et al. 2009). A noncovalent ubiquitin binding site was also identified on the N lobe of another C2-WW HECT E3, Smurf2, and was shown to be required for efficient polyubiquitination of the HECT domain itself and its substrate, Smurf2. The authors thus propose that the ubiquitin binding site functions in positioning and stabilizing binding of mono-ubiquitinated substrate to the HECT (Ogunjimi, Wiesner et al.).

An important parameter to consider in the context of polyubiquitin chain assembly is how the topology of the ubiquitin chain is generated. The ubiquitin chain linkage preference has been documented for numerous RING and HECT E3s. For example, some RING-E2 pairs exclusively synthesize polyubiquitin chains linked through Lys6 (Wu-Baer, Lagrazon et al. 2003; Nishikawa, Ooka et al. 2004), Lys48 (Chau, Tobias et al. 1989; Feldman, Correll et al.

1997), and Lys63 (Hofmann and Pickart 1999). The observation that E2 enzymes can direct polyubiquitin chain topology even in the absence of an E3, and that in cases where a single RING domain recruits different E2s, the chain topology is dictated by the E2's known preference of lysine usage (David, Ziv et al. ; Christensen, Brzovic et al. 2007; Kim, Kim et al. 2007), suggests that for E2-RING pairs, chain topology is dictated by the E2. There are a few notable exceptions, in which an E2 synthesizes different chain linkages with different partner E3s (Deshaies and Joazeiro 2009).   HECT E3s with known ubiquitin chain assembly specificity include human E6AP, which assembles Lys48-linked polyubiquin chains (Wang and Pickart 2005; Kim, Kim et al. 2007), and *S. cerevisiae* Rsp5, which preferentially assembles Lys63-linked polyubiquitin chains (Kee, Lyon et al. 2005; Kee, Munoz et al. 2006). In contrast to the RING E3s, the HECT domain governs chain type specificity (Wang and Pickart 2005; Kim and Huibregtse 2009).

Deubiquitinating enzymes/proteases

Ub conjugation, like other post-translational modifications, is reversible. Ubiquitin conjugation is counterbalanced by the action of deubiquitinating enzymes (DUBs). DUBs are proteases that function in several different capacities to proteolyse ubiquitin polymers or remove ubiquitin from target proteins. First, Ub is encoded in the human genome as head-to-tail fusions of several ubiquitin monomers or as an N-terminal fusion with ribosomal proteins. After translation, Ub fusion proteins are proteolytically processed by DUBs to produce an active Ub monomer with a free C-terminus for conjugation. Second, DUBs cleave mono- or polyubiquitin chains from ubiquitinated substrate proteins, thereby regulating their activity or rescuing them from proteasomal degradation. Finally, DUBs remove ubiquitin chains from proteins targeted to

the proteasome for degradation, recycling Ub and preventing it from being degraded by the proteasome (Amerik and Hochstrasser 2004). Ubiquitin-like modifiers are similarly processed or deconjugated from target proteins, although less is known about ubiquitin like-proteases. SUMO-specific proteases (SENPs) process newly synthesized SUMO precursor proteins and remove SUMO from target proteins (Mukhopadhyay and Dasso 2007). The COP9 signalosome (CSN) and NEDP1 (DEN1) remove NEDD8 from specific substrate (Lyapina, Cope et al. 2001; Mendoza, Shen et al. 2003; Chan, Yoon et al. 2008). A single ISG15-specific protease has been identified, UBP43/USP18 (Malakhov, Malakhova et al. 2002). Some proteases possess dual specificity: for example, UCHL1, UCHL3 and USP21 deubiquitinating enzymes also function as deNeddylases (Gong, Kamitani et al. 2000; Amerik and Hochstrasser 2004; Hemelaar, Borodovsky et al. 2004).

The human genome encodes ~100 DUBs, which fall into five families: four families of cysteine proteases, and one family of zinc-dependent metalloproteases (Nijman, Luna-Vargas et al. 2005). The Cys protease families are: ubiquitin-specific proteases (USP), ubiquitin C-terminal hydrolases (UCH), otubain proteases (OTU), and Machado/Joseph (MJD) proteases. Cys proteases utilize an active site-cysteine residue to catalyze nucleophilic attack on the carbonyl carbon of the scissile peptide bond. The Cys is activated by a nearby His residue that lowers its pKa, and often a third residue, Asn or Asp, that positions and stabilizes the His residue. The acyl-enzyme intermediate is resolved by nucleophilic attack of water to regenerate the free DUB and release product (Figure 7). The Jab1/MPN (JAMM) family of metalloproteases employs a zinc-catalyzed mechanism of hydrolysis, in which a zinc atom, chelated by His and Asp residues, activates a water molecule in nucleophilic attack on the carbonyl carbon of the isopeptide bond (Amerik and Hochstrasser 2004).

Figure 7.
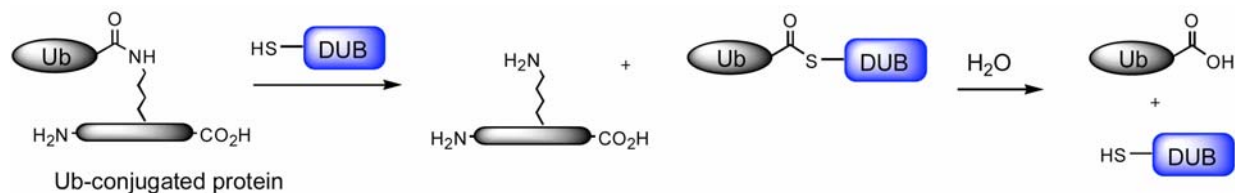
Figure 7 Catalysis by the cysteine protease DUBs.

Deubiquitination of Ub-conjugated proteins by DUBs. Enzymes of the UCH, USP, MJD, and OTU classes are cysteine proteases, whereas JAMMs are metalloproteases. The active site cysteine residue of cysteine proteases performs a nucleophilic attack on the carbonyl carbon atom of Ub's C-terminal glycine residue that is in isopeptide linkage to a substrate lysine residue. The resulting acyl-enzyme intermediate is resolved by the nucleophilic attack of water, allowing the release of free DUB and Ub. Figure courtesy of Howard Hang.

DUBs regulate numerous cellular processes, including signal transduction, chromatin remodeling, DNA repair, cell-cycle progression, and apoptosis (Wilkinson 2009). Their importance to maintaining cellular function is underscored by the fact that mutation in or misregulation of specific DUBs is associated with malignant transformation and disease including ataxia (Nijman, Luna-Vargas et al. 2005). The identification, and biochemical and structural characterization of DUBs has greatly benefited from the development of function-dependent methodologies, and in particular, activity-based protein profiling (ABPP).

Activity-based protein profiling (ABPP)

Genome sequencing efforts have tabulated an enormous catalogue of predicted protein products. The assignment of function to these proteins is a challenging task: methods such as

bioinformatics and the genetic alteration of expression have generated insight into function, but are limited by pre-existing knowledge of protein families and perturbing expression to infer function, respectively (Evans and Cravatt 2006; Cravatt, Wright et al. 2008). Proteomics methods, including profiling protein expression and modification state by LC-MS analysis, protein microarrays, and protein-protein interaction techniques, have further advanced knowledge of the proteome (Gygi, Rist et al. 1999; Washburn, Wolters et al. 2001; Ito, Ota et al. 2002; MacBeath 2002; Zhu, Bilgin et al. 2003; Petricoin and Liotta 2004). These methods, however, do not report directly report on the functional state of enzymes, whose activity can be regulated in many ways, for example, by proteolytic cleavage, post-translational modification, or subcellular localization. A powerful method for the global analysis of protein expression and function is activity-based protein profiling (ABPP).

ABPP is a chemical strategy that employs active site-directed covalent probes to query the functional state of enzymes in complex mixtures (Cravatt, Wright et al. 2008) (Figure 8). ABPP can provide information on an active set of enzymes, not just the expressed set of enzymes, under physiological conditions, during a cell state change, or in pathogenic settings. Activity based probes are designed to target a subset of the proteome, usually sharing similar catalytic features. A dozen different enzyme classes have been targeted by ABPs, including kinases, phosphatases, oxidoreductases, and proteases (Cravatt, Wright et al. 2008). The design of an ABP relies on three components: a chemical moiety designed to react covalently with a catalytic residue in the enzyme active site; a binding group to target the ABP to a specific class of enzymes; and an analytic handle, such as a fluorophore or haemagluttinin (HA) tag, for visualization or recovery of probe-reacted enzyme complexes. Thus, the design of an ABP requires some knowledge of the target enzyme class: its catalytic mechanism, preference for

binding small molecules or substrate, and/or structure. Knowledge of these properties facilitates

the design of a "mechanism-based" inhibitor to selectively target a specific enzyme class, as well

as a high-affinity binding group to guide probe specificity. Enzymes that are less well-

characterized can be targeted using a "non-directed" strategy in which a library of probes

containing less potent electrophiles and a variety of binding groups is used to target a broad

group of enzyme classes (Evans and Cravatt 2006).

Figure 8.
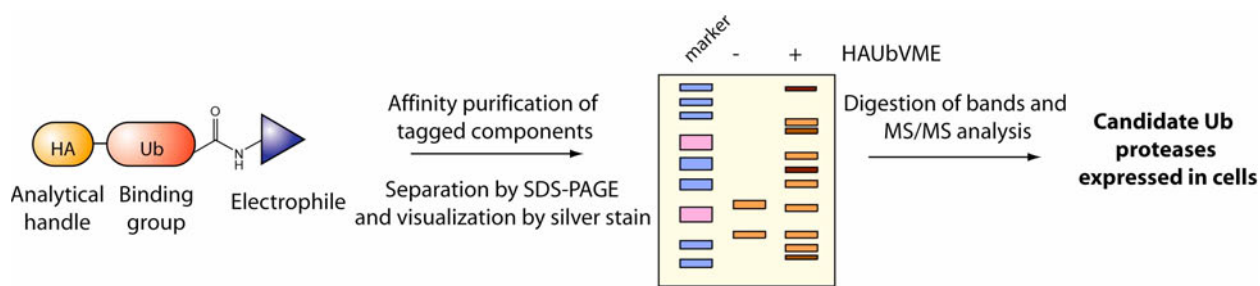
Figure 8. A typical activity-based protein profiling (ABPP) experiment.

A typical activity-based protein profiling experiment makes use of an active site-directed chemical probe that covalently binds to an active site residue of a subset of enzymes in a complex proteome. The probe is incubated with cell lysate, and the analytical handle is used to retrieve labeled complexes. The complexes are separated by SDS-PAGE and visualized by silver stain. A cartoon of an ABPP result is shown, in which incubation of lysate with the HAUbVME probe is seen to label numerous species.   Enzymes labeled with HAUbVME can be identified by tandem mass spectrometry to obtain a list of candidate Ub proteases expressed in cells.

DUB-specific activity-based probes evolved from the development of DUB substrates

consisting of Ub with C-terminal modifications: Ub ethyl ester (Wilkinson, Cox et al. 1986) and

the fluorogenic derivative Ub-AMC (Dang, Melandri et al. 1998), and DUB inhibitors Ub-

aldehyde (Pickart and Rose 1986; Hershko and Rose 1987; Lam, Xu et al. 1997) and Ub-nitrile

(Lam, Xu et al. 1997). An intein-based protein ligation system was later developed for Ub probe synthesis. Epitope-tagged Ub is expressed with an intein-chitin binding domain fused to its C-terminus for purification and introduction of glycine-based electrophilic groups (Borodovsky, Ovaa et al. 2002). These electrophiles, chosen for their reactivity with Cys nucleophiles, have included vinyl methylsulfone, vinyl methylester, alkyl halides, and vinyl cyanide (Figure 9). Following recovery of probe-labeled complexes using the analytic handle, the identity of labeled proteins is determined by MS/MS sequencing and database searching of peptide hits.

Figure 9.
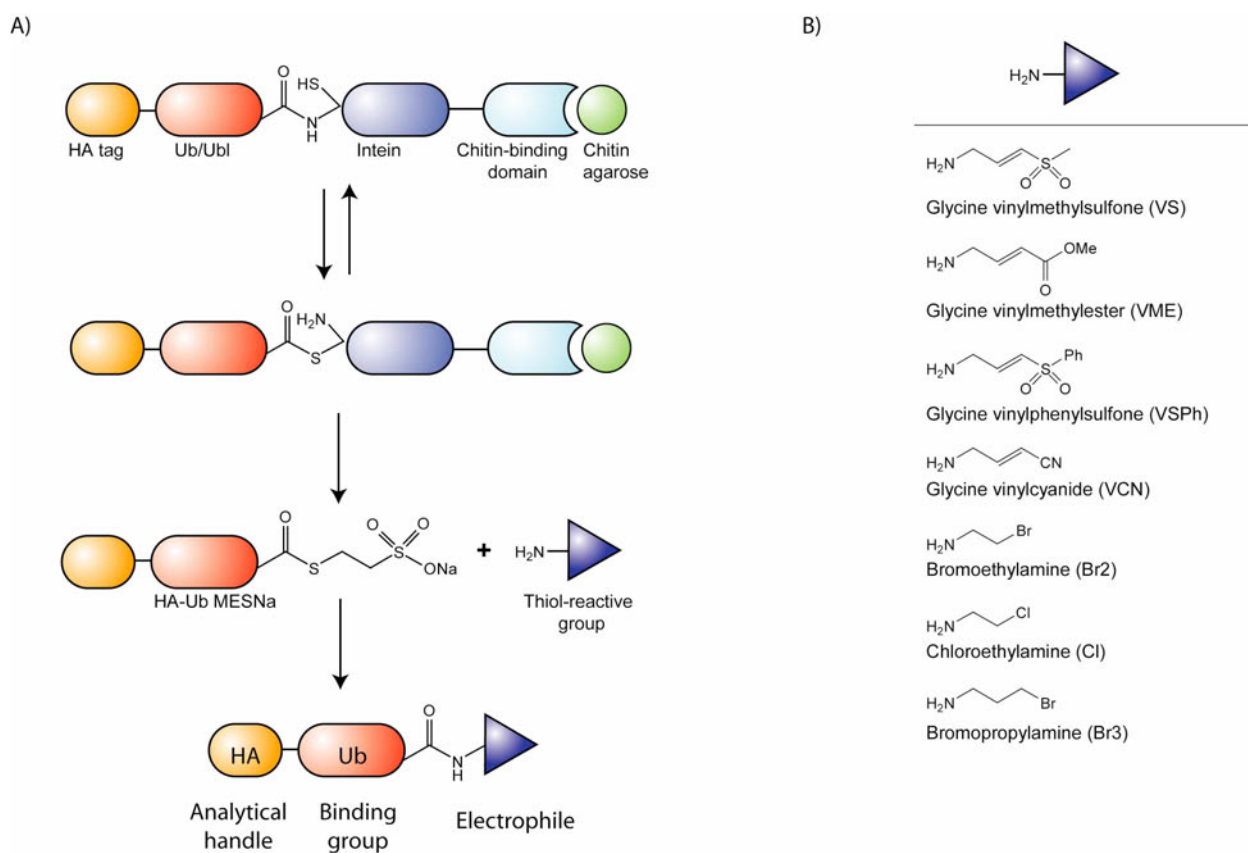
Figure 9. Synthesis of Ub-based chemical probes.

(**A**) HAUb-derived probes are synthesized using an intein-based chemical ligation. Recombinant HA-tagged Ub/Ubls are expressed with a C-terminal intein-chitin binding domain for purification using chitin agarose. Bound proteins are eluted with a thiol agent, such as β-mercaptoethane solfonic acid (MESNa), resulting in a Ub-thioester capable of chemical ligation. (**B**) Table of glycine-based electrophiles synthesized for attachment to the C-terminus of HAUb probes, used in (Borodovsky, Ovaa et al. 2002). Figure from (Love, Catic et al. 2007).

ABPP of ubiquitin proteases was first undertaken in a murine thymoma (EL-4) cell line and identified 23 DUBs (Borodovsky, Ovaa et al. 2002). Subsequently, Ub active site-directed probes have successfully identified bacterial, viral, and parasite-encoded DUBs (Kattenhorn, Korbel et al. 2005; Schlieker, Korbel et al. 2005; Zhou, Monack et al. 2005; Artavanis-Tsakonas, Misaghi et al. 2006; Misaghi, Balsara et al. 2006; Catic, Misaghi et al. 2007; Frickel, Quesada et al. 2007; Rytkonen, Poh et al. 2007). The existence of pathogen-encoded DUBs suggests that microbes may utilize protease activity to confer selective advantages during infection and to reverse the ubiquitination of host proteins required for the host's defense against microbes (Angot, Vergunst et al. 2007; Rytkonen and Holden 2007; Wilkinson 2009). DUB profiling using activity-based probes has also been used to inform how Ub protease activity changes during malignant transformation in B cell malignancies (Ovaa, Kessler et al. 2004) and in human papillomavirus (HPV) cervical carcinoma (Rolen, Kobzeva et al. 2006).

Activity-based probes are invaluable tools for the structural analysis of DUBs. The deubiquitinating enzyme HAUSP, which removes ubiquitin from the tumor suppressor protein p53, was crystallized alone and bound to its inhibitor, Ub aldehyde (Hu, Li et al. 2002). These structures revealed that inhibitor binding triggers a major conformational change in the enzyme active site, rearranging the catalytic residues for productive catalysis. The crystal structure of UCHL3 bound at its active site to UbVME confirmed the probe's mechanism of inhibition and

illustrated the conformational changes that occur in UCHL3's N-terminus to accommodate Ub binding (Misaghi, Galardy et al. 2005). Finally, the crystallization of the murine cytomegalovirus M48(USP) was only possible in its inhibitor-bound state. This structure revealed a novel configuration of active site residues and Ub-interaction surface that established it as a founding member of a new class of DUBs – the herpesvirus tegument USP (Schlieker, Weihofen et al. 2007).

Because earlier campaigns using Ub C-terminal electrophilic probes identified approximately half of the ~100 proposed mammalian DUBs, we hypothesized that incorporation of "warheads" with greater electrophilicity should retrieve a larger number of DUBs. In Chapter 2, we report the design and use of an expanded set of Ub C-terminal electrophilic probes, and their utility in recovering enzymes of the Ub activating, conjugating, and ligase classes. One ligase we identified, termed HUWE1, was particularly intriguing due to its misregulation in several tumor types and its reported role in regulating cell proliferation and apoptosis. We therefore chose this enzyme for further biochemical and structural characterization (Chapter 3).

HUWE1 E3 Ub ligase

HUWE1 (HECT, UBA, and WWE domain containing 1) is a large (482-kDa) E3 Ub ligase of the SI(ngle) class (Figure 10). This protein functions in many cellular pathways: cell proliferation, apoptosis, DNA damage response, base excision repair, and cell attachment (D'Arca, Zhao et al. ; Zahreddine, Zhang et al. ; Adhikary, Marinoni et al. 2005; Chen, Kon et al. 2005; Zhong, Gao et al. 2005; Hall, Kow et al. 2007; Herold, Hock et al. 2008; Zhao, Heng et al. 2008; Zhao, D et al. 2009). It is overexpressed in several tumor types, including breast and lung (Adhikary, Marinoni et al. 2005; Chen, Kon et al. 2005). HUWE1 overexpression has also been

identified in colon carcinomas, where its expression directly correlates with tumor stage, and

inversely correlates with p53 protein levels (Adhikary, Marinoni et al. 2005; Yoon, Lee et al.

2005). Despite the number of reports on HUWE1 function and substrates, its cellular role is still

under investigation. The first two reports identifying this E3 ligase described opposite

phenotypes as a result of its knockdown in the same cell line (Chen, Kon et al. 2005; Zhong, Gao

et al. 2005). One report observed increased survival, by linking HUWE1 function to its substrate

Mcl-1 (an antiapoptotic protein), whereas another group observed increased apoptosis, as a

consequence of its substrate p53 (a proapoptotic protein) (Chen, Kon et al. 2005). HUWE1

functions in the DNA damage response by ubiquitinating its substrates CDC6, TopBP1, and

DNA polymerase beta (Pol beta), the major base excision repair DNA polymerase (Hall, Kow et

al. 2007; Herold, Hock et al. 2008; Parsons, Tait et al. 2009). HUWE1 is reported to build

Lys63-linked polyubiquitin chains on the oncoprotein c-Myc, thus promoting recruitment of its

coactivator p300 and c-Myc-dependent gene transactivation (Adhikary, Marinoni et al. 2005).

However, another group reported that HUWE1 ubiquitinates N-myc *in vivo*, thereby regulating

neural proliferation and promoting neuronal differentiation (D'Arca, Zhao et al.; Zhao, Heng et

al. 2008; Zhao, D et al. 2009). Because this ligase plays a fundamental role in critical cellular

pathways, we chose this enzyme for biochemical characterization following its recovery in

immunoprecipitations with Ub C-terminal electrophiles (Love, Pandya et al. 2009).

Figure 10.
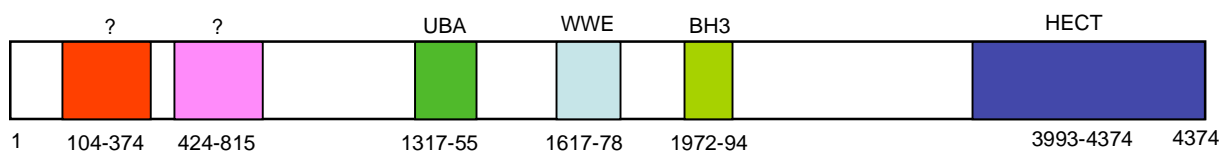
Figure 10. Domain structure of the HUWE1 E3 Ub ligase.

HUWE1 is a large (482-kDa) protein that is composed of multiple domains: from the N-terminus, two domains of unknown function; a UBA domain; that associates with Ub, a WWE domain, which has been found in E3 ligases; a BH3 domain, which binds one of its substrates, the anti-apoptotic Bcl-2 family member Mcl-1; and the catalytic HECT domain. Shown are residue numbers indicating the positions of these domains.

Conclusions

In this thesis, I will describe work relating to the development of an expanded class of Ub C-terminal electrophilic probes (Chapter 2), the structural characterization of the HECT domain of the E3 Ub ligase HUWE1 (Chapter 3), and a method that we hope will be useful to probe the role of conformational flexibility to HECT domain function (Chapter 4). The work in Chapter 2 was motivated by the observation that the first generation of activity-based Ub electrophiles recovered deubiquitinating enzymes from cell lysates, but not Ub conjugating enzymes, despite the presence of active site-cysteine residues in the latter class of enzymes. As discussed above, the functional identification of Ub conjugation enzymes will prove useful to complement existing bioinformatics and gene manipulation studies to identify enzyme function. Our work in solving the structure of the HUWE1 HECT domain (Chapter 3) was motivated, in part, to understand why the HUWE1 HECT domain reacted with Ub electrophilic probes at multiple cysteines, and also to crystallize a complex between the HECT domain and the Ub electrophile. Finally, the results in Chapter 4 give an example of a methodology that we are developing to study how conformational changes are important for enzyme function.

References

Adhikary, S., F. Marinoni, et al. (2005). "The ubiquitin ligase HectH9 regulates transcriptional activation by Myc and is essential for tumor cell proliferation." Cell **123**(3): 409-21.

Amerik, A. Y. and M. Hochstrasser (2004). "Mechanism and function of deubiquitinating enzymes." Biochim Biophys Acta **1695**(1-3): 189-207.

Angot, A., A. Vergunst, et al. (2007). "Exploitation of eukaryotic ubiquitin signaling pathways by effectors translocated by bacterial type III and type IV secretion systems." PLoS Pathog **3**(1): e3.

Artavanis-Tsakonas, K., S. Misaghi, et al. (2006). "Identification by functional proteomics of a deubiquitinating/deNeddylating enzyme in Plasmodium falciparum." Mol Microbiol **61**(5): 1187-95.

Bernassola, F., M. Karin, et al. (2008). "The HECT family of E3 ubiquitin ligases: multiple players in cancer development." Cancer Cell **14**(1): 10-21.

Bernier-Villamor, V., D. A. Sampson, et al. (2002). "Structural basis for E2-mediated SUMO conjugation revealed by a complex between ubiquitin-conjugating enzyme Ubc9 and RanGAP1." Cell **108**(3): 345-56.

Borodovsky, A., H. Ovaa, et al. (2002). "Chemistry-based functional proteomics reveals novel members of the deubiquitinating enzyme family." Chem Biol **9**(10): 1149-59.

Brzovic, P. S., A. Lissounov, et al. (2006). "A UbcH5/ubiquitin noncovalent complex is required for processive BRCA1-directed ubiquitination." Mol Cell **21**(6): 873-80.

Buchwald, G., P. van der Stoop, et al. (2006). "Structure and E3-ligase activity of the Ring-Ring complex of polycomb proteins Bmi1 and Ring1b." EMBO J **25**(11): 2465-74.

Cadwell, K. and L. Coscoy (2005). "Ubiquitination on nonlysine residues by a viral E3 ubiquitin ligase." Science **309**(5731): 127-30.

Catic, A., S. Misaghi, et al. (2007). "ElaD, a Deubiquitinating protease expressed by E. coli." PLoS One **2**(4): e381.

Chan, Y., J. Yoon, et al. (2008). "DEN1 deneddylates non-cullin proteins in vivo." J Cell Sci **121**(Pt 19): 3218-23.

Chau, V., J. W. Tobias, et al. (1989). "A multiubiquitin chain is confined to specific lysine in a targeted short-lived protein." Science **243**(4898): 1576-83.

Chen, B., J. Mariano, et al. (2006). "The activity of a human endoplasmic reticulum-associated degradation E3, gp78, requires its Cue domain, RING finger, and an E2-binding site." Proc Natl Acad Sci U S A **103**(2): 341-6.

Chen, D., N. Kon, et al. (2005). "ARF-BP1/Mule is a critical mediator of the ARF tumor suppressor." Cell **121**(7): 1071-83.

Chen, Z. J. and L. J. Sun (2009). "Nonproteolytic functions of ubiquitin in cell signaling." Mol Cell **33**(3): 275-86.

Chiu, Y. H., Q. Sun, et al. (2007). "E1-L2 activates both ubiquitin and FAT10." Mol Cell **27**(6): 1014-23.

Christensen, D. E., P. S. Brzovic, et al. (2007). "E2-BRCA1 RING interactions dictate synthesis of mono- or specific polyubiquitin chain linkages." Nat Struct Mol Biol **14**(10): 941-8.

Cook, W. J., L. C. Jeffrey, et al. (1994). "Structure of tetraubiquitin shows how multiubiquitin chains can be formed." J Mol Biol **236**(2): 601-9.

Cravatt, B. F., A. T. Wright, et al. (2008). "Activity-based protein profiling: from enzyme chemistry to proteomic chemistry." Annu Rev Biochem **77**: 383-414.

D'Arca, D., X. Zhao, et al. "Huwe1 ubiquitin ligase is essential to synchronize neuronal and glial differentiation in the developing cerebellum." Proc Natl Acad Sci U S A **107**(13): 5875-80.

Dang, L. C., F. D. Melandri, et al. (1998). "Kinetic and mechanistic studies on the hydrolysis of ubiquitin C-terminal 7-amido-4-methylcoumarin by deubiquitinating enzymes." Biochemistry **37**(7): 1868-79.

Das, R., J. Mariano, et al. (2009). "Allosteric activation of E2-RING finger-mediated ubiquitylation by a structurally defined specific E2-binding region of gp78." Mol Cell **34**(6): 674-85.

David, Y., T. Ziv, et al. "The E2 ubiquitin-conjugating enzymes direct polyubiquitination to preferred lysines." J Biol Chem **285**(12): 8595-604.

Deng, L., C. Wang, et al. (2000). "Activation of the IkappaB kinase complex by TRAF6 requires a dimeric ubiquitin-conjugating enzyme complex and a unique polyubiquitin chain." Cell **103**(2): 351-61.

Deshaies, R. J. and C. A. Joazeiro (2009). "RING domain E3 ubiquitin ligases." Annu Rev Biochem **78**: 399-434.

Desterro, J. M., M. S. Rodriguez, et al. (1999). "Identification of the enzyme required for activation of the small ubiquitin-like protein SUMO-1." J Biol Chem **274**(15): 10618-24.

Dikic, I., S. Wakatsuki, et al. (2009). "Ubiquitin-binding domains - from structures to functions." Nat Rev Mol Cell Biol **10**(10): 659-71.

Dominguez, C., A. M. Bonvin, et al. (2004). "Structural model of the UbcH5B/CNOT4 complex revealed by combining NMR, mutagenesis, and docking approaches." Structure **12**(4): 633-44.

Duda, D. M., L. A. Borg, et al. (2008). "Structural insights into NEDD8 activation of cullin-RING ligases: conformational control of conjugation." Cell **134**(6): 995-1006.

Duda, D. M., H. Walden, et al. (2005). "Structural analysis of Escherichia coli ThiF." J Mol Biol **349**(4): 774-86.

Durfee, L. A., M. L. Kelley, et al. (2008). "The basis for selective E1-E2 interactions in the ISG15 conjugation system." J Biol Chem **283**(35): 23895-902.

Dye, B. T. and B. A. Schulman (2007). "Structural mechanisms underlying posttranslational modification by ubiquitin-like proteins." Annu Rev Biophys Biomol Struct **36**: 131-50.

Eddins, M. J., C. M. Carlile, et al. (2006). "Mms2-Ubc13 covalently bound to ubiquitin reveals the structural basis of linkage-specific polyubiquitin chain formation." Nat Struct Mol Biol **13**(10): 915-20.

Eletr, Z. M., D. T. Huang, et al. (2005). "E2 conjugating enzymes must disengage from their E1 enzymes before E3-dependent ubiquitin and ubiquitin-like transfer." Nat Struct Mol Biol **12**(10): 933-4.

Evans, M. J. and B. F. Cravatt (2006). "Mechanism-based profiling of enzyme families." Chem Rev **106**(8): 3279-301.

Feldman, R. M., C. C. Correll, et al. (1997). "A complex of Cdc4p, Skp1p, and Cdc53p/cullin catalyzes ubiquitination of the phosphorylated CDK inhibitor Sic1p." Cell **91**(2): 221-30.

French, M. E., B. R. Kretzmann, et al. (2009). "Regulation of the RSP5 ubiquitin ligase by an intrinsic ubiquitin-binding site." J Biol Chem **284**(18): 12071-9.

Frickel, E. M., V. Quesada, et al. (2007). "Apicomplexan UCHL3 retains dual specificity for ubiquitin and Nedd8 throughout evolution." Cell Microbiol **9**(6): 1601-10.

Gong, L., T. Kamitani, et al. (2000). "Identification of a novel isopeptidase with dual specificity for ubiquitin- and NEDD8-conjugated proteins." J Biol Chem **275**(19): 14212-6.

Gong, L., B. Li, et al. (1999). "Molecular cloning and characterization of human AOS1 and UBA2, components of the sentrin-activating enzyme complex." FEBS Lett **448**(1): 185-9.

Gong, L. and E. T. Yeh (1999). "Identification of the activating and conjugating enzymes of the NEDD8 conjugation pathway." J Biol Chem **274**(17): 12036-42.

Gygi, S. P., B. Rist, et al. (1999). "Quantitative analysis of complex protein mixtures using isotope-coded affinity tags." Nat Biotechnol **17**(10): 994-9.

Hall, J. R., E. Kow, et al. (2007). "Cdc6 stability is regulated by the Huwe1 ubiquitin ligase after DNA damage." Mol Biol Cell **18**(9): 3340-50.

Hamilton, K. S., M. J. Ellison, et al. (2001). "Structure of a conjugating enzyme-ubiquitin thiolester intermediate reveals a novel role for the ubiquitin tail." Structure **9**(10): 897-904.

Hemelaar, J., A. Borodovsky, et al. (2004). "Specific and covalent targeting of conjugating and deconjugating enzymes of ubiquitin-like proteins." Mol Cell Biol **24**(1): 84-95.

Herold, S., A. Hock, et al. (2008). "Miz1 and HectH9 regulate the stability of the checkpoint protein, TopBP1." EMBO J **27**(21): 2851-61.

Hershko, A. and I. A. Rose (1987). "Ubiquitin-aldehyde: a general inhibitor of ubiquitin-recycling processes." Proc Natl Acad Sci U S A **84**(7): 1829-33.

Hicke, L. (2001). "Protein regulation by monoubiquitin." Nat Rev Mol Cell Biol **2**(3): 195-201.

Hochstrasser, M. (2006). "Lingering mysteries of ubiquitin-chain assembly." Cell **124**(1): 27-34.

Hochstrasser, M. (2009). "Origin and function of ubiquitin-like proteins." Nature **458**(7237): 422-9.

Hofmann, R. M. and C. M. Pickart (1999). "Noncanonical MMS2-encoded ubiquitin-conjugating enzyme functions in assembly of novel polyubiquitin chains for DNA repair." Cell **96**(5): 645-53.

Hu, M., P. Li, et al. (2002). "Crystal structure of a UBP-family deubiquitinating enzyme in isolation and in complex with ubiquitin aldehyde." Cell **111**(7): 1041-54.

Huang, A., R. N. de Jong, et al. (2009). "E2-c-Cbl recognition is necessary but not sufficient for ubiquitination activity." J Mol Biol **385**(2): 507-19.

Huang, D. T., O. Ayrault, et al. (2009). "E2-RING expansion of the NEDD8 cascade confers specificity to cullin modification." Mol Cell **33**(4): 483-95.

Huang, D. T., H. W. Hunt, et al. (2007). "Basis for a ubiquitin-like protein thioester switch toggling E1-E2 affinity." Nature **445**(7126): 394-8.

Huang, D. T., D. W. Miller, et al. (2004). "A unique E1-E2 interaction required for optimal conjugation of the ubiquitin-like protein NEDD8." Nat Struct Mol Biol **11**(10): 927-35.

Huang, D. T., A. Paydar, et al. (2005). "Structural basis for recruitment of Ubc12 by an E2 binding domain in NEDD8's E1." Mol Cell **17**(3): 341-50.

Huang, D. T., H. Walden, et al. (2004). "Ubiquitin-like protein activation." Oncogene **23**(11): 1958-71.

Huang, L., E. Kinnucan, et al. (1999). "Structure of an E6AP-UbcH7 complex: insights into ubiquitination by the E2-E3 enzyme cascade." Science **286**(5443): 1321-6.

Huibregtse, J. M., M. Scheffner, et al. (1995). "A family of proteins structurally and functionally related to the E6-AP ubiquitin-protein ligase." Proc Natl Acad Sci U S A **92**(7): 2563-7.

Huibregtse, J. M., M. Scheffner, et al. (1994). "E6-AP directs the HPV E6-dependent inactivation of p53 and is representative of a family of structurally and functionally related proteins." Cold Spring Harb Symp Quant Biol **59**: 237-45.

Humbard, M. A., H. V. Miranda, et al. "Ubiquitin-like small archaeal modifier proteins (SAMPs) in Haloferax volcanii." Nature **463**(7277): 54-60.

Ito, T., K. Ota, et al. (2002). "Roles for the two-hybrid system in exploration of the yeast protein interactome." Mol Cell Proteomics **1**(8): 561-6.

Jin, J., X. Li, et al. (2007). "Dual E1 activation systems for ubiquitin differentially regulate E2 enzyme charging." Nature **447**(7148): 1135-8.

Jin, L., A. Williamson, et al. (2008). "Mechanism of ubiquitin-chain formation by the human anaphase-promoting complex." Cell **133**(4): 653-65.

Joazeiro, C. A., S. S. Wing, et al. (1999). "The tyrosine kinase negative regulator c-Cbl as a RING-type, E2-dependent ubiquitin-protein ligase." Science **286**(5438): 309-12.

Johnson, E. S. (2004). "Protein modification by SUMO." Annu Rev Biochem **73**: 355-82.

Kamadurai, H. B., J. Souphron, et al. (2009). "Insights into ubiquitin transfer cascades from a structure of a UbcH5B approximately ubiquitin-HECT(NEDD4L) complex." Mol Cell **36**(6): 1095-102.

Kattenhorn, L. M., G. A. Korbel, et al. (2005). "A deubiquitinating enzyme encoded by HSV-1 belongs to a family of cysteine proteases that is conserved across the family Herpesviridae." Mol Cell **19**(4): 547-57.

Kee, Y., N. Lyon, et al. (2005). "The Rsp5 ubiquitin ligase is coupled to and antagonized by the Ubp2 deubiquitinating enzyme." EMBO J **24**(13): 2414-24.

Kee, Y., W. Munoz, et al. (2006). "The deubiquitinating enzyme Ubp2 modulates Rsp5-dependent Lys63-linked polyubiquitin conjugates in Saccharomyces cerevisiae." J Biol Chem **281**(48): 36724-31.

Kerscher, O. (2007). "SUMO junction-what's your function? New insights through SUMO-interacting motifs." EMBO Rep **8**(6): 550-5.

Kerscher, O., R. Felberbaum, et al. (2006). "Modification of proteins by ubiquitin and ubiquitin-like proteins." Annu Rev Cell Dev Biol **22**: 159-80.

Kim, H. C. and J. M. Huibregtse (2009). "Polyubiquitination by HECT E3s and the determinants of chain type specificity." Mol Cell Biol **29**(12): 3307-18.

Kim, H. T., K. P. Kim, et al. (2007). "Certain pairs of ubiquitin-conjugating enzymes (E2s) and ubiquitin-protein ligases (E3s) synthesize nondegradable forked ubiquitin chains containing all possible isopeptide linkages." J Biol Chem **282**(24): 17375-86.

Kim, K. I., N. V. Giannakopoulos, et al. (2004). "Interferon-inducible ubiquitin E2, Ubc8, is a conjugating enzyme for protein ISGylation." Mol Cell Biol **24**(21): 9592-600.

Kirisako, T., K. Kamei, et al. (2006). "A ubiquitin ligase complex assembles linear polyubiquitin chains." EMBO J **25**(20): 4877-87.

Kolman, C. J., J. Toth, et al. (1992). "Identification of a portable determinant of cell cycle function within the carboxyl-terminal domain of the yeast CDC34 (UBC3) ubiquitin conjugating (E2) enzyme." EMBO J **11**(8): 3081-90.

Komander, D., F. Reyes-Turcu, et al. (2009). "Molecular discrimination of structurally equivalent Lys 63-linked and linear polyubiquitin chains." EMBO Rep **10**(5): 466-73.

Kuo, M. L., W. den Besten, et al. (2004). "N-terminal polyubiquitination and degradation of the Arf tumor suppressor." Genes Dev **18**(15): 1862-74.

Kurz, T., N. Ozlu, et al. (2005). "The conserved protein DCN-1/Dcn1p is required for cullin neddylation in C. elegans and S. cerevisiae." <u>Nature</u> **435**(7046): 1257-61.

Lake, M. W., M. M. Wuebbens, et al. (2001). "Mechanism of ubiquitin activation revealed by the structure of a bacterial MoeB-MoaD complex." <u>Nature</u> **414**(6861): 325-9.

Lam, Y. A., W. Xu, et al. (1997). "Editing of ubiquitin conjugates by an isopeptidase in the 26S proteasome." <u>Nature</u> **385**(6618): 737-40.

Lee, I. and H. Schindelin (2008). "Structural insights into E1-catalyzed ubiquitin activation and transfer to conjugating enzymes." <u>Cell</u> **134**(2): 268-78.

Lehmann, C., T. P. Begley, et al. (2006). "Structure of the Escherichia coli ThiS-ThiF complex, a key component of the sulfur transfer system in thiamin biosynthesis." <u>Biochemistry</u> **45**(1): 11-9.

Li, W., M. H. Bengtson, et al. (2008). "Genome-wide and functional annotation of human E3 ubiquitin ligases identifies MULAN, a mitochondrial E3 that regulates the organelle's dynamics and signaling." <u>PLoS ONE</u> **3**(1): e1487.

Li, W., D. Tu, et al. (2007). "A ubiquitin ligase transfers preformed polyubiquitin chains from a conjugating enzyme to a substrate." <u>Nature</u> **446**(7133): 333-7.

Li, W., D. Tu, et al. (2009). "Mechanistic insights into active site-associated polyubiquitination by the ubiquitin-conjugating enzyme Ube2g2." <u>Proc Natl Acad Sci U S A</u> **106**(10): 3722-7.

Liakopoulos, D., G. Doenges, et al. (1998). "A novel protein modification pathway related to the ubiquitin system." <u>EMBO J</u> **17**(8): 2208-14.

Lois, L. M. and C. D. Lima (2005). "Structures of the SUMO E1 provide mechanistic insights into SUMO activation and E2 recruitment to E1." <u>EMBO J</u> **24**(3): 439-51.

Lorick, K. L., J. P. Jensen, et al. (1999). "RING fingers mediate ubiquitin-conjugating enzyme (E2)-dependent ubiquitination." <u>Proc Natl Acad Sci U S A</u> **96**(20): 11364-9.

Love, K. R., A. Catic, et al. (2007). "Mechanisms, biology and inhibitors of deubiquitinating enzymes." <u>Nat Chem Biol</u> **3**(11): 697-705.

Love, K. R., R. K. Pandya, et al. (2009). "Ubiquitin C-terminal electrophiles are activity-based probes for identification and mechanistic study of ubiquitin conjugating machinery." <u>ACS Chem Biol</u> **4**(4): 275-87.

Lyapina, S., G. Cope, et al. (2001). "Promotion of NEDD-CUL1 conjugate cleavage by COP9 signalosome." <u>Science</u> **292**(5520): 1382-5.

MacBeath, G. (2002). "Protein microarrays and proteomics." <u>Nat Genet</u> **32 Suppl**: 526-32.

Malakhov, M. P., O. A. Malakhova, et al. (2002). "UBP43 (USP18) specifically removes ISG15 from conjugated proteins." <u>J Biol Chem</u> **277**(12): 9976-81.

Matsushita, N., H. Kitao, et al. (2005). "A FancD2-monoubiquitin fusion reveals hidden functions of Fanconi anemia core complex in DNA repair." <u>Mol Cell</u> **19**(6): 841-7.

McKenna, S., T. Moraes, et al. (2003). "An NMR-based model of the ubiquitin-bound human ubiquitin conjugation complex Mms2.Ubc13. The structural basis for lysine 63 chain catalysis." <u>J Biol Chem</u> **278**(15): 13151-8.

Mendoza, H. M., L. N. Shen, et al. (2003). "NEDP1, a highly conserved cysteine protease that deNEDDylates Cullins." <u>J Biol Chem</u> **278**(28): 25637-43.

Misaghi, S., Z. R. Balsara, et al. (2006). "Chlamydia trachomatis-derived deubiquitinating enzymes in mammalian cells during infection." <u>Mol Microbiol</u> **61**(1): 142-50.

Misaghi, S., P. J. Galardy, et al. (2005). "Structure of the ubiquitin hydrolase UCH-L3 complexed with a suicide substrate." <u>J Biol Chem</u> **280**(2): 1512-20.

Miura, T., W. Klaus, et al. (1999). "Characterization of the binding interface between ubiquitin and class I human ubiquitin-conjugating enzyme 2b by multidimensional heteronuclear NMR spectroscopy in solution." <u>J Mol Biol</u> **290**(1): 213-28.

Moraes, T. F., R. A. Edwards, et al. (2001). "Crystal structure of the human ubiquitin conjugating enzyme complex, hMms2-hUbc13." <u>Nat Struct Biol</u> **8**(8): 669-73.

Mukhopadhyay, D. and M. Dasso (2007). "Modification in reverse: the SUMO proteases." <u>Trends Biochem Sci</u> **32**(6): 286-95.

Nakasato, N., K. Ikeda, et al. (2006). "A ubiquitin E3 ligase Efp is up-regulated by interferons and conjugated with ISG15." <u>Biochem Biophys Res Commun</u> **351**(2): 540-6.

Narasimhan, J., M. Wang, et al. (2005). "Crystal structure of the interferon-induced ubiquitin-like protein ISG15." <u>J Biol Chem</u> **280**(29): 27356-65.

Nijman, S. M., M. P. Luna-Vargas, et al. (2005). "A genomic and functional inventory of deubiquitinating enzymes." <u>Cell</u> **123**(5): 773-86.

Nishikawa, H., S. Ooka, et al. (2004). "Mass spectrometric and mutational analyses reveal Lys-6-linked polyubiquitin chains catalyzed by BRCA1-BARD1 ubiquitin ligase." <u>J Biol Chem</u> **279**(6): 3916-24.

Ogunjimi, A. A., D. J. Briant, et al. (2005). "Regulation of Smurf2 ubiquitin ligase activity by anchoring the E2 to the HECT domain." <u>Mol Cell</u> **19**(3): 297-308.

Ogunjimi, A. A., S. Wiesner, et al. "The ubiquitin binding region of the Smurf HECT domain facilitates polyubiquitylation and binding of ubiquitylated substrates." <u>J Biol Chem</u> **285**(9): 6308-15.

Olsen, S. K., A. D. Capili, et al. "Active site remodelling accompanies thioester bond formation in the SUMO E1." <u>Nature</u> **463**(7283): 906-12.

Osaka, F., H. Kawasaki, et al. (1998). "A new NEDD8-ligating system for cullin-4A." <u>Genes Dev</u> **12**(15): 2263-8.

Ovaa, H., B. M. Kessler, et al. (2004). "Activity-based ubiquitin-specific protease (USP) profiling of virus-infected and malignant human cells." <u>Proc Natl Acad Sci U S A</u> **101**(8): 2253-8.

Ozkan, E., H. Yu, et al. (2005). "Mechanistic insight into the allosteric activation of a ubiquitin-conjugating enzyme by RING-type ubiquitin ligases." <u>Proc Natl Acad Sci U S A</u> **102**(52): 18890-5.

Parsons, J. L., P. S. Tait, et al. (2009). "Ubiquitin ligase ARF-BP1/Mule modulates base excision repair." <u>EMBO J</u> **28**(20): 3207-15.

Pearce, M. J., J. Mintseris, et al. (2008). "Ubiquitin-like protein involved in the proteasome pathway of Mycobacterium tuberculosis." <u>Science</u> **322**(5904): 1104-7.

Pelzer, C., I. Kassner, et al. (2007). "UBE1L2, a novel E1 enzyme specific for ubiquitin." <u>J Biol Chem</u> **282**(32): 23010-4.

Peng, J., D. Schwartz, et al. (2003). "A proteomics approach to understanding protein ubiquitination." <u>Nat Biotechnol</u> **21**(8): 921-6.

Petricoin, E. F. and L. A. Liotta (2004). "SELDI-TOF-based serum proteomic pattern diagnostics for early detection of cancer." <u>Curr Opin Biotechnol</u> **15**(1): 24-30.

Petroski, M. D. and R. J. Deshaies (2005). "Function and regulation of cullin-RING ubiquitin ligases." <u>Nat Rev Mol Cell Biol</u> **6**(1): 9-20.

Petroski, M. D. and R. J. Deshaies (2005). "Mechanism of lysine 48-linked ubiquitin-chain synthesis by the cullin-RING ubiquitin-ligase complex SCF-Cdc34." <u>Cell</u> **123**(6): 1107-20.

Pickart, C. M. (2001). "Mechanisms underlying ubiquitination." Annu Rev Biochem **70**: 503-33.

Pickart, C. M. and M. J. Eddins (2004). "Ubiquitin: structures, functions, mechanisms." Biochim Biophys Acta **1695**(1-3): 55-72.

Pickart, C. M. and D. Fushman (2004). "Polyubiquitin chains: polymeric protein signals." Curr Opin Chem Biol **8**(6): 610-6.

Pickart, C. M. and I. A. Rose (1986). "Mechanism of ubiquitin carboxyl-terminal hydrolase. Borohydride and hydroxylamine inactivate in the presence of ubiquitin." J Biol Chem **261**(22): 10210-7.

Pierce, N. W., G. Kleiger, et al. (2009). "Detection of sequential polyubiquitylation on a millisecond timescale." Nature **462**(7273): 615-9.

Pitluk, Z. W., M. McDonough, et al. (1995). "Novel CDC34 (UBC3) ubiquitin-conjugating enzyme mutants obtained by charge-to-alanine scanning mutagenesis." Mol Cell Biol **15**(3): 1210-9.

Ravid, T. and M. Hochstrasser (2007). "Autoregulation of an E2 enzyme by ubiquitin-chain assembly on its catalytic residue." Nat Cell Biol **9**(4): 422-7.

Reverter, D. and C. D. Lima (2005). "Insights into E3 ligase activity revealed by a SUMO-RanGAP1-Ubc9-Nup358 complex." Nature **435**(7042): 687-92.

Riedinger, C., and J.A. Endicott (2009). "All change: protein conformation and the ubiquitination reaction cascade." F1000 Biology Reports **1**(19).

Rodrigo-Brenni, M. C. and D. O. Morgan (2007). "Sequential E2s drive polyubiquitin chain assembly on APC targets." Cell **130**(1): 127-39.

Rolen, U., V. Kobzeva, et al. (2006). "Activity profiling of deubiquitinating enzymes in cervical carcinoma biopsies and cell lines." Mol Carcinog **45**(4): 260-9.

Rudolph, M. J., M. M. Wuebbens, et al. (2001). "Crystal structure of molybdopterin synthase and its evolutionary relationship to ubiquitin activation." Nat Struct Biol **8**(1): 42-6.

Ryabov, Y. and D. Fushman (2006). "Interdomain mobility in di-ubiquitin revealed by NMR." Proteins **63**(4): 787-96.

Rytkonen, A. and D. W. Holden (2007). "Bacterial interference of ubiquitination and deubiquitination." Cell Host Microbe **1**(1): 13-22.

Rytkonen, A., J. Poh, et al. (2007). "SseL, a Salmonella deubiquitinase required for macrophage killing and virulence." Proc Natl Acad Sci U S A **104**(9): 3502-7.

Saeki, Y., T. Kudo, et al. (2009). "Lysine 63-linked polyubiquitin chain may serve as a targeting signal for the 26S proteasome." EMBO J **28**(4): 359-71.

Saha, A. and R. J. Deshaies (2008). "Multimodal activation of the ubiquitin ligase SCF by Nedd8 conjugation." Mol Cell **32**(1): 21-31.

Sampson, D. A., M. Wang, et al. (2001). "The small ubiquitin-like modifier-1 (SUMO-1) consensus sequence mediates Ubc9 binding and is essential for SUMO-1 modification." J Biol Chem **276**(24): 21664-9.

Scheffner, M. and O. Staub (2007). "HECT E3s and human disease." BMC Biochem **8 Suppl 1**: S6.

Schlieker, C., G. A. Korbel, et al. (2005). "A deubiquitinating activity is conserved in the large tegument protein of the herpesviridae." J Virol **79**(24): 15582-5.

Schlieker, C., W. A. Weihofen, et al. (2007). "Structure of a herpesvirus-encoded cysteine protease reveals a unique class of deubiquitinating enzymes." Mol Cell **25**(5): 677-87.

Schulman, B. A. and J. W. Harper (2009). "Ubiquitin-like protein activation by E1 enzymes: the apex for downstream signalling pathways." Nat Rev Mol Cell Biol **10**(5): 319-31.

Seol, J. H., R. M. Feldman, et al. (1999). "Cdc53/cullin and the essential Hrt1 RING-H2 subunit of SCF define a ubiquitin ligase module that activates the E2 enzyme Cdc34." <u>Genes Dev</u> **13**(12): 1614-26.

Silver, E. T., T. J. Gwozd, et al. (1992). "A chimeric ubiquitin conjugating enzyme that combines the cell cycle properties of CDC34 (UBC3) and the DNA repair properties of RAD6 (UBC2): implications for the structure, function and evolution of the E2s." <u>EMBO J</u> **11**(8): 3091-8.

Sullivan, M. L. and R. D. Vierstra (1991). "Cloning of a 16-kDa ubiquitin carrier protein from wheat and Arabidopsis thaliana. Identification of functional domains by in vitro mutagenesis." <u>J Biol Chem</u> **266**(35): 23878-85.

Sutter, M., F. F. Damberger, et al. "Prokaryotic ubiquitin-like protein (Pup) is coupled to substrates via the side chain of its C-terminal glutamate." <u>J Am Chem Soc</u> **132**(16): 5610-2.

Tait, S. W., E. de Vries, et al. (2007). "Apoptosis induction by Bid requires unconventional ubiquitination and degradation of its N-terminal fragment." <u>J Cell Biol</u> **179**(7): 1453-66.

Thrower, J. S., L. Hoffman, et al. (2000). "Recognition of the polyubiquitin proteolytic signal." <u>EMBO J</u> **19**(1): 94-102.

Tokunaga, F., S. Sakata, et al. (2009). "Involvement of linear polyubiquitylation of NEMO in NF-kappaB activation." <u>Nat Cell Biol</u> **11**(2): 123-32.

VanDemark, A. P., R. M. Hofmann, et al. (2001). "Molecular insights into polyubiquitin chain assembly: crystal structure of the Mms2/Ubc13 heterodimer." <u>Cell</u> **105**(6): 711-20.

Varshavsky, A. (2005). "Regulated protein degradation." <u>Trends Biochem Sci</u> **30**(6): 283-6.

Verdecia, M. A., C. A. Joazeiro, et al. (2003). "Conformational flexibility underlies ubiquitin ligation mediated by the WWP1 HECT domain E3 ligase." <u>Mol Cell</u> **11**(1): 249-59.

Walden, H., M. S. Podgorski, et al. (2003). "The structure of the APPBP1-UBA3-NEDD8-ATP complex reveals the basis for selective ubiquitin-like protein activation by an E1." <u>Mol Cell</u> **12**(6): 1427-37.

Walsh, C. T. (2006). <u>Posttranslational modification of proteins: expanding nature's inventory</u>. Greenwood Village, Roberts and Company.

Walsh, C. T., S. Garneau-Tsodikova, et al. (2005). "Protein posttranslational modifications: the chemistry of proteome diversifications." <u>Angew Chem Int Ed Engl</u> **44**(45): 7342-72.

Wang, C., J. Xi, et al. (2001). "Solution structure of ThiS and implications for the evolutionary roots of ubiquitin." <u>Nat Struct Biol</u> **8**(1): 47-51.

Wang, M. and C. M. Pickart (2005). "Different HECT domain ubiquitin ligases employ distinct mechanisms of polyubiquitin chain synthesis." <u>EMBO J</u> **24**(24): 4324-33.

Wang, X., R. A. Herr, et al. (2009). "Ube2j2 ubiquitinates hydroxylated amino acids on ER-associated degradation substrates." <u>J Cell Biol</u> **187**(5): 655-68.

Washburn, M. P., D. Wolters, et al. (2001). "Large-scale analysis of the yeast proteome by multidimensional protein identification technology." <u>Nat Biotechnol</u> **19**(3): 242-7.

Wilkinson, K. D. (2009). "DUBs at a glance." <u>J Cell Sci</u> **122**(Pt 14): 2325-9.

Wilkinson, K. D., M. J. Cox, et al. (1986). "Synthesis and characterization of ubiquitin ethyl ester, a new substrate for ubiquitin carboxyl-terminal hydrolase." <u>Biochemistry</u> **25**(21): 6644-9.

Winn, P. J., T. L. Religa, et al. (2004). "Determinants of functionality in the ubiquitin conjugating enzyme family." <u>Structure</u> **12**(9): 1563-74.

Wong, J. J., Y. F. Pung, et al. (2006). "HERC5 is an IFN-induced HECT-type E3 protein ligase that mediates type I IFN-induced ISGylation of protein targets." <u>Proc Natl Acad Sci U S A</u> **103**(28): 10735-40.

Wu, P. Y., M. Hanlon, et al. (2003). "A conserved catalytic residue in the ubiquitin-conjugating enzyme family." <u>EMBO J</u> **22**(19): 5241-50.

Wu-Baer, F., K. Lagrazon, et al. (2003). "The BRCA1/BARD1 heterodimer assembles polyubiquitin chains through an unconventional linkage involving lysine residue K6 of ubiquitin." <u>J Biol Chem</u> **278**(37): 34743-6.

Xu, P., D. M. Duong, et al. (2009). "Quantitative proteomics reveals the function of unconventional ubiquitin chains in proteasomal degradation." <u>Cell</u> **137**(1): 133-45.

Ye, Y. and M. Rape (2009). "Building ubiquitin chains: E2 enzymes at work." <u>Nat Rev Mol Cell Biol</u> **10**(11): 755-64.

Yoon, S. Y., Y. Lee, et al. (2005). "Over-expression of human UREB1 in colorectal cancer: HECT domain of human UREB1 inhibits the activity of tumor suppressor p53 protein." <u>Biochem Biophys Res Commun</u> **326**(1): 7-17.

Yunus, A. A. and C. D. Lima (2006). "Lysine activation and functional analysis of E2-mediated conjugation in the SUMO pathway." <u>Nat Struct Mol Biol</u> **13**(6): 491-9.

Zahreddine, H., H. Zhang, et al. "CRT-1/calreticulin and the E3 ligase EEL-1/HUWE1 control hemidesmosome maturation in C. elegans development." <u>Curr Biol</u> **20**(4): 322-7.

Zhang, M., M. Windheim, et al. (2005). "Chaperoned ubiquitylation--crystal structures of the CHIP U box E3 ubiquitin ligase and a CHIP-Ubc13-Uev1a complex." <u>Mol Cell</u> **20**(4): 525-38.

Zhao, C., S. L. Beaudenon, et al. (2004). "The UbcH8 ubiquitin E2 enzyme is also the E2 enzyme for ISG15, an IFN-alpha/beta-induced ubiquitin-like protein." <u>Proc Natl Acad Sci U S A</u> **101**(20): 7578-82.

Zhao, X., D. A. D, et al. (2009). "The N-Myc-DLL3 cascade is suppressed by the ubiquitin ligase Huwe1 to inhibit proliferation and promote neurogenesis in the developing brain." <u>Dev Cell</u> **17**(2): 210-21.

Zhao, X., J. I. Heng, et al. (2008). "The HECT-domain ubiquitin ligase Huwe1 controls neural differentiation and proliferation by destabilizing the N-Myc oncoprotein." <u>Nat Cell Biol</u> **10**(6): 643-53.

Zheng, N., P. Wang, et al. (2000). "Structure of a c-Cbl-UbcH7 complex: RING domain function in ubiquitin-protein ligases." <u>Cell</u> **102**(4): 533-9.

Zhong, Q., W. Gao, et al. (2005). "Mule/ARF-BP1, a BH3-only E3 ubiquitin ligase, catalyzes the polyubiquitination of Mcl-1 and regulates apoptosis." <u>Cell</u> **121**(7): 1085-95.

Zhou, H., D. M. Monack, et al. (2005). "Yersinia virulence factor YopJ acts as a deubiquitinase to inhibit NF-kappa B activation." <u>J Exp Med</u> **202**(10): 1327-32.

Zhu, H., M. Bilgin, et al. (2003). "Proteomics." <u>Annu Rev Biochem</u> **72**: 783-812.

Zou, W. and D. E. Zhang (2006). "The interferon-inducible ubiquitin-protein isopeptide ligase (E3) EFP also functions as an ISG15 E3 ligase." <u>J Biol Chem</u> **281**(7): 3989-94.

CHAPTER 2: UBIQUITIN C-TERMINAL ELECTROPHILES ARE ACTIVITY-BASED PROBES FOR IDENTIFICATION AND MECHANISTIC STUDY OF UBIQUITIN CONJUGATING MACHINERY

Abstract

Protein modification by ubiquitin (Ub) and ubiquitin-like modifiers (Ubl) requires the action of activating (E1), conjugating (E2), and ligating (E3) enzymes and is a key step in the specific destruction of proteins. Deubiquitinating enzymes (DUBs) deconjugate substrates modified with Ub/Ubls and recycle Ub inside the cell. Genome mining based on sequence homology to proteins with known function has assigned many enzymes to this pathway without confirmation of either conjugating or DUB activity. Function-dependent methodologies are still the most useful for rapid identification or assessment of biological activity of expressed proteins from cells. Activity-based protein profiling (ABPP) uses chemical probes that are active-site directed for the classification of protein activities in complex mixtures. Here we show that the design and use of an expanded set of Ub-based electrophilic probes allowed us to recover and identify members of each enzyme class in the ubiquitin-proteasome system, including E3 ligases and DUBs with previously unverified activity. We show that epitope-tagged Ub-electrophilic probes can be used as activity-based probes for E3 ligase identification by *in vitro* labeling and activity studies of purified enzymes identified from complex mixtures in cell lysate. Furthermore, the reactivity of our probe with the HECT domain of the E3 Ub ligase ARF-BP1 suggests that multiple cysteines may be in the vicinity of the E2-binding site and are capable of the transfer of Ub to self or to a substrate protein.

Introduction

The addition of ubiquitin (Ub), a 76 amino acid polypeptide, or a ubiquitin-like modifier (Ubl) to proteins via a primary amino group serves to modulate protein function in a variety of ways. Mono- and multi-ubiquitination play a critical role in transcriptional activation(*1*), as well as receptor internalization and trafficking(*2-4*), while poly-ubiquitination typically leads to protein degradation by the proteasome and is therefore important for regulation of many cellular functions(*5*). Dysregulation of Ub/Ubl substrate modification has been implicated in a growing number of human diseases, including cancer(*6, 7*) and neurodegenerative disorders(*8-11*).

Ub/Ubls are installed on substrate proteins in a complex cascade involving Ub/Ubl-activating enzymes (E1 enzymes), Ub/Ubl-conjugating enzymes (E2 enzymes), and Ub/Ubl-ligating enzymes (E3 enzymes)(*12, 13*). E1 enzymes activate the C-terminus of Ub/Ubl for nucleophilic attack via ATP-dependent thioester formation with an active site cysteine. This activated Ub/Ubl intermediate is then transferred from E1 to E2 as a thioester and is finally installed on a recipient lysine by an E3 ligase, which contains a substrate binding region and ultimately confers specificity. The action of the ligation machinery is balanced by the activity of deubiquinating enzymes (DUBs) and Ubl-specific proteases (ULPs) – proteases that remove Ub/Ubl from modified substrates, thereby rescuing proteins from proteasomal degradation(*14, 15*). DUBs/ULPs themselves may be key players in disease pathology, as they are known regulators of the cell cycle machinery and can act as either oncoproteins(*16*) or tumor suppressors(*17, 18*). The identification of members of this pathway is important for understanding substrate specificity, regulation of the Ub-proteasome system, and ultimately for the development of specific inhibitors for possible use in treatment of disease(*19, 20*).

Activity-based protein profiling (ABPP) has proved an essential complement to *in silico* efforts for the identification of DUBs/ULPs(*14*). Novel members of this class of proteases were previously identified by Ub-based active site-directed probes(*21*). The recombinant expression of an epitope-tagged Ub fusion protein allowed the installation of electrophilic groups at the C-terminus via intein-based chemical ligation. Incubation of these first generation probes with cell lysate led to the isolation and identification of 23 known DUBs by MS/MS analysis(*21*). Additionally, an OTU domain-containing protein was isolated on the basis of probe reactivity and was shown to have DUB-like activity *in vitro*. An ABPP-based approach was also used to identify DUBs and ULPs encoded by both viral(*22, 23*) and bacterial genomes(*24, 25*), as well as eukaryotic pathogens like *Plasmodium falciparum*(*26*) and *Toxoplasma gondii*(*27*). This strategy proved essential for the identification of the M48^{USP} – a DUB within the N-terminal 500 residues of the large tegument protein of the herpes simplex virus 1 (HSV1), which bears no homology to any known host DUBs(*28*). UbVME was confirmed to be a mechanism-based suicide inhibitor as it was crystallized covalently bound to the active site cysteine of UCH-L3(*29*) and M48(*28*).

Since earlier campaigns using the C-terminal electrophilic probes identified no more than half of the ~100 proposed mammalian DUBs (*21, 30, 31*), we postulated that incorporation of "warheads" with greater electrophilicity should retrieve a larger number of DUBs. Here we report the synthesis and reactivity of an expanded set of Ub-based chemical probes. Enzymes modified by the probes were isolated from whole cell lysate and identified by tandem mass spectrometry. While several new DUBs were recovered, including two members of the Josephin-domain subfamily (JOS1 and JOS2)(*32*), we were surprised to recover numerous members of the Ub/Ubl conjugating machinery including a gene product containing a HECT

(homologous to E6-AP carboxy terminus) domain, but with no reported ligase activity.

Previously, only recombinantly expressed and purified E1, E2 or E3 enzymes had shown any

reactivity with electrophilic Ub derivatives(*21, 33*). One E3 ligase we identified, ARF-BP1, was

particularly intriguing due to recent interest in one of its target proteins, Mcl-1, as a potential

tumor marker(*34*). Further characterization of the binding interaction between hemagluttinin

(HA)-tagged UbVME and the HECT domain of ARF-BP1 revealed that the probe modified

cysteines present in this domain. Mutagenesis of probe-labeled cysteines indicates that several

residues in the HECT domain may participate in the transfer of Ub to self or substrate proteins,

with, as expected, a dominant role in the reaction for the catalytic cysteine.

Results and Discussion

Synthesis and Characterization of Second Generation HAUb-Electrophilic Probes

Known Ub-based active site-directed probes were synthesized as previously reported

(Figure 1A)(*21*). Three new glycine-based electrophiles were synthesized (see the Supporting

Information available with this article online for schemes of chemical syntheses and compound

characterization) and installed using an intein-based chemical ligation on a recombinantly

expressed HAUb lacking the C-terminal glycine (G76). The product of each ligation reaction

was purified using cation-exchange chromatography and characterized by mass spectrometry

(LC-ESI-MS, see Supporting Information). These second generation glycine derivatives,

including a vinylethoxysulfone (OEtVS), a β-lactone (*35*) and a 2,6-

trifluoromethylbenzyloxymethylketone (TF$_3$BOK) were chosen for increased electrophilicity as

compared to compounds synthesized earlier(*21*), and the likelihood to retain specificity for

cysteine over serine proteases in reactions with complex mixtures of proteins(*36*). All three

HAUb probes should react at the position corresponding to the C-terminal carbonyl group of the G76, as this is the position of conjugation between Ub and peptide substrates. HAUbVME, which is the most reactive first generation probe in retrieval of diverse DUBs, was used as a comparison for probe reactivity.

Profiling and Identification of Enzymes Modified by Newly Synthesized HAUb-Electrophilic Probes in EL-4 and HMLE Cell Lysate

To identify potentially uncharacterized DUBs using an ABPP approach, our new set of probes was used to label whole-cell lysate. The EL-4 mouse thymoma cell line was initially chosen(*21*) since it is known to express a diverse set of DUBs/ULPs(*37*), and was selected for sake of comparison with previous ABPP experiments. For identification of human orthologs of particular DUBs/ULPs reactive with our HAUb electrophilic probes, we chose the immortalized human mammary epithelial cell line (HMLE)(*38*). Cell lysate was incubated with HAUb-derived probes and enzymes modified were visualized by anti-HA immunoblotting (Figure 2). Titrations and time courses were conducted to determine the optimal concentrations of each probe and the optimal time for labeling enzymes present in EL-4 cell lysate (data not shown). Significant enrichment of probe-reactive material was observed by immunoblotting of samples incubated with 0.2 μg of each HAUb electrophile per 30 μg cell lysate for more than 3h. Extended reaction times or increased quantities of probe beyond 0.2 μg per 30 μg cell lysate, however, did not affect the number of distinct polypeptides retrieved. HAUb-derived probes have different activities and specificities using otherwise identical labeling conditions and probe concentrations (Figure 2). Furthermore, the pattern of labeled DUBs/ULPs differs between the two cell types – as expected, EL-4 and HMLE cells contain diverse and differentially expressed

DUBs/ULPs. In all cases, labeling could be blocked by preincubation of lysate with the

alkylating agent N-ethylmaleimide (NEM) (Supplementary Figure 1), consistent with active site

cysteine modification by the HAUb-derived probes. The increased electrophilicity of our newly

synthesized probes did not translate into greater reactivity with proteins in cell lysates – the first

generation HAUbVME probe was still the most broadly reactive (Figure 2). The increased

chemical reactivity of these newly synthesized probes likely means they are also more quickly

hydrolyzed during the labeling reaction, which may explain their seemingly lower reactivity with

cell lysates.

To isolate the proteins modified by each of the HAUb probes, we immunoprecipitated

labeled proteins from either EL-4 or HMLE cell lysate using agarose-conjugated anti-HA

antibody as described(*21*). Precipitated proteins were separated by reducing SDS-PAGE (10%)

and visualized by silver staining (data not shown). Polypeptides were excised from the gel,

trypsinized and analyzed by MS/MS. MS/MS data were subjected to database searches using the

US NCBI expressed sequence tag (EST) databases. Proteins identified were corrected for

nonspecific interactions with the antibody and agarose against untreated, immunoprecipitated

cell lysate using the MScomp program(*39*). 29 DUBs were identified from EL-4 cell extracts

and 23 DUBs and one NEDD8-specific ULP were identified from HMLE cell extracts (see

Supplementary Table 1).

We observed selective reactivity with DUBs for each HAUb-electrophilic probe, with

HAUbVME being the most diversely reactive probe. HAUbTF$_3$BOK was the next most DUB-

reactive probe and showed significant overlap of labeled species with HAUbVME in EL-4

lysate. Ubiquitin C-terminal hydrolases, including UCH-L1, -L3, and -L4 displayed broad

reactivity with all probes in EL-4 lysate, while UCH-L3 and -L5 had similar reactivity in HMLE

extracts. Several DUBs not previously identified using this ABPP approach were recovered: Otubain-domain containing DUB Cezanne 2 (OTUD-7A) and U2afl-rs1, an uncharacterized peptidase C19 family member with putative DUB activity toward polyubiquitinated peptides, were identified in EL-4 cell lysate using HAUbVME and HAUbLac respectively. Otubain-domain containing DUBs OTUD4 (isoform 3) and OTUD5 were identified from HMLE extracts using HAUbVME, as were Josephin domain (JD)-containing DUBs JOS1 and JOS2(*32*). Josephin-type DUBs represent a new class of DUBs to be identified using a chemical biology approach. Finally, the identification of one ULP, SENP8 – a NEDD8 specific protease, in HMLE extracts using HAUbVME was not surprising considering the fact that Ub and NEDD8 contain the same 4 C-terminal residues and share ~60% sequence identity(*40*). Reactivity of HAUbVME toward a different subset of DUBs, as compared to those identified previously, could be attributed to either altered DUB expression particular to this EL-4 cell culture, or to the longer incubation times with probe and increased probe concentrations used here, which allows the retrieval of enzymes that contain more weakly nucleophilic active site cysteines.

Recovery of diverse members of the Ub/Ubl conjugation machinery was also observed (Table 1). Since previous experiments failed to retrieve any such enzymes from cell lysate, this observation was surprising, but not altogether unexpected – most Ub/Ubl conjugating enzymes also contain an active site cysteine that participates in the conjugation of these modifiers to substrate peptides. Ub/Ubl installation on substrate lysines via the E1 to E2 to E3 thioester cascade hinges on reversible interaction of the active site cysteines in these enzymes with the Ub/Ubl C terminus. In fact, the pK_a of the active site cysteine residue of several E2 enzymes is approximately 2 pH units above that of a free cysteine, likely preventing these residues from reacting non-specifically with other thiol-reactive groups in the cell(*41*). The increased potency

of the newly synthesized HAUb probes should encourage labeling of more weakly nucleophilic

cysteine residues; indeed, HAUbTF$_3$BOK was the most reactive probe toward these types of

proteins. Representative members of all three classes of conjugating enzymes, including E1s and

E2s for both Ub and Ubls and both HECT and RING domain E3 Ub ligases, were identified in

EL-4 and HMLE lysate. One protein we recovered, Trip 12, contains both WWE and HECT

domains characteristic of a Ub E3 ligase, but its activity as such had not been verified either *in

vivo* or *in vitro*. We expressed the HECT domain of Trip12 (expressed as a GST fusion to

improve solubility) and confirmed that it has autoubiquitination activity that is E1/E2 dependent

(Supplementary Figure 2)(*42, 43*).

        While active site cysteines capable of being modified by HAUb-electrophilic probes do

exist in most classes of conjugating enzymes, some proteins might be retrieved as part of larger

multi-protein complexes containing only a single probe-reactive species. This may apply in

particular to RING ligases, which do not utilize an active site cysteine, but rather activate

Ub/Ubls using two zinc ions coordinated in the active site by eight conserved cysteine and

histidine residues(*13*). For example, the RING ligases containing CUL-4A and CUL-4B consist

of a multi-subunit complex containing the cullin scaffold with C-terminally associated substrate

binding proteins and an N-terminally associated RING-domain protein, which recruits the E2-

conjugating enzyme to form the active ligase complex(*44*). While the cullin scaffold itself is not

capable of reacting with Ub-based electrophiles, reaction of the E2 protein with probe could lead

to recovery of these associated scaffold proteins in our immunoprecipitations as performed using

non-denaturing conditions. Indeed, this is the case for one example RING E3, UBAC1, which

can be identified in EL-4 lysate by immunoblotting, but unreactive with HAUbVME as indicated

by the presence of a single unmodified species following incubation with probe (Supplementary

Figure 3). UBC9 and other Ubl-conjugating enzymes may be retrieved either due to cross

reactivity with Ub(*45*) under the in vitro labeling conditions, or as part of a complex with its

interacting E1, which in the case of UBC9 was also recovered from EL-4 lysate (Aos1).

HAUb-Electrophilic probes are activity-based probes for E3 Ub ligases

After demonstrating the capability of our panel of probes to identify Ub conjugating machinery,

we were interested in validating the utility of these proteins for mechanistic study of purified

enzymes. The HECT Ub E3 ligase that was recovered with the most diverse panel of

electrophilic probes using both types of cell lysate was the protein ARF-BP1. ARF-BP1 (Mule)

is a 482 kD HECT-domain-containing Ub E3 ligase that has several known substrates: p53(*46*),

Cdc6(*47*), Mcl-1(*48, 49*), N-Myc(*50*), C-Myc(*51*), TopBP1 (*51*), and histones (*52*). ARF-BP1 is

a key player in both p53-dependent and independent functions of the ARF tumor suppressor(*46*)

and regulates DNA damage-induced apoptosis(*47-49*). ARF-BP1 is interesting not only because

its substrates function in multiple pathways, but also because a catalytic mutant of ARF-BP1 in

which the active site cysteine is mutated to alanine (C4341A) or serine (C4341S)(*51*) reduces,

but does not abolish ligase activity. We therefore selected this protein for verification of

reactivity with HAUbVME and confirmation of enzyme activity as an E3 Ub ligase.

To verify that HAUbVME does indeed bind to the active site-cysteine of ARF-BP1, we

incubated HAUbVME for three hours with recombinantly expressed ARF-BP1 HECT domain

(residues 4012-4374). The reaction mixture was separated by reducing 10% SDS-PAGE and

visualized by coomassie stain. We observed multiple species, each corresponding to covalent

modification of ARF-BP1 (Figure 3, panel A) which appear to occur only in the context of

folded HECT domain – modification of ARF-BP1 by HAUbVME following denaturation in 6.4

M urea is nearly abolished. In contrast, incubation of recombinant DUB enzymes with

HAUbVME invariably produces a single modified species (*53*). We identified the nature of the

modified species using MS/MS analysis of polypeptides excised from the gel. Three out of the

six cysteines within the expressed HECT domain were modified by HAUbVME: C4099, C4341,

and C4367 (hereafter called Cys 1, Cys 5, and Cys 6 in reference to their sequential position

from the N terminus of the HECT domain). The modification of Cys 5 was expected, as it was

identified as the likely catalytic residue based on multiple sequence alignment (*54*). We

reasoned that the modification of the other two residues should correlate with the ability of these

cysteines to contribute to product formation. To investigate this possibility, we expressed and

purified ARF-BP1 HECT domain mutants (residues 4012-4374) in which cysteines 1, 5, and 6

were mutated to alanine either singly or in combination. We then tested the activity of these

proteins *in vitro* using one of two assays: autoubiquitination, or ubiquitination of the anti-

apoptotic protein Mcl-1, a substrate of ARF-BP1 (*54*).

  When wild-type ARF-BP1 is incubated for ten minutes at room temperature in the

presence of recombinant E1, the E2 UbcH7, [^{32}P]-Ub, and an ATP-regenerating system, the E3

efficiently catalyzes polyubiquitination of itself (Figure 3, panel B). Following separation of

reaction mixture on 10% SDS-PAGE, ubiquitinated products are quantified using

phosphoimaging (Figure 3, panel D). Mutation of the catalytic cysteine (Cys 5) to alanine

greatly reduces activity but does not abolish it; the mutant forms 8.2% of wild-type product after

a 10 minute reaction. Mutation of Cys 6 reduces product formation in the autoubiquitination

assay to 56.27% of the wild type level. Finally, the mutation of Cys 1 alone does not affect

activity. The mutation of Cys 1 in combination with either Cys 5 or Cys 6 does dramatically

alter autoubiquitination activity: in combination with a Cys 6 mutation, activity is restored; in the

context of a Cys 5 mutation, ARF-BP1 fails to ubiquitinate itself. Finally, mutation of all three

probe-labeled cysteines (1, 5, and 6) abolishes all activity.

Although we cannot exclude that these cysteine mutations affect binding to Ub or

UbcH7, these results suggest that mutation of probe-labeled cysteines affects activity of the

ARF-BP1 HECT domain. We next asked whether this holds true for ARF-BP1-catalyzed

ubiquitination of its substrate protein Mcl-1. In this case, ARF-BP1 is incubated with

recombinant E1, the E2 UbcH7, Ub, an ATP-regenerating system, and [^{32}P]-Mcl-1 for one hour

at 37ºC as described(*48*). Reaction mixtures are separated on SDS-PAGE and quantified as

described above. Wild-type ARF-BP1 catalyzes multi-ubiquitination of Mcl-1 as reported

(Figure 1, panel C). We observed that the cysteine-to-alanine mutants of ARF-BP1 show a

similar pattern of reduced activity as seen in the autoubiquitination assay; however, the relative

contributions of cysteines 5 and 6 toward total activity differ in this assay as compared to the

autoubiquitination assay. As in the autoubiquitination assay, mutation of Cys 1 has no effect on

activity toward Mcl-1.   More significantly, mutation of either Cys 5 or Cys 6 reduces activity to

a similar extent (30% and 40.7%, respectively) after a 1 h incubation, suggesting that both of

these residues participate in ubiquitination of Mcl-1. The pattern of activity of the double

mutants in the autoubiquitination assay resembles the pattern for substrate activity: the 1,6

mutant resembles wild-type ARF-BP1, whereas the 1,5 mutant is inactive. Again, the triple

mutant lacking cysteines 1, 5, and 6 shows no activity.

Multiple Cysteines in ARF-BP1 form Thioesters with Ub

The mechanism of catalysis by HECT E3 ligases involves several steps. The E3 enzyme

binds Ub-loaded E2, followed by Ub transfer from the E2 catalytic cysteine to the E3 catalytic

cysteine. The E3 then catalyzes isopeptide bond formation between Ub and a recipient lysine

residue on substrate, which may be the E3 itself, Ub, or another protein. A crucial determinant

in isopeptide bond formation is the presence of a conserved phenylalanine located four amino

acids from the C terminus of most HECT E3s (*55*). Truncations which remove this residue

abolish Ub transfer to substrate, trapping the E3 with the catalytic cysteine in a thioester linkage

to Ub (*55*). We reasoned that if more than one cysteine is capable of receiving Ub from the

associated E2, we should be able to detect the presence of multiple Ub-thioesters in an ARF-BP1

HECT domain truncation mutant (ARF-BP1 Δ4) lacking the conserved phenylalanine.

We therefore expressed and purified two versions of the ARF-BP1 HECT domain lacking

the terminal four amino acids: wild-type (WTΔ4) and a Cys5 to Ala mutant (C5AΔ4) and

assayed these mutants, along with the full-length ARF-BP1 HECT domain (WT FL) for Ub

thioester formation. In this assay, ARF-BP1 is incubated with recombinant E1, the E2 UbcH7,

Ub, and an ATP regenerating system for 10 minutes at room temperature. The reaction is

quenched by urea denaturation followed by addition of SDS-PAGE loading buffer with or

without β-mercaptoethanol, separated on 10% SDS-PAGE, and analyzed by anti-Ub

immunoblot. Under these conditions, WT FL ARF-BP1 efficiently catalyzes autoubiquitination

(Figure 4, panel A). In contrast, WTΔ4 ARF-BP1 forms a mono-ubiquitylated species when the

reaction is quenched with reducing sample buffer, indicating that the activity of this protein is

compromised by the truncation. The ability of the WTΔ4 ARF-BP1 to form a

monoubiquitylated species depends on Cys 5 (Figure 4). Interestingly, quenching the reaction

with non-reducing sample buffer preserves multiple Ub-thioesters on WTΔ4 ARF-BP1. We

detect the persistence of a single Ub-thioester in the C5AΔ4 ARF-BP1 mutant, which is likely

due to Ub binding to a cysteine in the HECT domain. The apparent thioester formation

catalyzed by both WTΔ4 and C5AΔ4 ARF-BP1 is E1/E2 dependent (Figure 4, panel B). These results indicate that at least two cysteines in ARF-BP1 simultaneously can form Ub-thioesters and that one of these cysteines is Cys 5.

We predicted that the Δ4 truncation would abolish the ability of ARF-BP1 to ubiquitinate Mcl-1, and indeed we find this to be the case (Figure 4, panel C). WTΔ4 ARF-BP1 catalyzes monoubiquitylation of Mcl-1 in a manner dependent on Cys 5 and the presence of E1 and E2 enzymes (Figure 4, panel D). As this small amount of ligase activity persists after complete denaturation of samples in 4 M urea, it must correspond to covalent lysine modification.

Given that our probes were designed to act as electrophiles capable of reaction with local nucleophiles following specific binding by Ub-reactive proteins, it is likely that the probe's reactivity with cysteines other than the catalytic residue means that these residues are close in proximity to the electrophilic warhead within the tertiary structure of the ARF-BP1 HECT domain. We proceeded to construct a threaded structure based on the structures available for the HECT domains of WWP1 (*56*) and SMURF2 (*57*), the HECT domains with highest homology to ARF-BP1 (> 40% identity, data not shown). In our threaded structure, Cys 6 appears to be equidistant to Cys 5 in proximity to the E2 binding site and all three reactive cysteines are along a single face of the domain. We next ask if these three residues from the human ARF-BP1 sequence are conserved across eukaryotes (Figure 5). As expected, Cys 5 is conserved across all species examined, and Cys 6 is conserved within the animal kingdom. Cys 1, the most weakly reactive residue toward our Ub-based electrophiles, is conserved only through bony fishes (Danio rerio), but is also observed in Hydra. Altogether, these data link the ability of our probes to identify residues with the potential to react with Ub, either due to catalytic activity or proximity.

Conclusions

The ubiquitin-proteasome system is critical for the regulation of protein function in eukaryotes. Here we extend an earlier effort to allow the isolation and identification of members of all enzyme classes that comprise the ubiquitin-proteasome system. While we continue to find novel enzymes of the DUB family, we have also demonstrated the utility of Ub-based electrophiles as activity-based probes for certain HECT domain E3 ligases. In studying the covalent modification of the HECT domain of E3 ligase ARF-BP1 with HAUbVME, we observed that the probe covalently labels three out of the six cysteines found in the ARF-BP1 HECT domain (C4099 (Cys 1), C4341 (the canonical catalytic residue, Cys 5), and C4367 (Cys 6)). We provide evidence for the formation of multiple thioester-linked Ub molecules during catalysis by wild-type ARF-BP1 HECT domain, supporting the notion that the HAUbVME probe is capable of identifying residues that are competent nucleophiles for Ub tranfer. We are eager to see our hypotheses about the positioning of nucleophilic residues in the ARF-BP1 HECT domain confirmed with structural data. The utility of Ub electrophilic probes as mechanism-based chemical tools to study E3 ligase structure and function will likely provide further insights into the mechanism employed by ARF-BP1 and other HECT E3 Ub ligases.

Methods

Synthesis and Purification of HAUb-electrophilic Probes

Electrophilic glycine analogs 4-amino but-1-enyl ethoxysulfonate, serine-β-lactone, and 2,6-trifluoromethylbenzyloxy glycine methyl ketone were synthesized according to literature procedures (*58-60*) (see Supporting Information for synthesis details and compound characterization). HAUb$_{75}$-MESNa (500 μL, ~10-15 mg/mL), synthesized as previously reported(*21*) from an Ub-intein-chitin domain fusion protein, was treated with 1 mM N-hydroxysuccinimide, immediately followed by 0.5 mM of the desired electrophilic glycine analog in 1.1 mL (total volume) of a 1 M NaHCO$_3$ (pH 8.0) solution. These conjugation reactions were incubated overnight at 37°C. The resulting products were dialyzed and purified as previously reported(*21*). Each purified HAUb-electrophilic probe was characterized by LC/MS using a Michrom Paradigm MS4 HPLC equipped with a Waters Symmetry C8 2.1 mm X 50 mm column using standard reverse-phase gradients. The effluent from the column was mass analyzed using a Waters LCT Electrospray Time-OF-Flight Mass Spectrometer (see Supporting Information for MS characterization).

Preparation of EL-4 and HMLE Cell Lysate and Labeling with HAUb-electrophilic Probes

EL-4 cells (cultured in DMEM supplemented with 10% IFS and 1% penicillin/streptomycin at 37°C with 5% CO$_2$) were harvested, washed once with culture media and once with PBS. Cell pellets were lysed with glass beads as previously reported(*21*). 30 μg of protein extract was incubated with 0.2 μg of each HAUb-electrophilic probe (2 μM, 10 μL total volume per sample) for 5 h at room temperature. After terminating the reactions with reducing SDS-PAGE sample

buffer and boiling 10 min, reaction mixtures were separated by SDS-PAGE (10%) and analyzed

by immunoblotting with anti-HA antibody (3F10, Roche).

The immortalized, nontransformed HMLE line, expressing the SV40 large-T oncogene, and

hTERT, was cultured as previously described(*38*) using a 2:1:1 mixture of mammary epithelial

growth medium (MEGM, Clonetics), DMEM, and F12 medium supplemented with EGF (10

ng/ml), insulin (10 µg/ml), and hydrocortisone (1 µg/ml). Cells were harvested at a confluence

of 90% and washed once with PBS. Cell pellets were lysed with glass beads as previously

reported(*21*). 7.5 mg of cell lysate were incubated with 1 µg of each HAUb-electrophilic probe

(0.2 µM) 5 h at room temperature. A sample of labeled proteins (30 µg protein extract) were

separated by SDS-PAGE (8%) and analyzed by immunoblotting with anti-HA antibody (3F10,

Roche).

Anti-HA Immunoprecipitation of Labeled Proteins and Identification by Tandem Mass

Spectrometry

EL-4 and HMLE lysate were prepared as above. 7 mg EL-4 protein extract or 7.5 mg HMLE

protein extract were incubated with 1 µg (0.2 µM) of each HAUb-electrophilic probe for 5 h at

room temperature in 50 mM Tris (pH 8.0), 150 mM NaCl. Anti-HA agarose (3F10 antibody,

Roche) was incubated with the samples overnight at 4°C. The immunoprecipitations were

washed extensively with NET buffer (50 mM Tris [pH 7.5], 150 mM NaCl, 5 mM EDTA, 0.5%

NP40) and the bound proteins were eluted by boiling for 10 min with reducing SDS-PAGE

sample buffer, separated by SDS-PAGE (10%), and visualized by silver stain using standard

conditions. Bands were excised, reduced, alkylated and digested with trypsin at 37°C overnight.

The resulting peptides were extracted, concentrated and injected onto a Waters NanoAcquity HPLC equipped with a self-packed Jupiter 3 μm C18 analytical column (0.075 mm by 10 cm, Phenomenex). Peptides were eluted using standard reverse-phase gradients. The effluent from the column was analyzed using a Thermo LQT linear ion trap mass spectrometer (nanospray configuration) operated in a data dependent manner. The resulting fragmentation spectra were correlated against the known database using SEQUEST. Bioworks browser was used to provide consensus reports of the proteins identified.

ARF-BP1 Labeling with HAUbVME

Recombinantly expressed and purified ARF-BP1 HECT domain (5 μg) was incubated with HAUbVME (2.0 μM) in 50 mM Tris, 150 mM NaCl, pH 8.0 for 3h at room temperature. The specificity of probe labeling was tested by first denaturing the ARF-BP1 HECT domain with 6.4 M urea (30 min incubation at 30°C) and then diluting the sample to 0.6 M urea before the addition of HAUbVME (2.0 μM). Activity of HAUbVME was tested with ARF-BP1 in 50 mM Tris, 150 mM NaCl, pH 8.0 containing 0.6 M urea to ensure that probe reactivity was not compromised in dilute concentrations of urea. All of the above labeling reactions were quenched by addition of reducing sample buffer, boiled for 10 min and separated by SDS-PAGE (10%). Labeled and unlabeled species were visualized by coomassie staining and bands were excised and treated as above for MS/MS analysis. Modified cysteine residues were identified by the presence of the mass change corresponding to the C-terminus of the VME probe (= 172.08 Da).

ARF-BP1 Autoubiquitination and Substrate Ubiquitination Assays with Wild-type and Mutant HECT Domain proteins

Autoubiquitination activity was tested in a 20 µL reaction by incubating ARF-BP1 HECT

domain (10 µg) with 100 ng human E1 (Ube1, Boston Biochem), 1 µg UbcH7, and 10 µg [^{32}P]-

Ub (see Supporting Information for plasmid construction, protein expression and purification

conditions, and [^{32}P]-labeling) with an ATP regenerating system (50 mM Tris [pH 7.6], 5 mM

MgCl$_2$, 5 mM ATP, 10 mM creatine phosphate, 3.5 U/mL creatine kinase) for 10 min at room

temperature. Substrate ubiquitination activity was tested by adding 1 µg [^{32}P]-Mcl-1 (see

Supporting Information for plasmid construction, protein expression and purification conditions,

and [^{32}P]-labeling) to the above reaction containing 100 µg non-radiolabeled Ub and incubating

the mixture for 1 h at 37°C. A control reaction was run without ARF-BP1 HECT domain, but

containing all other reaction components for each case. After terminating the reactions with

reducing SDS-PAGE sample buffer and boiling 10 min, reaction mixtures were separated by

SDS-PAGE (10%) and analyzed by phosphorimaging. Product formation by ARF-BP1 HECT

domain mutants was calculated as a percentage of total (background corrected) [^{32}P] counts

attributable to ubiquitinated product in the wild type HECT domain. The average and standard

deviation of 9 experiments is shown.

Ub-thioester assays

To test ARF-BP1 thioester formation, reaction mixtures (10 µL) were set up in duplicate

containing 100 ng human E1 (Ube1, Boston Biochem), 1 µg UbcH7, 10 µg ARF-BP1 Δ4 HECT

domain, 10 µg Ub, 50 µM DTT, and an ATP regenerating system, and incubated for 10 min at

room temperature. Reactions were terminated with 10 µL 8M urea and incubated 15 min at

30°C. One set of samples received reducing SDS-PAGE sample buffer, the other set received

non-reducing SDS-PAGE sample buffer, and were then boiled 10 min, separated on 10% SDS-

PAGE, and analyzed by immunoblotting with anti-Ub antibody (Sigma). To test the activity of

the ARF-BP1 Δ4 proteins against substrate, reactions were set up as above except with 100 μg

Ub and 1 μg Flag-Mcl-1 and were incubated 1 hr at 37°C. Reactions were terminated as above,

separated on 10% SDS-PAGE, and analyzed by immunoblotting with anti-Flag antibody

(Sigma).

Acknowledgements

References

1.   Hicke, L. (2001) Protein regulation by monoubiquitin. Nat. Rev. Mol. Cell Biol. 2, 195-201.

2.   Hicke, L., Schnell, J., and Stamenova, S. (2005) Regulation of receptor endocytosis by monoubiquitin signals. FASEB J. 19, A1689-A1689.

3.   Hicke, L., and Dunn, R. (2003) Regulation of membrane protein transport by ubiquitin and ubiquitin-binding proteins. Ann.Rev. Cell Dev. Biol. 19, 141-172.

4.   Haglund, K., Di Fiore, P. P., and Dikic, I. (2003) Distinct monoubiquitin signals in receptor endocytosis. Trends Biochem. Sci. 28, 598-603.

5.   Pickart, C. M., and Eddins, M. J. (2004) Ubiquitin: Structures, functions, mechanisms. Biochem. Biophys. Acta (BBA) - Mol. Cell Res. 1695, 55-72.

6.   Newton, K., and Vucic, D. (2007) Ubiquitin ligases in cancer: Ushers for degradation. Cancer Invest. 25, 502 - 513.

7.   Ohta, T., and Fukuda, M. (2004) Ubiquitin and breast cancer. Oncogene 23, 2079-2088.

8.   Cooper, E. M., Hudson, A. W., Amos, J., Wagstaff, J., and Howley, P. M. (2004) Biochemical analysis of angelman syndrome-associated mutations in the e3 ubiquitin ligase e6-associated protein. J. Biol. Chem. 279, 41208-41217.

9.   Davies, J., Sarkar, S., and Rubinsztein, D. (2007) The ubiquitin proteasome system in huntington's disease and the spinocerebellar ataxias. BMC Biochemistry 8, S2.

10.   Upadhya, S., and Hegde, A. (2007) Role of the ubiquitin proteasome system in alzheimer's disease. BMC Biochemistry 8, S12.

11.   Lim, K.-L., and Tan, J. (2007) Role of the ubiquitin proteasome system in parkinson's disease. BMC Biochemistry 8, S13.

12.   Kerscher, O., Felberbaum, R., and Hochstrasser, M. (2006) Modification of proteins by ubiquitin and ubiquitin-like proteins. Ann.Rev. Cell Dev. Biol. 22, 159-180.

13.   Dye, B. T., and Schulman, B. A. (2007) Structural mechanisms underlying posttranslational modification by ubiquitin-like proteins. Ann. Rev. Biophys. Biomol. Struct. 36, 131-150.

14.   Love, K. R., Catic, A., Schlieker, C., and Ploegh, H. L. (2007) Mechanisms, biology and inhibitors of deubiquitinating enzymes. Nat. Chem. Biol. 3, 697-705.

15.   Amerik, A. Y., and Hochstrasser, M. (2004) Mechanism and function of deubiquitinating enzymes. Biochem. Biophys. Acta (BBA) - Mol. Cell Res. 1695, 189-207.

16.   Jensen, D. E., and Rauscher, F. J. (1999) Defining biochemical functions for the brca1 tumor suppressor protein: Analysis of the brca1 binding protein bap1. Cancer Lett. 143, S13-S17.

17.   Brooks, C. L., and Gu, W. (2006) P53 ubiquitination: Mdm2 and beyond. Mol. Cell 21, 307-315.

18.   Trompouki, E., Hatzivassiliou, E., Tsichritzis, T., Farmer, H., Ashworth, A., and Mosialos, G. (2003) Cyld is a deubiquitinating enzyme that negatively regulates nf-kappa b activation by tnfr family members. Nature 424, 793-796.

19.   Ciechanover, A., and Schwartz, A. L. (2004) The ubiquitin system: Pathogenesis of human diseases and drug targeting. Biochem. Biophys. Acta (BBA) - Mol. Cell Res. 1695, 3.

20.   Nicholson, B., Marblestone, J. G., Butt, T. R., and Mattern, M. R. (2007) Deubiquitinating enzymes as novel anticancer targets. Fut. Oncol. 3, 191-199.

21.   Borodovsky, A., Ovaa, H., Kolli, N., Gan-Erdene, T., Wilkinson, K. D., Ploegh, H. L., and Kessler, B. M. (2002) Chemistry-based functional proteomics reveals novel members of the deubiquitinating enzyme family. Chem. Biol. 9, 1149-1159.

22.   Kattenhorn, L. M., Korbel, G. A., Kessler, B. M., Spooner, E., and Ploegh, H. L. (2005) A deubiquitinating enzyme encoded by hsv-1 belongs to a family of cysteine proteases that is conserved across the family herpesviridae. Mol. Cell 19, 547-557.

23.   Schlieker, C., Korbel, G. A., Kattenhorn, L. M., and Ploegh, H. L. (2005) A deubiquitinating activity is conserved in the large tegument protein of the herpesviridae. J. Virol. 79, 15582-15585.

24.   Misaghi, S., Balsara, Z. R., Catic, A., Spooner, E., Ploegh, H. L., and Starnbach, M. N. (2006) Chlamydia trachomatis-derived deubiquitinating enzymes in mammalian cells during infection. Mol. Microbiol. 61, 142-150.

25.   Catic, A., Misaghi, S., Korbel, G. A., and Ploegh, H. L. (2007) Elad, a deubiquitinating protease expressed by e. Coli. PLoS One 2, e381.

26.   Artavanis-Tsakonas, K., Misaghi, S., Comeaux, C. A., Catic, A., Spooner, E., Duraisingh, M. T., and Ploegh, H. L. (2006) Identification by functional proteomics of a deubiquitinating/deneddylating enzyme in plasmodium falciparum. Mol. Microbiol. 61, 1187-1195.

27.   Frickel, E.-M., Quesada, V., Muething, L., Gubbels, M.-J., Spooner, E., Ploegh, H., and Artavanis-Tsakonas, K. (2007) Apicomplexan uchl3 retains dual specificity for ubiquitin and nedd8 throughout evolution. Cell. Microbiol. 9, 1601-1610.

28.   Schlieker, C., Weihofen, W. A., Frijns, E., Kattenhorn, L. M., Gaudet, R., and Ploegh, H. L. (2007) Structure of a herpesvirus-encoded cysteine protease reveals a unique class of deubiquitinating enzymes. Mol. Cell 25, 677-687.

29.   Misaghi, S., Galardy, P. J., Meester, W. J. N., Ovaa, H., Ploegh, H. L., and Gaudet, R. (2005) Structure of the ubiquitin hydrolase uch-l3 complexed with a suicide substrate. J. Biol. Chem. 280, 1512-1520.

30.   Ovaa, H., Kessler, B. M., Rolen, U., Galardy, P. J., Ploegh, H. L., and Masucci, M. G. (2004) Activity-based ubiquitin-specific protease (usp) profiling of virus-infected and malignant human cells. Proc. Natl. Acad. Sci. U. S. A. 101, 2253-2258.

31.   Gredmark, S., Schlieker, C., Quesada, V., Spooner, E., and Ploegh, H. L. (2007) A functional ubiquitin-specific protease embedded in the large tegument protein (orf64) of murine gammaherpesvirus 68 is active during the course of infection. J. Virol. 81, 10300-10309.

32.   Tzvetkov, N., and Breuer, P. (2007) Josephin domain-containing proteins from a variety of species are active de-ubiquitination enzymes. Biol. Chem. 388, 973-978.

33.   Hemelaar, J., Borodovsky, A., Kessler, B. M., Reverter, D., Cook, J., Kolli, N., Gan-Erdene, T., Wilkinson, K. D., Gill, G., Lima, C. D., Ploegh, H. L., and Ovaa, H. (2004) Specific and covalent targeting of conjugating and deconjugating enzymes of ubiquitin-like proteins. Mol. Cell. Biol. 24, 84-95.

34.   Thomadaki, H., and Scorilas, A. (2006) Bcl2 family of apoptosis-related genes: Functions and clinical implications in cancer. Crit. Rev. Clin. Lab. Sci. 43, 1-67.

35.   Powers, J. C., Asgian, J. L., Ekici, O. D., and James, K. E. (2002) Irreversible inhibitors of serine, cysteine, and threonine proteases. Chem. Rev. 102, 4639-4750.

36.   Borodovsky, A., Kessler, B. M., Casagrande, R., Overkleeft, H. S., Wilkinson, K. D., and Ploegh, H. L. (2001) A novel active site-directed probe specific for deubiquitylating enzymes reveals proteasome association of usp14. EMBO J. 20, 5187-5196.

37.   Elenbaas, B., Spirio, L., Koerner, F., Fleming, M. D., Zimonjic, D. B., Donaher, J. L., Popescu, N. C., Hahn, W. C., and Weinberg, R. A. (2001) Human breast cancer cells generated by oncogenic transformation of primary mammary epithelial cells. Genes Dev. 15, 50-65.

(38.   The MScomp is a custom script written in visual basic for the comparison of protein sequences identified in tandem mass spectrometry.

39.   Whitby, F. G., Xia, G., Pickart, C. M., and Hill, C. P. (1998) Crystal structure of the human ubiquitin-like protein nedd8 and interactions with ubiquitin pathway enzymes. J. Biol. Chem. 273, 34983-34991.

40.   Tolbert, B. S., Tajc, S. G., Webb, H., Snyder, J., Nielsen, J. E., Miller, B. L., and Basavappa, R. (2005) The active site cysteine of ubiquitin-conjugating enzymes has a significantly elevated pk(a): Functional implications. Biochemistry 44, 16385-16391.

41.   Park, Y., Yoon, S. K., and Yoon, J. B. (2008) Trip12 functions as an e3 ubiquitin ligase of app-bp1. Biochem. Biophys. Res. Comm. 374, 294-298.

42.   Park, Y., Yoon, S. K., and Yoon, J. B. (2009) The hect domain of trip12 ubiquitinates substrates of the ubiquitin fusion degradation pathway. J. Biol. Chem. 284, 1540-1549.

43.   Petroski, M. D., and Deshaies, R. J. (2005) Function and regulation of cullin-ring ubiquitin ligases. Nat. Rev. Mol. Cell Biol. 6, 9-20.

44.   Huang, D. T., Zhuang, M., Ayrault, O., and Schulman, B. A. (2008) Identification of conjugation specificity determinants unmasks vestigial preference for ubiquitin within the nedd8 e2. Nature Structural & Molecular Biology 15, 280-287.

45.   Chen, D. L., Kon, N., Li, M. Y., Zhang, W. Z., Qin, J., and Gu, W. (2005) Arf-bp1/mule is a critical mediator of the arf tumor suppressor. Cell 121, 1071-1083.

46.   Hall, J. R., Kow, E., Nevis, K. R., Lu, C. K., Luce, K. S., Zhong, Q., and Cook, J. G. (2007) Cdc6 stability is regulated by the huwe1 ubiquitin ligase after DNA damage. Mol. Biol. Cell 18, 3340-3350.

47.   Zhong, Q., Gao, W. H., Du, F. H., and Wang, X. D. (2005) Mule/arf-bp1, a bh3-only e3 ubiquitin ligase, catalyzes the polyubiquitination of mcl-1 and regulates apoptosis. Cell 121, 1085-1095.

48.   Warr, M. R., Acoca, S., Liu, Z. Q., Germain, M., Watson, M., Blanchette, M., Wing, S. S., and Shore, G. C. (2005) Bh3-ligand regulates access of mcl-1 to its e3 ligase. FEBS Lett. 579, 5603-5608.

49.   Zhao, X. D., Heng, J. I. T., Guardavaccaro, D., Jiang, R., Pagano, M., Guillemot, F., Iavarone, A., and Lasorella, A. (2008) The hect-domain ubiquitin ligase huwe1 controls neural differentiation and proliferation by destabilizing the n-myc oncoprotein. Nat. Cell Biol. 10, 643-653.

50.   Adhikary, S., Marinoni, F., Hock, A., Hulleman, E., Popov, N., Beier, R., Bernard, S., Quarto, M., Capra, M., Goettig, S., Kogel, U., Scheffner, M., Helin, K., and Eilers, M. (2005) The ubiquitin ligase hecth9 regulates transcriptional activation by myc and is essential for tumor cell proliferation. Cell 123, 409-421.

51.   Herold, S., Hock, A., Herkert, B., Berns, K., Mullenders, J., Beijersbergen, R., Bernards, R., and Eilers, M. (2008) Miz1 and hecth9 regulate the stability of the checkpoint protein, topbp1. EMBO J. 27, 2851-2861.

52.   Liu, Z. Q., Oughtred, R., and Wing, S. S. (2005) Characterization of e3(histone), a novel testis ubiquitin protein ligase which ubiquitinates histones. Mol. Cell. Biol. 25, 2819-2831.

53.   Schlieker, C., Korbel, G. A., Kattenhorn, L. M., and Ploegh, H. L. (2005) A deubiquitinating activity is conserved in the large tegument protein of the herpesviridae. J Virol 79, 15582-15585.

54.   Zhong, Q., Gao, W., Du, F., and Wang, X. (2005) Mule/arf-bp1, a bh3-only e3 ubiquitin ligase, catalyzes the polyubiquitination of mcl-1 and regulates apoptosis. Cell 121, 1085-1095.

55.   Salvat, C., Wang, G., Dastur, A., Lyon, N., and Huibregtse, J. M. (2004) The -4 phenylalanine is required for substrate ubiquitination catalyzed by hect ubiquitin ligases. J Biol Chem 279, 18935-18943.

56.   Verdecia, M. A., Joazeiro, C. A. P., Wells, N. J., Ferrer, J. L., Bowman, M. E., Hunter, T., and Noel, J. P. (2003) Conformational flexibility underlies ubiquitin ligation mediated by the wwp1hect domain e3 ligase. Mol. Cell 11, 249-259.

57.   Ogunjimi, A. A., Briant, D. J., Pece-Barbara, N., Le Roy, C., Di Guglielmo, G. M., Kavsak, P., Rasmussen, R. K., Seet, B. T., Sicheri, F., and Wrana, J. L. (2005) Regulation of smurf2 ubiquitin ligase activity by anchoring the e2 to the hect domain. Mol. Cell 19, 297-308.

58.   Reddick, J. J., Cheng, J. M., and Roush, W. R. (2003) Relative rates of michael reactions of 2 '-(phenethyl)thiol with vinyl sulfones, vinyl sulfonate esters, and vinyl sulfonamides relevant to vinyl sulfonyl cysteine protease inhibitors. Org. Lett. 5, 1967-1970.

59.   Lall, M. S., Ramtohul, Y. K., James, M. N. G., and Vederas, J. C. (2002) Serine and threonine beta-lactones: A new class of hepatitis a virus 3c cysteine proteinase inhibitors. J. Org. Chem 67, 1536-1547.

60.   Krantz, A., Copp, L. J., Coles, P. J., Smith, R. A., and Heard, S. B. (1991) Peptidyl (acyloxy)methyl ketones and the quiescent affinity label concept - the departing group as a variable structural element in the design of inactivators of cysteine proteinases. Biochemistry 30, 4678-4687.

61.   Larkin, M. A., Blackshields, G., Brown, N. P., Chenna, R., McGettigan, P. A., McWilliam, H., Valentin, F., Wallace, I. M., Wilm, A., Lopez, R., Thompson, J. D., Gibson, T. J., and Higgins, D. G. (2007) Clustal w and clustal x version 2.0. Bioinformatics 23, 2947-2948.

Figure and Table Legends

Figure 1. ABPP approach for identifying DUBs, Ub/Ubl activating enzymes, conjugating enzymes and ligases.

(a) Synthesis of HAUb-derived probes using an intein-based chemical ligation. Recombinant HA-tagged Ub was expressed as a C-terminal fusion with an intein-chitin binding domain (CBD) for purification and introduction of reactive groups. Addition of β-mercaptoethane sulfonic acid (MESNa) to the chitin agarose (CA) with bound HAUb fusion protein results in elution of a species containing a thioester capable of chemical ligation.

(b) A table of new glycine-based electrophiles synthesized for attachment to the C-terminus of HAUb. HAUbVME, a first generation probe, was used for comparison of second generation probe reactivity. Figure adapted with permission from *Nature Chemical Biology*, ref. 14.

Figure 2. Different HAUb-derived probes show distinct activities and labeling profiles.

(a) EL4 cell lysates (30 μg) were incubated with 0.2 μg of each HAUb (2 μM) probe for 5 h at room temperature (22°C). The labeled proteins were resolved by SDS-PAGE (10%) under reducing conditions and immunoblotted with anti-HA antibody. The HAUbVME probe is the most reactive as visualized by labeling intensity in this immunoblot. Labeling is not observed using HAUbLac at the concentration used.

(b) HMLE cell lysates (7.5 mg) were incubated with 1 μg of each HAUb probe (0.2 μM) for 5 h at room temperature (22°C). A sample of labeled proteins (30 μg protein extract) were resolved by SDS-PAGE (8%) under reducing conditions and immunoblotted with anti-HA antibody. The amount of sample loaded onto the gel and the exposure times of this immunoblot were varied to

account for differences in the reactivity and decomposition of the C-terminal electrophiles in each Ub-based probe.

Table 1. Ub/Ubl activating enzymes (E1s), conjugating enzymes (E2s) and ligases (E3s) identified from (a) mouse lymphoma (EL4) and (b) human mammary epithelial cell lysates (HMLE).

Figure 3. Biochemical analysis of probe-labeled cysteines in ARF-BP1.

(a) Incubation of HAUbVME with recombinant ARF-BP1 HECT domain covalently labels multiple cysteines as identified using tandem M/S analysis. 5 µg recombinant ARF-BP1 HECT domain was incubated with 2.0 µM HAUbVME for 3 h at 22°C. Labeled species were resolved by 10% SDS-PAGE and detected by coomassie staining. The labeled peptides were excised from the gel, trypsizined, and subject to MS/MS analysis. Residues C4099 (Cys 1), C4341 (Cys 5), and C4367 (Cys 6) were modified by probe. Probe labeling is specific for these sites, as HECT domain denatured in 6.4 M urea for 30 minutes at 30°C and then diluted with reaction buffer to 0.6 M urea before probe addition no longer efficiently binds HAUbVME.   ARF-BP1 HECT domain and HAUbVME retain activity when incubated initially with 0.6 M urea. Ub ligase activity of wild-type (*6*) or cysteine-to-alanine mutant ARF-BP1 HECT domains was assayed using (b) [^{32}P]-Ub for autoubiqutination or (c) [^{32}P]-Mcl-1 for substrate ubiquitination. Reaction components contained recombinant UBE1, UbcH7, an ATP regenerating system, and either no ligase (N), WT, or a mutant ligase as indicated. Ligation reaction mixtures were separated by 10% SDS-PAGE and visualized by phosphorimaging.

(d) Product formation by wild type or mutant ARF-BP1 in the autoubiquitination assay or Mcl-1

ubiquitination assay was calculated by averaging the percent wild-type activity quantified using

phosphorimaging data from nine independent experiments.

Figure 4. Detection of Ub-thioesters in ARF-BP1 HECT domain.

(a) Ub-thioester assay with the indicated ARF-BP1 HECT domain proteins. Purified ARF-BP1

HECT domain proteins were incubated with recombinant E1 and E2 (UbcH7), an ATP

regenerating system, and Ub. Reactions were stopped with 4 M urea and either reducing (left

panel) or non-reducing (right panel) SDS-PAGE sample buffer, separated by SDS-PAGE, and

analyzed by immunoblot with anti-Ub antibody.

(b) Ub thioester assay with the indicated ARF-BP1 truncation proteins was performed with all

necessary components; without UBE1; or without UbcH7.

(c) Substrate ubiquitination assay using the indicated ARF-BP1 HECT domain proteins and

recombinant Mcl-1 as substrate. Reactions contained recombinant UBE1, UbcH7, Ub, an ATP

regenerating system, and 1 μg recombinant Flag-labeled Mcl-1. Reaction mixtures were

quenched as above, separated on SDS-PAGE and analyzed by anti-Flag immunoblot.

(d) Substrate ubiquitination assay using the indicated ARF-BP1 HECT domain with all

components; no UBE1; and no UbcH7.

Figure 5. Multiple sequence alignment of ARF-BP1 HECT domain.

Sequence conservation of ARF-BP1 HECT domain across diverse eukaryotes. The region

depicted represents two portions of ARF-BP1 C-terminus and includes Cys 1 (C4099), Cys 5

(C4341), and Cys 6 (C4367), each marked above with an asterik. Residues depicted in red are

small or hydrophobic, those depicted in blue are acidic, those depicted in magenta are basic, and

the remainders are depicted in green. Alignment made with Clustal W(*35*).

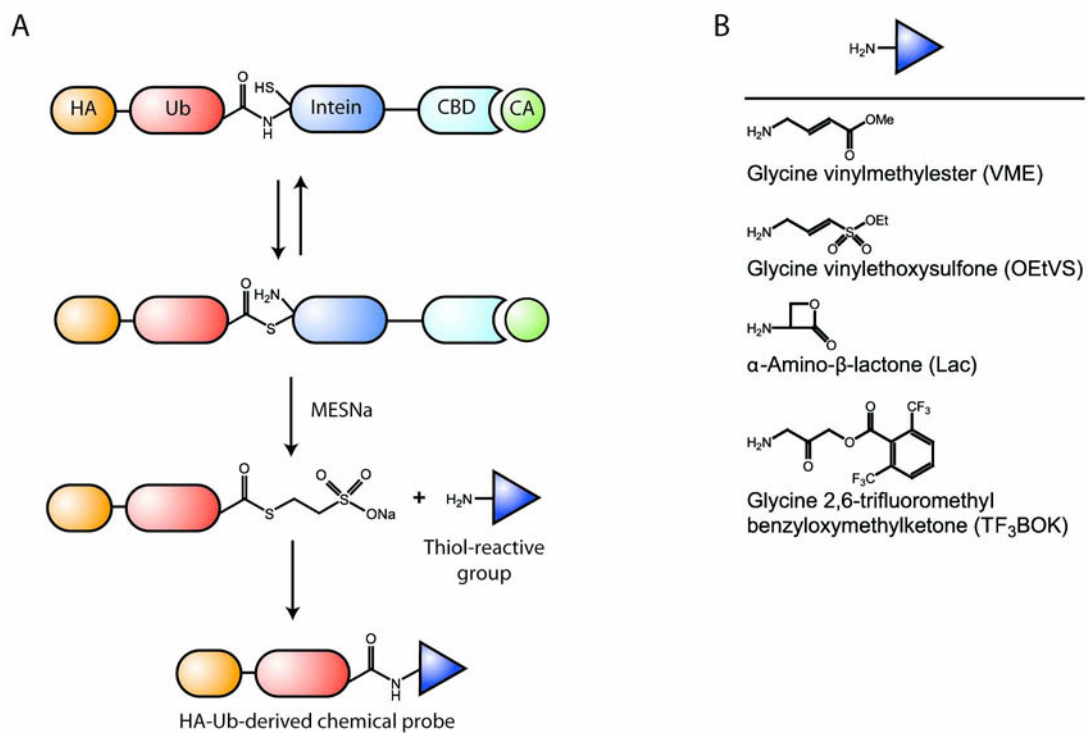## Figure 1

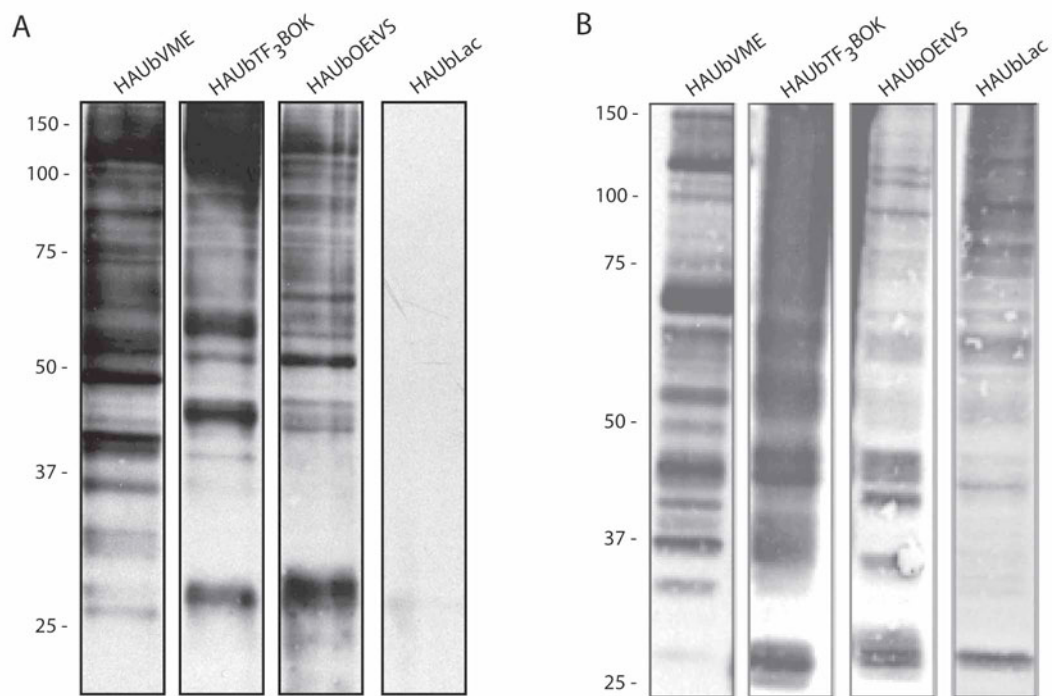

A

MESNa

Thiol-reactive group

HA-Ub-derived chemical probe

B

Glycine vinylmethylester (VME)

Glycine vinylethoxysulfone (OEtVS)

α-Amino-β-lactone (Lac)

Glycine 2,6-trifluoromethyl benzyloxymethylketone (TF$_3$BOK)

Figure 2

Table 1.
A.

Protein identified	Protein activity	Accession number (NCBI)	Predicted MW (kDa)	HAUb probe used for retrieval
UBE1	E1 Ub-activating enzyme	267190	118	TF₃BOK
UBE1-L2	E1 Ub-activating enzyme	27370032	118	TF₃BOK
UBE1 (Chromosome X)	E1 Ub-activating enzyme	148878383	118	TF₃BOK
UBA2	E1 Ubl-activating enzyme	32493410	70.5	TF₃BOK
Aos1	E1 Ubl-activating enzyme	18490720	38.5	TF₃BOK
UBC9	E2 Ubl-conjugating enzyme	54039792	18	TF₃BOK
UBC12	E2 Ubl-conjugating enzyme	46577656	21	TF₃BOK
UBC13	E2 Ub-conjugating enzyme	18017605	17	TF₃BOK
UB2V1	E2 Ub-conjugating enzyme	51702141	16	TF₃BOK
UB2V2	E2 Ub-conjugating enzyme	51702142	16	TF₃BOK
UBE2-L3 (UbcM4)	E2 Ub-conjugating enzyme	54039806	18	TF₃BOK
UBE2S	E2 Ub-conjugating enzyme	53734650	24	TF₃BOK
UBE2O	E2 Ub-conjugating enzyme	50234896	141	TF₃BOK
E6-AP (Ube3A)	HECT E3 Ub ligase	76880500	97.5	VME
Nedd4 (Rsp5)	HECT E3 Ub ligase	32172436	103	OEtVS, TF₃BOK

ARF-BP1 (Mule)	HECT E3 Ub ligase	73915354	482	VME, Lac, TF₃BOK
Trip12	Putative HECT E3 Ub ligase	91932791	224	VME, TF₃BOK
UBAC1 (KPC2)	RING E3 Ub ligase	19527050	45	VME
UBR2	RING E3 Ub ligase	73622074	199	TF₃BOK
CUL-4A	RING E3 Ub ligase	108936014	88	OEtVS
TRAF2	RING E3 Ub ligase	83921633	56	OEtVS

B.

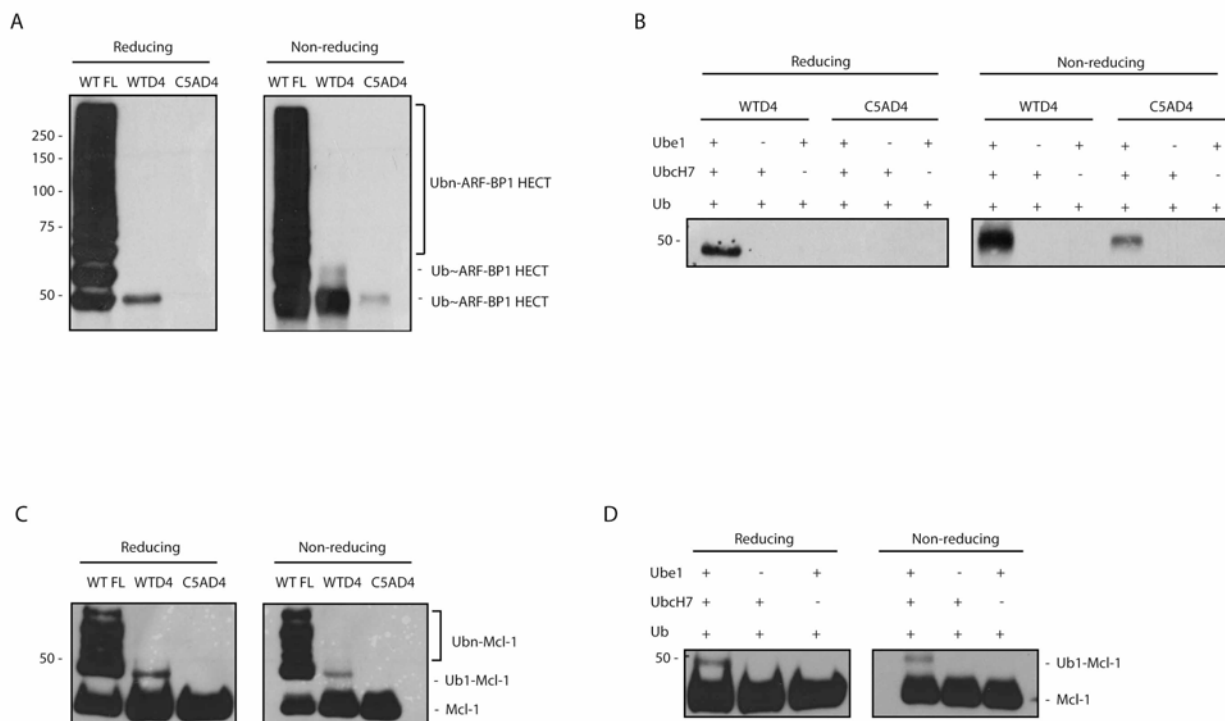| Protein identified	Protein activity	Accession number (NCBI)	Predicted MW (kDa)	HAUb probe used for retrieval
UBE1	E1 Ub-activating enzyme	24418865	117.8	VME, OEtVS, TF$_3$BOK
UBC1	E2 Ub-conjugating enzyme	46577658	22.4	VME, Lac, TF$_3$BOK
UB2E2	E2 Ub-conjugating enzyme	47606201	22.2	VME, TF$_3$BOK
UBE2N	E2 Ub-conjugating enzyme	46577660	17.1	VME, Lac, TF$_3$BOK
UBE2S	E2 Ub-conjugating enzyme	23829978	23.8	TF$_3$BOK
UBE2C (isoform 4)	E2 Ub-conjugating enzyme	32967289	46.4	TF$_3$BOK
UBE2T	E2 Ub-conjugating enzyme	73622065	22.5	TF$_3$BOK
E6-AP (isoform 3, Ube3A)	HECT E3 Ub ligase	19718764	100	VME
ARF-BP1	HECT E3 Ub ligase	73915353	481.6	VME, TF$_3$BOK
Trip12	Putative HECT E3 Ub ligase	2499839	220.3	TF$_3$BOK
RN138	RING E3 Ub ligase	74733576	28.2	Lac
CUL-4A	RING E3 Ub ligase	108936013	87.6	Lac
CUL-4B (isoform 2)	RING E3 Ub ligase	121114302	102.2	VME, Lac
SH3R2	Putative RING E3 Ub ligase	122070123	79.2	Lac, TF$_3$BOK

Figure 3

A

Probe-modified ARF-BP1 HECT
ARF-BP1 HECT

B

C

D
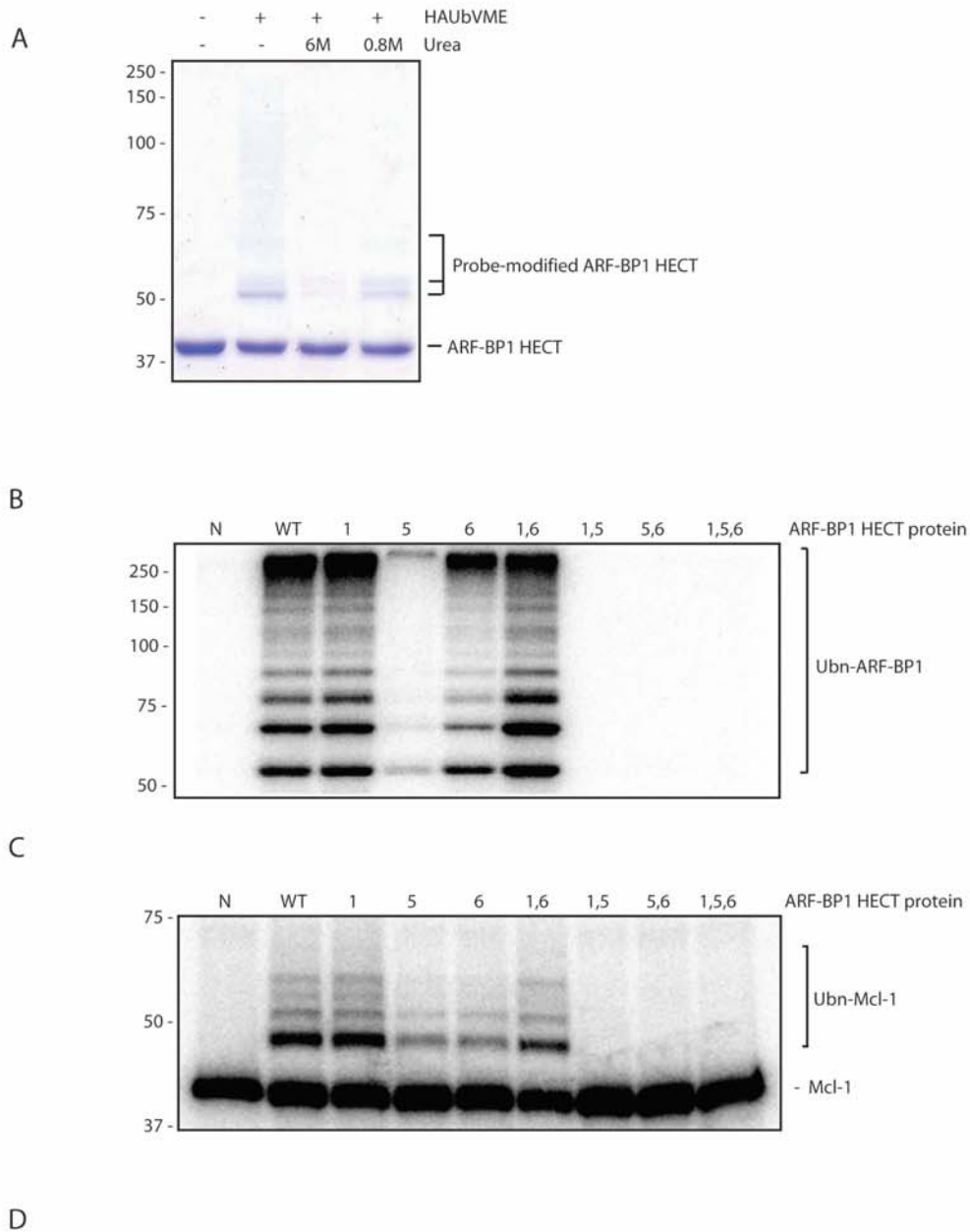
ARF-BP1 mutant	Product formed as a % WT (SD) in a 10 min AutoUb reaction	Product formed as a % WT (SD) in a 60 min Mcl-1 Ub
1 (C4099A)	94.03 (22.15)	104.32 (40.39)
5 (C4341A)	8.17 (3.78)	30.04 (7.32)
6 (C4367A)	56.27 (12.69)	40.70 (20.15)
1,6 (C4099A, C4367A)	101.96 (31.15)	73.58 (36.92)
1,5 (C4099A, C4341A)	NP*	NP
5,6 (C4341A, C4367A)	NP	NP
1,5,6 (C4099A, C4341A, C4367A)	NP	NP

NP indicates no product formation was observed for this mutant. *Negligible product detected.

Figure 4

Figure 5

```
                                 *                              *                         *
Homo sapiens              4086  DRVTYT INPSSHCN PNH LSY FK  410 8…432 8  DRST DRLP SAHTC FNQ LDLPA YES FEKLR HMLLLAI QECS EGFGLA  437 4
Macaca mulatta            4069  DRVTYT INPSSHCN PNH LSY FK  4 091…411 1  DRST DRLP SAHTC FNQ LDLPA YES FEKLR HMLLLAI QECS EGFGLA  4357
Bos Taurus                4087  DRVTYT INPSSHCN PNH LSY FK  410 9…432 9  DRST DRLP SAHTC FNQ LDLPA YES FEKLR HMLLLAI QECS EGFGLA  437 5
Canis familiaris          4087  DRVTYT INPSSHCN PNH LSY FK  410 9…432 9  DRST DRLP SAHTC FNQ LDLPA YES FEKLR HMLLLAI QECS EGFGLA  437 5
Mus musculus              4090  DRVTYT INPSSHCN PNH LSY FK  411 2…43 32  DRST DRLP SAHTC FNQ LDLPA YES FEKLR HMLLLAI QECS EGFGLA  437 8
Danio rerio               4072  DRVTYT INPSSHCN PNH LSY FK  4 094…411 4  DRST DRLP SAHTC FNQ LDLPA YESY EKLR HMLLLAI QECS EGFGLA  436 0
Tribolium castaneum       3661  DRVTYMI NSASHYN PNH LCYY K  36 83…390 3  DRST DRLP SAHTC FNQ LDLPV YETY DKLRSY LL KAI HECS EGFGFA  394 9
Drosophila melanogaster   4858  DRVTYMI NPSSH ANPNH LSY FK  48 80…5100   DRST DRLP CAHTC FNQ LDLPM YKSY DKLRSC LL KAI HECS EGFGFA  514 6
Hydra magnipapillata      2002  EKSTY LPNQHSHCN PNH LSY FK  202 4…219 4  DRST DRLP CAHTC FNQ LDLPA YETY DKLHSQ ML KAI NECP EGFGLA  224 0
Aspergillus nidulans      3735  DRTT FHPNRLSG VNPEH LMFF K  375 7…397 6  YGN KDRLP SSHTC FNQ LDLP EYDSY ETLRQRL YIAM TTGS EY FGFA  402 2
Pichia guilliermondii     2987  DE TT FHPNRTS FI NPEH LSFF K  300 9…322 8  YGTT DRLP SSHTC FNQ IDLPA YETY ETLRGS LLLAI TEGH EGFGLA  3274
```

CHAPTER 3: A STRUCTURAL ELEMENT WITHIN THE HUWE1 HECT DOMAIN MODULATES SELF-UBIQUITINATION AND SUBSTRATE UBIQUITINATION ACTIVITIES

Abstract

E3 ubiquitin ligases catalyze the final step of ubiquitin conjugation and regulate numerous cellular processes. The HECT class of E3 Ub ligases directly transfers Ub from bound E2 enzyme to a myriad of substrates. The catalytic domain of HECT Ub ligases has a bilobal architecture that separates the E2-binding region and catalytic site. An important question regarding HECT domain function is the control of ligase activity and specificity. Here we present a functional analysis of the HECT domain of the E3 ligase HUWE1, based on crystal structures, and show that a single, N-terminal helix significantly stabilizes the HECT domain. We observe that this element modulates HECT domain activity, as measured by self-ubiquitination induced in the absence of this helix, as distinct from its effects on Ub conjugation of substrate Mcl-1. Such subtle changes to the protein may be at the heart of the vast spectrum of substrate specificities displayed by HECT domain E3 ligases.

Introduction

Ubiquitin (Ub) conjugation regulates many cellular processes, including protein stability, cell cycle control, DNA repair, transcription, signal transduction, and protein trafficking (2-4). An enzymatic cascade consisting of Ub activating enzyme (E1), Ub conjugating enzyme (E2), and Ub ligase (E3) is responsible for catalyzing Ub conjugation to target proteins. The E1 enzyme activates Ub for transfer by adenylating its C terminus in an ATP-dependent step. Ub is then transferred to the E1 active site cysteine, forming a thioester bond between E1 and Ub. The activated Ub is transferred to E2 enzyme in a transthiolation reaction and is conjugated to target proteins by the action of E3 Ub ligases (4). The E2 and E3 enzymes provide substrate specificity to the Ub conjugation reaction (5). Approximately 600 E3s exist in the human proteome, 28 of which belong to the HECT (homologous to E6AP C terminus) domain family (6). HECT domain E3s possess a ~350 amino acid C-terminal HECT domain containing a conserved catalytic cysteine that participates in the transfer of Ub to substrate. Mutation, abnormal expression, or misregulation of these enzymes predisposes to the development of cancer and disease (2,7).

Structural studies describe the canonical HECT domain architecture and provide insight into its mechanism of catalysis (8-10). HECT domains are composed of two subdomains connected by a flexible peptide linker. The N-terminal (N) lobe contains the E2 binding region, and the C-terminal (C) lobe contains the catalytic cysteine. In the structure of the E6AP-UbcH7 complex (Protein Data Bank (PDB) codes IC4Z and ID5F), the catalytic cysteines of E2 and E3 are separated by 41 Å, suggesting that a substantial conformational rearrangement is required to achieve Ub transfer (8). Analysis of the structure of the WWP1 HECT domain (PDB code 1ND7) partially addresses how Ub is transferred from the E2 to the E3 catalytic cysteine by illustrating conformational flexibility of the HECT domain (10). In the WWP1 structure

modeled in a complex with UbcH5, the C-lobe is rotated about the hinge region, placing it in closer proximity to the E2 cysteine, and closing the distance between active site cysteines to 16 Å. Mutations in this hinge loop that restrict HECT domain rotation decrease activity (10). Additional structural elements within the HECT domain that modulate conformation or activity remain unknown.

HUWE1 (also called ARF-BP1, Mule, Lasu1, Ureb1, E3 histone, and HectH9) is a large 482-kDa HECT domain E3 Ub ligase implicated in the regulation of cell proliferation, apoptosis, DNA damage response, and base excision repair (11-17). We recovered this enzyme in immunoprecipitations using Ub C-terminal electrophilic probes (18). Following an initial biochemical characterization (18), we completed a structural and biophysical analysis of the HECT domain to understand modulation of its robust in vitro activity. Here we present crystal structures of the HUWE1 HECT domain and characterize a structural element that both stabilizes this domain and modulates its activity. This structural element, the α1 helix, is an important component of the HECT domain that largely restricts its autoubiquitination activity, while only nominally affecting Mcl-1 ubiquitination activity.

Results

Structure of the HUWE1 HECT domain.

We first attempted to crystallize the HUWE1 HECT domain using a fragment defined by the founding member of the HECT domain E3 ligase family, E6AP (PDB codes 1C4Z and ID5F) (8). The crystals diffracted to only 3.5 Å (data not shown), with fairly high temperature factors indicating vibrational disorder within the protein crystals. By sequence comparison, we noted the significance of a conserved N-terminal helix that seals the hydrophobic core of the N-lobe in

the structures of WWP1, Smurf2, and Nedd4-like (residues 546-560 in WWP1 and 371-387 in

Smurf2) (9,10). The presence of this helix is conserved in over 13 HECT domain E3 ligases

based on sequence comparison (Figure 1a) and (10), highlighting its structural importance. The

α1 helix has been previously described as a critical element for structural stability, yet an

element dispensable for HECT domain function (8,10). Initial model-building into the 3.5 Å

electron density showed a noticeable hydrophobic groove on the surface of helices 5, 11, 12, and

13, possibly indicating an additional helix being bound here. As sequence conservation drops off

N-terminal of this α1 helix (Figure 1b), we hypothesized that this element is an important part of

the HECT domain. We note that expression of the HECT domain of Nedd4 yielded soluble

folded product when the homologous helical segment was included in the expression construct,

but was not successful in its absence (E. Maspero and S. Polo, personal communication). We

therefore asked whether addition of helix α1 would not only assist in our crystallographic efforts

but also affect the catalytic activity of the HECT domain.

Addition of helix α1 greatly stabilizes the HECT domain, as made evident in thermal

denaturation experiments (Figure 1c), shifting the transition midpoint by 16°C from 44 °C to

60°C. Although thermal stability differs between the two versions of the HECT domain, the

level of secondary structure remains the same (Figure 1d), indicating that the absence of helix α1

does not lead to unfolding, but to less rigidity of the domain. We solved the structure of the

helix-extended HECT domain by molecular replacement using the E3 ligase WWP1 (10) as a

search model. The final model (R/R$_{free}$ 16.6%/22.9%) was built and refined to 1.9 Å resolution

(Table 1). The structure of HUWE1 HECT domain closely resembles that of WWP1, with

which it shares 41.3% sequence identity (Figure 2a). The HUWE1 HECT domain contains two

distinct lobes similar to previously determined HECT domain structures (E6AP, Smurf2,

97

WWP1). The larger N lobe (residues 3993-4252) contains the E2 binding region, and the

smaller C lobe (residues 4259-4374) contains the conserved catalytic cysteine (C4341). The N

lobe is composed of 13 α-helices and 7 β-strands, and the C lobe is composed of 4 α-helices and

4 β-strands. Residues 4253-4258 form the hinge that connects the two lobes. A rotary

movement about this linker likely repositions the N and C lobes to bring the catalytic cysteine of

the cognate Ub-loaded E2 in proximity to its E3 counterpart (10). Like WWP1, HUWE1 is

oriented in an inverted T shape (⊥), in which the C lobe is positioned over the middle of the N

lobe, with approximately 800 Å^2 of contact surface area (Figure 2b). Hydrogen bonds between

Glu4248 (N lobe) and Ser4304 (C lobe), as well as Gln4245 (N lobe) and Gln4298 (C lobe), and

a salt bridge between Glu4246 and Lys4295, stabilize the ⊥ conformation. The ⊥ conformation

is further stabilized by water-mediated hydrogen bonds between the two lobes, involving

residues Arg4130, Glu4147, Ser4148, and Glu4244 from the N lobe and Gln4298, Thr4340,

Gly4302, and Lys4295 in the C lobe. The orientation of the N and C lobes of the HUWE1

HECT domain differs from the more open conformation observed in the crystal structures of

E6AP and Smurf2 (Figure 2c) (8,9), although we cannot exclude the possibility that crystal

contacts influence the observed orientation of the C lobe. The stabilizing nature of helix α1 is

apparent from the extended structure, as it closes the hydrophobic core of the N-lobe (Figure 2a,

d).

The most notable difference between HUWE1 HECT domain and previously solved

structures concerns the E2 binding region (residues 4150-4200). Most of the hydrophobic

residues in WWP1 that mediate contact with the E2 are similar to those in HUWE1, obvious

from the alignment between HECT E3 ligases (Figure 2e). The HUWE1 E2 binding region

differs from that of WWP1, in that it contains additional structured elements – mainly ordered β-

strands not previously identified. The well-ordered β-strands in the E2 binding region of the

HUWE1 HECT domain extend farther from the helical core of the protein than seen in the

structure of WWP1, and the loop is folded back on itself to complete the β3 strand and form the

α8 helix (Figure 2a). It is possible that HUWE1 uses its unique E2 binding region to interact

with a specific set of E2 enzymes in vivo that differ from WWP1.

A comparison of our two HUWE1 HECT domain structures shows that they are nearly

identical with respect to the positioning of the N and C lobes (Supplementary Figure 1a, b). For

the structure lacking the α1 helix, the additional β-strands and α-helix seen in the E2 binding

region remain unresolved, likely due to the low resolution data and high temperature factors.

Catalytic activity of the HECT domain.

As addition of the α1 helix to the HECT domain stabilized the protein, we asked whether

the presence of this structural element affected HECT domain catalytic activity. We

hypothesized its addition might confer altered catalytic properties to the HECT domain

compared to its helix-lacking counterpart. We therefore examined the ability of the HECT

domain to catalyze self-ubiquitination in the presence of E1 and E2 (UBE2L3) enzymes, an ATP

regenerating system, and $[^{32}P]$-Ub (Figure 3). The use of $[^{32}P]$-Ub allowed us to quantify the

amount of Ub adducts formed and calculate initial rates of product formation in HECT-domain

limiting conditions. In this assay, the HECT domain catalyzes the formation of a complex

mixture of self-ubiquitinated species (Figure 3a, b) that are not observed in absence of the HECT

domain (lane marked "N"). Immunoblotting using an anti-His antibody confirmed that these

species are ubiquitinated E3 enzyme, as it is the only species in this reaction that contains a

polyhistidine tag (data not shown). The pattern of autoubiquitination observed is similar

regardless of the presence of the α1 helix – both versions form multi- and polyubiquitinated species (Figure 3a, b). Although the pattern of product formation is similar, the presence of the α1 helix suppresses the autoubiquitination activity of the HECT domain by more than 25-fold (Figure 3c). As autoubiquitination is observed for many Ub ligases and is often used as a criterion of E3 Ub ligase activity, we sought to further characterize the reasons for its modulation.

The autoubiquitination reaction described above produces a complex mixture of products. We examined HECT domain activity in a single-turnover reaction to monitor the first round of Ub addition to the HECT domain. This assay encompasses two steps. In the first step, E2~Ub thioester is generated by incubating E1, E2, an ATP regenerating system, and Ub. After the E2~Ub thioester has formed, this reaction is quenched by the addition of EDTA to prevent further E1-catalyzed activation of Ub. In the second step, the HUWE1 HECT domain is added, and Ub is chased from the E2~thioester onto the HECT domain (22). The use of a mutant version of Ub, in which all lyines are mutated to arginine (K0 Ub), prevents polyubiquitin chain formation on the HECT domain. Ub-conjugated HECT domain is visualized using anti-Ub immunoblot (Figure 3d). We find that the HUWE1 Δ α1 HECT domain shows increased activity under single turnover conditions compared to the HECT domain containing helix α1 (Figure 3d), confirming the rate differences observed in the autoubiquitination assay.

Thioester formation in the HECT domain.

Catalysis by HECT domain E3 enzymes is a multi-step process. The E3 enzyme binds Ub-loaded E2 and substrate, followed by Ub transfer between the E2 and E3 catalytic cysteines. The E3 then catalyzes isopeptide bond formation between Ub and a lysine residue on the

substrate, which may be the E3 itself, Ub, or another protein. We next determined whether the presence of the α1 helix affects this upstream step, in which the catalytic cysteine of the E3 enzyme forms a thioester bond with ubiquitin.

We first attempted to assay thioester formation using the wild-type HECT domain, but the enzyme efficiently catalyzes formation of the isopeptide bond on a time scale too fast to measure (23,24). Instead, we analyzed thioester formation using a four-amino acid, C-terminal truncation of the HECT domain (25). This truncation removes a crucial determinant for isopeptide bond formation, a conserved phenylalanine located four amino acids from the C terminus of most HECT E3s (25). HUWE1 Δ4 displays a diminished rate of isopeptide bond formation, allowing us to monitor formation of thioester-linked Ub to the enzyme. After incubation of the HECT domain with E1, the E2 UBE2L3, Ub, and an ATP regenerating system, the reaction is quenched with SDS-PAGE loading buffer with or without β-mercaptoethanol, and following electrophoretic resolution, is analyzed by anti-Ub immunoblot. The presence of the α1 helix greatly reduces the rate of thioester formation (Figure 4), proportional to its suppression of autoubiquitination activity. The α1 helix, located on the back surface of the N lobe, is clearly not sufficiently close to interact with the E2 binding region of the HECT domain (Figure 2a), suggesting that the vibrational disorder in this protein contributes to the HECT domain-E2 interaction.

Substrate ubiquitination catalyzed by the HECT domain.

Having seen that removal of helix α1 destabilizes the HECT domain and increases its autoubiquitination activity, we asked whether this effect is also observed during substrate ubiquitination. The anti-apoptotic Bcl-2 family member Mcl-1 is an in vivo target of HUWE1

(15). HUWE1 recruits Mcl-1 via its BH3-domain, while the HECT domain presented here catalyzes Mcl-1 ubiquitination. Although Mcl-1 is a substrate of the full-length HUWE1, we use this assay with the isolated HECT domain here as a measure of non-self ubiquitination activity with an *in vivo* verified substrate of HUWE1. We examined initial rates of product formation, under HECT-domain limiting conditions, to determine whether the intrinsic activity of the HECT domain toward substrate is altered by the destabilizing effect of removing the $\alpha 1$ helix (Figure 5a, b). We find that the HECT domain lacking $\alpha 1$ helix is ~5-fold more active in catalyzing Mcl-1 ubiquitination than the more stable HECT domain containing helix $\alpha 1$ (Figure 5c). These results also suggest that autoubiquitination of the HECT domain does not impair catalytic activity toward substrate. The two versions of the HUWE1 HECT domain, which differ 25-fold in autoubiquitination rates, show only a 5-fold difference in their Mcl-1 ubiquitination rates. A similar observation was made for the heterodimeric complex of the minimal catalytic domains of Ring1a/Bmi1, in which autoubiquitination of the Ring1b protein did not affect E3 ligase activity toward its substrate, histone H2A, in an in vitro reconstituted system (26). We also observe similar differences in autoubiquitination and Mcl-1 ubiquitination activity between the two versions of the HECT domain at 37°C (Figure 6).

Catalytic activity of the C4341A mutants.

Mutation of the conserved catalytic cysteine to alanine (C4341A) abolishes activity of the HECT domain (Supplementary Figure 2). In the case of the helix-lacking HECT domain, we consistently observed that the C4341A mutant is capable of transferring a single ubiquitin to self (Supplementary Figure 2a) or Mcl-1 (Supplementary Figure 2c). These species are not generated when the HECT domain is omitted from the reaction (lane marked "N"). Although the failure of

mutation of the catalytic cysteine to abolish activity has been previously observed (11), quantification of the monoubiquitinated species shows that this activity represents at best a minor fraction of wild-type activity (Supplementary Figure 2e, f).

Discussion

We present here crystal structures of the HUWE1 HECT domain and identify a conserved structural element, helix α1, which stabilizes the HECT domain and tightly modulates its activity. Helix α1 is present in the structure of the WWP1 HECT domain (referred to in the WWP1 structure as H1') (10), where the authors note that it plays an obvious role in contributing to HECT domain stability. As the H1' helix is oriented between the C lobe and domains N-terminal to the HECT domain that presumably mediate protein-protein interactions, the authors suggested that H1' helix contributes to target protein specificity in reactions catalyzed by the HECT domain. We confirm that the α1 helix is indeed crucial for stability and identify a role for this structural element in modulating HECT domain activity, as judged by autoubiquitination and Mcl-1 ubiquitination assays. Further experiments will determine whether this conserved helix modulates activity of other members of the HECT domain family.

In the absence of the N-terminal α1 helix, the HUWE1 HECT domain gains activity relative to its helix-extended counterpart. What could be the reason for this unexpected behavior? Deletion of helix α1 might expose hydrophobic residues that trigger assembly of HUWE1 HECT domains into oligomers. Such behavior has been observed in the crystals of E6AP (PDB codes 1C4Z and 1D5F) (8). However, HUWE1 HECT Δ α1 behaves as a monomer and is properly folded in solution, as judged by several criteria (Figure 1d and data not shown).

103

Our structural data on HUWE1 shows that the HECT domain adopts the same conformation regardless of the presence of helix α1, and both variants contain the same helical content (Figure 1d). HUWE1 Δ α1, however, is far more active in catalyzing self-ubiquitination and in single-turnover assays. It also accepts Ub from the E2 UBE2L3 more readily than the helix-extended HECT domain. Furthermore, we observed elevated temperature factors, indicative of conformational flexibility, in the crystal structure of HUWE1 HECT Δ α1; a similar observation was made in the crystals of the E3 Ub ligase IpaH from the bacterial pathogen *Shigella flexneri* (23). We favor the interpretation that removal of helix α1 destabilizes the HECT domain to produce a more relaxed version of the enzyme that exhibits greater intra-domain flexibility. This increased flexibility allows the enzyme to sample more conformational states, thereby increasing its level of activity. Some of these conformational states may resemble the extended HECT domain structures observed in the crystal structures of Smurf2 and E6AP, in which the C-lobe has rotated about the flexible linker that connects the two subdomains of the HECT domain. In this scenario, removal of the α1 helix is analogous to the linker-extension mutations made in WWP1 (10). The removal of helix α1 may also shift the conformational equilibrium of the HECT domain into an orientation that facilitates the E2-HECT interaction or product release. This possibility is supported by evidence that enzymes exist in a dynamic range of conformations, and the equilibrium between these different conformers can be shifted by mutation (27).

We did not anticipate that destabilization of the HECT domain would increase enzymatic activity. The Ub transfer reaction involves defined regions including the ordered β-strands that describe the E2 binding region and the catalytic site surrounding residue C4341. However, other steps, such as product release, may contribute to catalytic rate and may be influenced by

increased conformational flexibility (28). A correlation between conformational flexibility and promiscuous activity has been observed for several other proteins (28). An example of a flexible enzyme is cytochrome P450, which can adopt a range of different conformations that allow it to act upon a variety of substrates. Among the P450 family of enzymes, the rigid CYP2A6 enzyme exhibits limited substrate specificity, whereas the highly flexible CYP3A4 is far more promiscuous (28). In the case of HUWE1 HECT domain, the $\alpha 1$ helix may serve to impose a constraint on the inherent flexibility of the catalytic domain, thus fine-tuning enzymatic activity.

Autoubiquitination is often used as a criterion of E3 Ub ligase activity and, for some ligases, has been proposed as a mechanism of self-regulation of stability and downstream signaling functions (29,30). Our data show that this type of activity can be largely suppressed by minor extensions of what has been considered the core catalytic domain. We note, however, that our study focuses on the HECT domain of a multi-domain protein, and there may exist other structural elements in the 482-kD Huwe1 protein that affect its activity. This has been observed for the E3 Ub ligases Smurf2 (30), IpaH9.8 (23), and SspH2 (31), in which domains N-terminal to the catalytic domain suppress autoubiquitination activity. While autoubiquitination is clear evidence of catalytic activity of Ub ligases, the functional relevance of this reaction remains to be established for many E3s, including HUWE1. The increase in activity seen in the absence of helix $\alpha 1$ appears to stem from increased conformational flexibility in the enzyme. It is difficult to rationalize this behavior from static crystal structures, yet increased thermal motion observed in the Δhelix $\alpha 1$ structure is at least an indirect indicator. The significance of thermal motion within a protein with respect to reaction parameters is an emerging theme (32). HECT domains may have diverged to arrive at their extant spectrum of substrates by modulating flexibility (28), in addition to more tractable changes of surface properties. We conclude that the activity of the

HUWE1 HECT domain is tightly modulated, through restriction of conformational space rather than steric considerations, by the presence of a 19-residue helix $\alpha 1$.

Experimental procedures

Plasmids.

HECT domain constructs of HUWE1 (amino acids 3993-4374 or amino acids 4012-4374) were cloned into a modified pET-28a plasmid (Novagen) containing a human rhinovirus 3C (HRV3C) protease site to generate an N-terminal His$_6$ fusion protein for use in biochemical assays. The catalytic mutants C4341A and C4099A/C4184A/C4367A were generated using site-directed mutagenesis (Stratagene). For biochemical assays with radiolabeled substrate, Flag-Mcl-1 (amino acids 1-327) and Ub were both cloned with an N-terminal protein kinase A (PKA) site for [^{32}P]-labeling into pET-16b and pET-28a with the HRV3C site, respectively, as previously reported (18). UBE2L3 was cloned into the pET-28a plasmid (Novagen).

Bacterial protein expression and purification.

All versions of the HUWE1 HECT domain were expressed and purified as previously reported (18). [^{32}P]-labeled proteins were purified and labeled as previously described (18). Native UBE2L3 was expressed in Rosetta (DE3) cells (Novagen). UBE2L3 was precipitated from bacterial lysate by addition of saturated ammonium sulfate to 90%. The precipitated protein was resuspended in 50 mM HEPES pH 7.4, 200 mM NaCl and purified by gel filtration (Superdex 75 PC 3.2/30, GE Healthcare).

Circular Dichroism.

HUWE1 Δ α1 and HUWE1 + α1 HECT domains were dialyzed into 5 mM HEPES pH 7.5, 100 mM NaCl immediately prior to the scanning and melting CD experiments using an AVIV model 202 CD spectrometer. HUWE1 Δ α1 HECT domain at 2.4 μM and HUWE1 + α1 HECT

domain at 2.8 μM were used for scanning experiments between 195 and 280 nm at 25°C. CD

signal at 222 nm of 4.8 μM HUWE1 Δ α1 and 5.6 μM HUWE1 + α1 was recorded every 2

degrees over a 20-94 °C temperature ramp with 2 minutes of equilibration time at every step.

Biochemical Assays.

Reaction mixtures (10 μl) for HUWE1 autoubiquitination assay contained 100 nM human E1

(Ube1, Boston Biochem), 5.6 μM E2 (UBE2L3), HECT domain, and 60 μM [^{32}P]-Ub with an

ATP regenerating system (50 mM Tris [pH 7.6], 5mM MgCl$_2$, 5 mM ATP, 10 mM creatine

phosphate, 3.5 U/ml creatine kinase). Reactions were incubated at room temperature and

aliquots were removed after the indicated amount of time and terminated in reducing SDS-PAGE

sample buffer. Samples were boiled 10 min. and separated on 8% Tris-tricine SDS-PAGE.

Dried gels were exposed to a phosphor screen. [^{32}P]-Ub bands were visualized by

autoradiography and quantitation of data was performed using a phosphorimager. Background

correction for each sample was performed by subtracting the counts from an equivalent area of

the gel from a lane containing all reaction components except E3 enzyme (lane marked "N").

The [^{32}P]-Ub signal from this lane was used to convert the observed sample counts to a

concentration value. The concentrations of HUWE1-[^{32}P]-Ub were measured and rates of

product formation determined by fitting the initial linear data points to a least squares regression

line.

Mcl-1 Ubiquitination Assay.

Reaction mixtures (10 μl) for the Mcl-1 ubiquitination assay were set up as above except with

the addition of 5 μM [^{32}P]-Flag-Mcl-1 and 100 μM Ub (Sigma). Reactions were quenched with

reducing sample buffer and separated on 10% SDS-PAGE. Bands from dried gels were analyzed as above.

Thioester assay.

Reaction mixtures for the thioester assay (10 µl) contained 100 nM human E1 (Ube1, Boston Biochem), 5.6 µM E2 (UBE2L3), 2 µM HUWE1 Δ4 HECT domain, and 60 µM Ub (Sigma) with an ATP regenerating system described above. Reactions were incubated at room temperature and aliquots were removed after the indicated amount of time and terminated in 4M urea and incubated 15 min. at 30°C, or terminated in reducing SDS-PAGE sample buffer. Samples were boiled 10 min., separated on 10% Tris-glycine SDS-PAGE, and analyzed by immunoblot using anti-Ub antibody (Sigma).

Single-turnover assay.

For the single-turnover assay, the E2~Ub thioester was generated in a 20 µl reaction containing 200 nM E1 (Boston Biochem), 8 µM E2, ATP regenerating system described above, 60 µM mutant Ub in which all lysines are mutated to arginine (K0 Ub) (Boston Biochem), and 1 µg/µl BSA incubated 25 min. at room temperature. Formation of the E2~Ub thioester was quenched with 50 mM EDTA on ice for 5 min. The E2~Ub thioester was diluted into chase mixture containing 2 µM HECT domain, 100 mM NaCl, 50 mM EDTA, and 1 µg/µl BSA, or the same reaction components lacking the HECT domain (labeled "N"). Reactions were incubated at room temperature and aliquots were removed after the indicated amount of time and terminated in either 4 M urea and incubated 15 min. at 30°C, or in reducing SDS-PAGE sample buffer.

Samples were boiled 10 min., separated on 10% Tris-glycine SDS-PAGE, and analyzed by immunoblot using anti-Ub antibody (Sigma).

Crystallization of HUWE1 HECT domain.

Crystallization experiments with purified HUWE1 HECT domain including the N-terminal His_6 tag, HRV3C protease site and with C4099A, C4184A, and C4341A mutations, were set up in 96-well sitting drop trays using commercially available sparse-matrix screens (Hampton Research, Qiagen). The initial crystals were improved in hanging-drop vapor diffusion setups. The HUWE1 + α1 HECT domain crystallized by mixing 1 μl of protein sample concentrated to 17 mg/ml with a 1 μl solution containing 0.1 M citric acid (pH 5.2) and 1.8 M $(NH_4)_2SO_4$. Birefringent crystals in the shape of thick rods with dimensions of approximately 80 x 40 x 40 μm grew within two days of incubation at 18 °C. The HUWE1 Δ α1 HECT domain crystallized by mixing a 1 μl solution containing $(Na/K)_2PO_4$ (pH 6.5) and 1.4 M $(Na/K)_2PO_4$. Thin rod-shaped crystals grew within 10 days at 23°C.

Data Collection and Processing.

For native X-ray diffraction studies, crystals were cryoprotected by soaking in 0.1 M citric acid (pH 5.2), 1.8 M $(NH_4)_2SO_4$, 12% glycerol for 30 sec prior to vitrifying in liquid nitrogen. X-ray diffraction data were collected on a single cryogenized crystal at beamline 24ID-E, Advanced Photon Source (Argonne, IL, USA), summarized in Table 1. Data were processed using *DENZO* and *SCALEPACK (19)*. The crystals belong to the monoclinic space group C2 and diffracted to 1.9 Å. Initial phases were obtained by molecular replacement using PHASER from the CCP4 crystallographic program suite (1,20), with the coordinates of the E3 ligase WWP1 (PDB

accession code 1ND7) as search model. The final model was refined at resolution of 1.9 Å using

PHENIX with four TLS groups (10). Details of refinement are given in Table 1. Figures were

made using PyMol (21).

Acknowledgements

The abbreviations used are: HECT, homologous to E6AP C-terminus; Ub, ubiquitin; HUWE1,

HECT, UBA and WWE domain containing 1.

References

1. Collaborative Computational Project, N. (1994) "The CCP4 Suite: Programs for Protein Crystallography". Acta Cryst.
2. Bernassola, F., Karin, M., Ciechanover, A., and Melino, G. (2008) *Cancer Cell* **14**, 10-21
3. Pickart, C. M. (2001) *Annu Rev Biochem* **70**, 503-533
4. Kerscher, O., Felberbaum, R., and Hochstrasser, M. (2006) *Annu Rev Cell Dev Biol* **22**, 159-180
5. Christensen, D. E., Brzovic, P. S., and Klevit, R. E. (2007) *Nat Struct Mol Biol* **14**, 941-948
6. Li, W., Bengtson, M. H., Ulbrich, A., Matsuda, A., Reddy, V. A., Orth, A., Chanda, S. K., Batalov, S., and Joazeiro, C. A. (2008) *PLoS ONE* **3**, e1487
7. Scheffner, M., and Staub, O. (2007) *BMC Biochem* **8 Suppl 1**, S6
8. Huang, L., Kinnucan, E., Wang, G., Beaudenon, S., Howley, P. M., Huibregtse, J. M., and Pavletich, N. P. (1999) *Science* **286**, 1321-1326
9. Ogunjimi, A. A., Briant, D. J., Pece-Barbara, N., Le Roy, C., Di Guglielmo, G. M., Kavsak, P., Rasmussen, R. K., Seet, B. T., Sicheri, F., and Wrana, J. L. (2005) *Mol Cell* **19**, 297-308
10. Verdecia, M. A., Joazeiro, C. A., Wells, N. J., Ferrer, J. L., Bowman, M. E., Hunter, T., and Noel, J. P. (2003) *Mol Cell* **11**, 249-259
11. Adhikary, S., Marinoni, F., Hock, A., Hulleman, E., Popov, N., Beier, R., Bernard, S., Quarto, M., Capra, M., Goettig, S., Kogel, U., Scheffner, M., Helin, K., and Eilers, M. (2005) *Cell* **123**, 409-421
12. Chen, D., Kon, N., Li, M., Zhang, W., Qin, J., and Gu, W. (2005) *Cell* **121**, 1071-1083
13. Hall, J. R., Kow, E., Nevis, K. R., Lu, C. K., Luce, K. S., Zhong, Q., and Cook, J. G. (2007) *Mol Biol Cell* **18**, 3340-3350
14. Zhao, X., Heng, J. I., Guardavaccaro, D., Jiang, R., Pagano, M., Guillemot, F., Iavarone, A., and Lasorella, A. (2008) *Nat Cell Biol* **10**, 643-653
15. Zhong, Q., Gao, W., Du, F., and Wang, X. (2005) *Cell* **121**, 1085-1095
16. Herold, S., Hock, A., Herkert, B., Berns, K., Mullenders, J., Beijersbergen, R., Bernards, R., and Eilers, M. (2008) *EMBO J* **27**, 2851-2861
17. Parsons, J. L., Tait, P. S., Finch, D., Dianova, II, Edelmann, M. J., Khoronenkova, S. V., Kessler, B. M., Sharma, R. A., McKenna, W. G., and Dianov, G. L. (2009) *EMBO J* **28**, 3207-3215
18. Love, K., Pandya, R., Spooner, E., and Ploegh, H. (2009) *ACS Chem Biol*
19. Otwinowski, X. (1993) *Proceedings of the CCP4 Study Weekend. Data Collection and Processing*, Warrington: Daresbury Laboratory
20. McCoy, A. J., Grosse-Kunstleve, R.W., Adams, P.D., Winn, M.D., Storoni, L.C., and Read, R.J. . (2007) *Phaser* Crystallographic Software. J. Appl. Cryst.
21. DeLano, W. L. (2002) The PyMOL Molecular Graphics System. DeLano Scientific, San Carlos, CA
22. Eletr, Z. M., Huang, D. T., Duda, D. M., Schulman, B. A., and Kuhlman, B. (2005) *Nat Struct Mol Biol* **12**, 933-934

23. Singer, A. U., Rohde, J. R., Lam, R., Skarina, T., Kagan, O., Dileo, R., Chirgadze, N. Y., Cuff, M. E., Joachimiak, A., Tyers, M., Sansonetti, P. J., Parsot, C., and Savchenko, A. (2008) *Nat Struct Mol Biol* **15**, 1293-1301
24. Wang, M., and Pickart, C. M. (2005) *EMBO J* **24**, 4324-4333
25. Salvat, C., Wang, G., Dastur, A., Lyon, N., and Huibregtse, J. M. (2004) *J Biol Chem* **279**, 18935-18943
26. Buchwald, G., van der Stoop, P., Weichenrieder, O., Perrakis, A., van Lohuizen, M., and Sixma, T. K. (2006) *EMBO J* **25**, 2465-2474
27. Eisenmesser, E. Z., Millet, O., Labeikovsky, W., Korzhnev, D. M., Wolf-Watz, M., Bosco, D. A., Skalicky, J. J., Kay, L. E., and Kern, D. (2005) *Nature* **438**, 117-121
28. Tokuriki, N., and Tawfik, D. S. (2009) *Science* **324**, 203-207
29. Varfolomeev, E., Blankenship, J. W., Wayson, S. M., Fedorova, A. V., Kayagaki, N., Garg, P., Zobel, K., Dynek, J. N., Elliott, L. O., Wallweber, H. J., Flygare, J. A., Fairbrother, W. J., Deshayes, K., Dixit, V. M., and Vucic, D. (2007) *Cell* **131**, 669-681
30. Wiesner, S., Ogunjimi, A. A., Wang, H. R., Rotin, D., Sicheri, F., Wrana, J. L., and Forman-Kay, J. D. (2007) *Cell* **130**, 651-662
31. Quezada, C. M., Hicks, S. W., Galan, J. E., and Stebbins, C. E. (2009) *Proc Natl Acad Sci U S A* **106**, 4864-4869
32. Lange, O. F., Lakomek, N. A., Fares, C., Schroder, G. F., Walter, K. F., Becker, S., Meiler, J., Grubmuller, H., Griesinger, C., and de Groot, B. L. (2008) *Science* **320**, 1471-1475
33. Davis, I. W., Leaver-Fay, A., Chen, V. B., Block, J. N., Kapral, G. J., Wang, X., Murray, L. W., Arendall, W. B., 3rd, Snoeyink, J., Richardson, J. S., and Richardson, D. C. (2007) *Nucleic Acids Res* **35**, W375-383

Protein coordinates have been deposited in the RCSB Protein Data Bank (accession code 3H1D).

Figure Legends

Figure 1. The α1 helix stabilizes the HUWE1 HECT domain.

(a) Multiple sequence alignment of helix α1 with a diverse set of human HECT E3 ligases. Residue conservation is indicated by degree of shading ranging from orange (most conserved) to light yellow (least conserved). Secondary structure is illustrated with α-helices as cylinders and β-sheets as arrows.

(b) Multiple sequence alignment with a diverse set of human HECT E3 ligases indicating that sequence conservation drops off N-terminal to the α1 helix. The N-terminus of the HECT domain + α1 helix is indicated.

(c) Thermostability of the HUWE1 HECT domain was measured in a CD melting experiment. HUWE1 HECT domain, +/Δ α1 helix, wild-type or with cysteine mutations, was heated in a circular dichroism cuvette and unfolding measured at 222 nm as a loss of helical content. Deletion of helix α1 results in a drastic reduction of thermostability.

(d) CD scan experiment demonstrates the structural similarities of the +/Δ α1 helix versions of the HECT domain.

Figure 2. Structure of the HUWE1 HECT domain.

(a) Stereo view of HUWE1 HECT domain (residues 3993-4374) showing the N- and C-lobes connected by the hinge loop. Helix α1 is colored green. The N-lobe contains the E2 binding region and the C-lobe contains the catalytic cysteine (C4341).

(b) Overlay of HUWE1 (blue) and WWP1 (orange; PDB 1ND7) crystal structures.

(c) Overlay of HUWE1 (blue) and Smurf2 (orange; PDB 1ZVD) crystal structures.

(d) Helix α1 plays a significant role in mediating hydrophobic contacts that maintain the core of the HUWE1 HECT domain. Hydrophobic residues in the α1 helix, Phe3994 and Phe4001, pack into hydrophobic pockets in the N lobe. Arg3998 and Asp4009 form hydrogen bonds stabilizing the N-lobe. Lys4014 and Tyr4119, C-terminal to the α1 helix, orient the α1 helix to further stabilize the N-lobe.

(e) Multiple sequence alignment of E2 binding region with a diverse set of human HECT E3 ligases. Residues important for E2 binding are indicated with blue circles.

Figure 3. E3 ubiquitin ligase activity of HUWE1 HECT domain.

(a,b) The autoubiquitination activity of HUWE1 HECT domain was tested using 60 μM [^{32}P]-Ub as substrate and (a) 2 μM WT Δ α1 or (b) 2.9 μM WT + α1 HECT domains incubated with UBE1, UBE2L3, and an ATP regenerating system. (Note the different time scale for the two variants of the HECT domain). HECT domain is omitted in the lane marked "N". Asterisk denotes a likely ubiquitin polymer; double asterisk denotes likely mono-ubiquitinated UBE2L3. Concentrations of HECT domain were chosen to obtain initial rate conditions.

(c) Ligation activity of the WT Δ α1 and WT + α1 HECT domains in the autoubiquitination assay. Activity is given as the ratio between initial velocity (pmol total [^{32}P]-Ub product/min) and total enzyme concentration E (pmol). Errors are the standard deviations calculated from three independent experiments, shown in parenthesis.

(d) Single turnover assay monitoring transfer of Ub from the UBE2L3~Ub thioester to a lysine in the WT Δ α1 and WT + α1 HECT domains. The UBE2L3~Ub thioester is generated in a pulse reaction containing E1, UBE2L3, ATP regenerating system, and a Ub mutant in which all lysines are mutated to arginine (K0 Ub). Ub is chased from the E2 enzyme to HECT domain added to

the reaction. Ub-conjugated HECT domain is visualized by anti-Ub immunoblot. Samples were terminated in reducing or non-reducing sample buffer as indicated. Panel marked "N" is a chase reaction performed in absence of HECT domain and terminated in non-reducing sample buffer.

Figure 4. Detection of Ub~thioesters in the HUWE1 HECT domains.

Ub-thioester assay with the indicated HUWE1 HECT domain proteins. Purified HECT domains containing a C-terminal truncation of the last four amino acids were incubated with E1, UBE2L3, an ATP regenerating system, and Ub for the indicated amount of time. Reactions were stopped with 4M urea and non-reducing sample buffer (upper panel) or reducing sample buffer (lower panel), separated by SDS-PAGE, and analyzed by immunoblot with anti-Ub antibody.

Figure 5. Substrate Ubiquitination activity of the HUWE1 HECT domains.

(a,b) The Mcl-1 ubiquitination activity of HUWE1 HECT domain was tested using 5 µM [^{32}P]-Mcl-1 as substrate and (a) 100 nM WT Δ α1 or (b) 300 nM WT + α1 HECT domains incubated with UBE1, UBE2L3, Ub, and an ATP regenerating system. HECT domain was omitted from the lane marked "N". Concentrations of HECT domain were chosen to obtain initial rate conditions.

(c) Ligation activity of the HECT domains in the Mcl-1 ubiquitination assay. Activity is given as the ratio between initial velocity (pmol total [^{32}P]-Ub product/min) and total enzyme concentration E (pmol). Errors are the standard deviations calculated from three independent experiments, shown in parenthesis.

(d. e) Graph showing percent ubiquitinated Mcl-1 as a function of time in the reactions shown in panels (a) and (b) catalyzed by HUWE1 Δ α1 (d) or HUWE1 + α1 (e) HECT domains.

Figure 6. Ubiquitination Activity of the HUWE1 HECT domains at 37°C.

(a) The autoubiquitination activity of HUWE1 HECT domain at 37°C was tested using 60 µM

Ub as substrate and 2 µM WT HECT domains incubated with UBE1, UBE2L3, and an ATP

regenerating system. (Note the different time scale for the two variants of the HECT domain).

Reaction mixtures were separated on SDS-PAGE and analyzed by anti-Ub immunoblot.

(b) The Mcl-1 ubiquitination activity of HUWE1 HECT domain at 37°C was tested using 5 µM

Flag Mcl-1 as substrate and 100 nM WT HECT domains incubated with UBE1, UBE2L3, Ub,

and an ATP regenerating system. Reaction mixtures were separated on SDS-PAGE and

analyzed by anti-Flag immunoblot.

Table 1. Data collection and refinement statistics.

Data Set	HUWE1 HECT + α1
Data Collection	
Wavelength	0.9793
Space group	C2
Cell dimensions:	
a,b,c (Å)	119.6, 56.6, 69.6
β (°)	122.5
Unique reflections	30,847
Resolution (Å)	30-1.9 (1.93-1.9)
R_{sym}[a]	0.069 (0.392)
$R_{r.i.m.}$[b]	0.084 (0.493)
$R_{p.i.m.}$[c]	0.048 (0.295)
Completeness	98.3 (96.3)
Redundancy	3.2 (2.5)
I/σ	17.2 (2.1)
Wilson B factor (Å^2)	25
Refinement	
Resolution (Å)	30-1.9
Nonhydrogen Atoms	3190
Water Molecules	357
R_{work}[d]	16.6
R_{free}[e]	22.9
R.m.s. deviations	
Bond lengths (Å)	0.01
Bond angles (°)	1.20
B factors (Å^2)	
Protein	30.0
Water	39.4
Coordinate error (Å)	0.68
Ramachandran plot[f]	
Most favored	376
Allowed	5
Outliers	0

[a] $R_{sym} = \sum |I_i - <I_i>|/\sum I_i$, where I_i is the intensity of the *i*th observation and $<I_i>$ is the mean intensity of the reflection.

[b] $R_{r.i.m.} = \sum_{hkl}[N/(N-1)]^{1/2} \sum_i |I_i(hkl) - <I(hkl)>|/\sum_{hkl} \sum_i I_i(hkl)$, where $I_i(hkl)$ is the observed intensity and $<I(hkl)>$ is the average intensity of multiple observations of symmetry-related reflections.

[c] $R_{p.i.m.} = \sum_{hkl}[1/(N-1)]^{1/2} \sum_i |I_i(hkl) - <I(hkl)>|/\sum_{hkl} \sum_i I_i(hkl)$, where $I_i(hkl)$ is the observed intensity and $<I(hkl)>$ is the average intensity of multiple observations of symmetry-related reflections.

[d] $R_{work} = \sum(||F_{obs}| - |F_{calc}|| / \sum|F_{obs}|)$

[e] $R_{free} = R$ value for a randomly selected subset (5%) of the data that were not used for minimization of the crystallographic residual.

Highest resolution shell is shown in parenthesis.

[f] Numer of residues calculated with the program MolProbity (33).

Figure 1

a

b

c

d

Figure 2

121

Figure 3

a

WT HECT Δ α1

30 40 50 60 70   N   sec.

250 –
150 –
100 –
75 –
50 –

25 –
20 –

15 –
10 –

Huwe1-Ub$_n$

**
*

– Ub

b

WT HECT + α1

2 2.5 3 4 5   N   min.

250 –
150 –
100 –
75 –
50 –

25 –
20 –

15 –
10 –

Huwe1-Ub$_n$

**
*

– Ub

c

Autoubiquitination Activity

Sample	Ligation rate (min^{-1})
WT HECT Δ α1	11.475 ± 2.19
WT HECT + α1	0.454 ± 0.053

d

WT HECT Δ α1   WT HECT + α1

1 3 5 7 9 12   1 3 5 7 9 12   min.

Reducing

150 –
75 –
50 –
37 –

25 –

– HUWE1-Ub$_1$

Non-reducing

150 –
75 –
50 –
37 –

25 –

– HUWE1-Ub$_1$

– UBE2L3~Ub

N

1 3 5 7 9 12   min.

150 –
75 –
50 –
37 –

25 –

– UBE2L3~Ub

Figure 4

Figure 5

a

WT HECT Δ α1

2 2.5 3 4 5   N   min.

50 –
37 –
⊐ Mcl-1-Ub_n
– Mcl-1

b

WT HECT + α1

2 2.5 3 4 5   N   min.

50 –
37 –
⊐ Mcl-1-Ub_n
– Mcl-1

c

Mcl-1 Ubiquitination Activity

Sample	Ligation rate (min^{-1})
WT HECT Δ α1	0.635 ± 0.184
WT HECT + α1	0.130 ± 0.033

d

WT HECT Δ α1

e

WT HECT + α1

Figure 6

a

WT HECT Δ α1   WT HECT + α1
30 40 50 60 70   30 40 50 60 70   sec.

250 -
150 -
100 -
75 -

50 -

Huwe1-Ub$_n$

b

WT HECT Δ α1   WT HECT + α1
2 2.5 3 4 5   2 2.5 3 4 5   min.
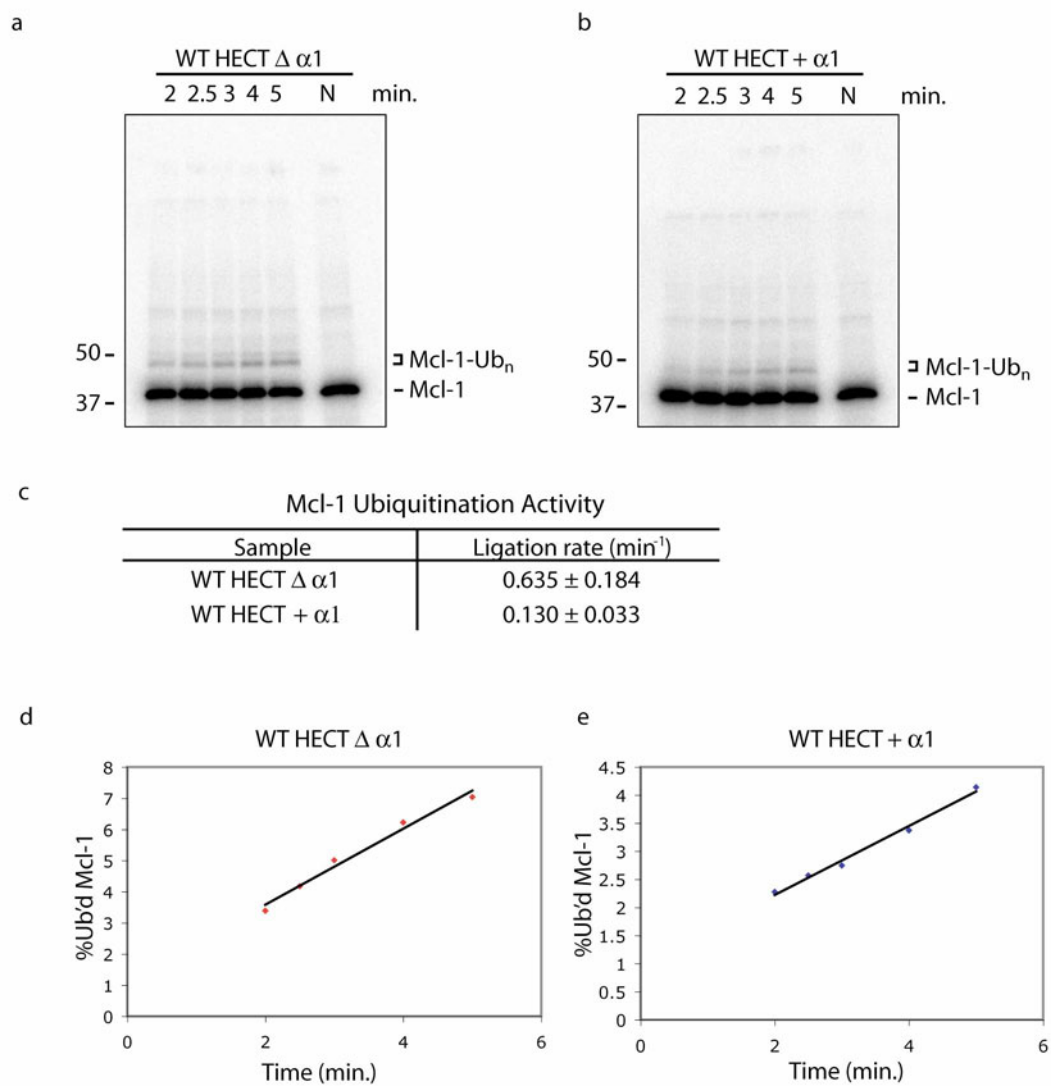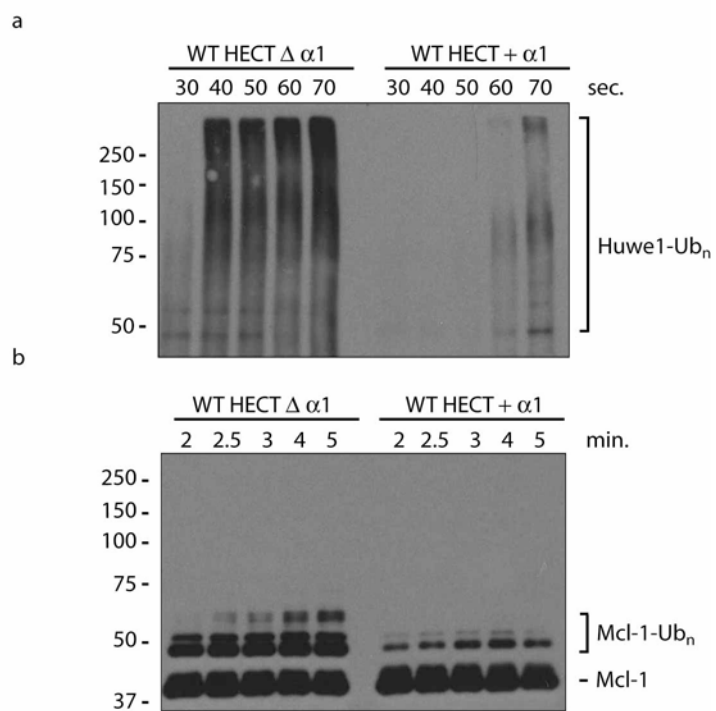
250 -
150 -
100 -

75 -

50 -

37 -

] Mcl-1-Ub$_n$
- Mcl-1

CHAPTER 4: SORTASE-CATALYZED CIRCULARIZATION OF HUWE1

HECT DOMAIN

Abstract

E3 Ub ligases catalyze the transfer of Ub to target proteins, providing a significant means of altering protein function in eukaryotes. The HECT class of Ub ligases interacts with E2~Ub thioester complex and substrate, forming a HECT~Ub thioester intermediate prior to catalyzing substrate ubiquitination. Crystal structures of E2-HECT complexes have shown that a significant rotation of the HECT C-lobe is required to bring E2 and E3 catalytic Cys in proximity to permit the transfer of Ub between active sites. We explored the requirement of conformational flexibility for HECT domain function using sortase-mediated circularization of the HECT domain. By ligating the N-and C-termini of the protein in a peptide linker of varying lengths, we show that restraining the motion of the HECT domain lobes perturbs HECT domain function, and we predict that function can be restored to circular HECT protein by increasing the length of the linker connecting the termini.

Introduction

The covalent attachment of ubiquitin (Scheffner and Staub) to target proteins regulates fundamental processes in eukaryotic cells, including cell cycle progression, signal transduction, DNA repair, and protein trafficking (Pickart 2001; Hershko 2005; Kerscher, Felberbaum et al. 2006; Bergink and Jentsch 2009; Broemer and Meier 2009). A sequential cascade of enzymatic reactions involving E1 activating enzyme, E2 conjugating enzyme, and E3 ligase catalyze Ub conjugation. The E1 enzyme binds ATP and Ub and catalyzes adenylation of Ub's C-terminus. The activated Ub is then transferred to the E1 active site-cysteine. The E1 enzyme interacts with a cognate E2 conjugating enzyme and transfers Ub to the E2 catalytic cysteine in a trans-thioesterification step. The final step of Ub conjugation is carried out by E3 Ub ligases, which bind both the E2~Ub (~ represents a covalent, high-energy thioester bond) and substrate and catalyze isopeptide bond formation between the Ub C-terminal glycine and a lysine residue in the substrate (Kerscher, Felberbaum et al. 2006). The human genome encodes approximately 28 E3 Ub ligases in the HECT (homologous to E6AP C terminus) class, which is defined by an ~350 amino acid C-terminal HECT domain containing a conserved catalytic cysteine that forms a thioester intermediate with Ub prior to its conjugation to a target lysine residue (Li, Bengtson et al. 2008). HECT domain E3 ligases serve numerous physiological roles – for example, in regulating cellular proliferation, apoptosis, and immune responses – and disruption of their function is associated with cancer and disease pathologies (Scheffner and Staub 2007; Bernassola, Karin et al. 2008).

An important question in discerning the mechanism of Ub conjugation is how Ub is transferred across the relatively large distance of juxtaposed enzyme active sites, a theme observed at multiple points in the Ub enzymatic cascade (Dye and Schulman 2007). For

example, a distance of 35 Å separates the Ub C terminus in the Ub E1 adenylation active site from the E1's active-site cysteine (Protein Data Bank (PDB) entry 3CMM (Lee and Schindelin 2008)); in the crystal structure of the E6AP-UbcH7 complex (PDB codes 1C4Z and 1D5F), the catalytic cysteines of E2 and E3 are separated by 41 Å (Huang, Kinnucan et al. 1999). Insights into the mechanism of Ub transfer have come from structural and biochemical studies of Ub enzymatic machinery. In the case of HECT domain E3 Ub ligases, structures of the WWP1 HECT domain, and more recently, the UbcH5B~Ub-HECT[NEDD4L] complex, have contributed to our understanding of this problem (Verdecia, Joazeiro et al. 2003; Kamadurai, Souphron et al. 2009). The WWP1 HECT domain, in comparison to the E6AP HECT domain, exhibits a ~100° rotation of the C-lobe with respect to the N-lobe about a flexible linker connecting the two subdomains, placing the E3 catalytic cysteine within 16 Å of the E2 UbcH5 modeled into its binding site on WWP1 (Verdecia, Joazeiro et al. 2003). The UbcH5B~Ub-HECT[NEDD4L] complex structure shows how, in addition to the conformational flexibility of the HECT domain, non-covalent interactions between the HECT C-lobe and UbcH5~Ub contribute to the E2 to E3 Ub transfer reaction. In the structure of this complex, the NEDD4L active site cysteine is 8 Å from the Ub C-terminus (Kamadurai, Souphron et al. 2009).

The HECT domain E3 ligase HUWE1 (also called ARF-BP1, Mule, Lasu1, E3 histone, and HectH9) is a large, 482-kDa protein that functions in the regulation of cell proliferation, apoptosis, DNA damage response, and base excision repair (Adhikary, Marinoni et al. 2005; Chen, Kon et al. 2005; Zhong, Gao et al. 2005; Hall, Kow et al. 2007; Herold, Hock et al. 2008; Zhao, Heng et al. 2008; Parsons, Tait et al. 2009). Following structural and biochemical characterization of the HUWE1 HECT domain (Pandya, Partridge et al.), we sought to gain insights into its mechanism of function that are difficult to obtain from static crystal structures.

We chose to employ a protein engineering method, sortagging (Popp, Antos et al. 2007), in an effort to perturb the conformational flexibility of the HECT domain and follow the consequences to its activity. Specifically, we applied sortase-catalyzed circularization (Antos, Popp et al. 2009) to the HECT domain. We reasoned that ligation of the HECT domain N- and C-termini would be a means of restraining the dynamic movement of the N- and C-lobes, with attendant, measurable consequences for activity. We report here our novel application of the sortagging technique to the study of HECT domain function.

Results and Discussion

Circularization of HUWE1-sortag1

Inspection of the HUWE1 crystal structure (PDB code 3H1D) shows that ~13.3 Å separates the N- and C-termini. As the eight residues at the C-terminus are not visible in the structure, this is the distance between the first residue in the native structure and E4366, the C-terminal most visible residue. We reasoned that this distance could be spanned by insertion of a minimal linker encoding the sortase recognition sequence. Addition of the sortase recognition sequence (LPETG) to a target protein's C-terminus permits sortase to catalyze site-specific installation of exogenously added, oligoglycine nucleophiles (Figure 1a (Popp, Antos et al. 2009)). If the oligoglycine nucleophile is appended to the target protein's N-terminus instead of provided exogenously, sortase catalyzes a circularization of the target protein through ligation of the N- and C-termini (Figure 1b; (Antos, Popp et al. 2009)). We designed a construct (referred to as HUWE1-sortag1) capable of undergoing sortase-catalyzed circularization by appending three glycines at the N-terminus of HUWE1, and the sortase recognition sequence (LPETG) followed by a short linker (GGS) and a His$_6$ tag at the C-terminus (GGG-HUWE1-LPETGGGS-

His$_6$). Incubation of recombinant HUWE1 containing these sequences with sortase A resulted in

~50% conversion to a product that migrated more rapidly on SDS-PAGE (Figure 2a, lane 2).

Incubation of the reaction mixture with NiNTA depleted unreacted HUWE1 and sortase A,

enriching for the putative circular HUWE1 (Figure 2a, lane 3). Evidence of circularization was

provided by mass spectral characterization of the input and circular HUWE1 proteins, revealing

a loss of 1098 Da after sortase-catalyzed circularization (Figure 2b). This mass change

correlates well with that calculated from the expected loss of the C-terminal peptide GGGSHis$_6$

(MW = 1099.1 Da) following sortase cleavage and transpeptidation reaction. MS/MS sequencing

of proteolytic peptides obtained from circular HUWE1 showed ligation of the termini (Figure

2c).

Previous reports noted that circular proteins possess increased thermal stability compared

to their linear counterparts (Iwai and Pluckthun 1999; Scott, Abel-Santos et al. 1999; Iwai,

Lingel et al. 2001; Antos, Popp et al. 2009). Consistent with these observations, the melting

temperature of circular HUWE1 (58.2 ℃) is 2.1 ℃ greater than linear HUWE1 (56.1 ℃, Figure

2d). Although the magnitude of thermal stability gained by HUWE1 upon circularization is

small, it suggests that circularization has not greatly destabilized the protein.

Biochemical characterization of circular HUWE1-sortag1

We hypothesized that ligation of HUWE1's N- and C-termini may have functional

consequences for HUWE1 activity. We first examined the ability of linear and circular HUWE1

proteins to bind the ubiquitin C-terminal electrophile HA-UbVME, a probe consisting of HA-

tagged ubiquitin derivitized at the C-terminus with the electrophilic vinyl methyl ester moiety.

HA-UbVME covalently reacts with multiple cysteines in HUWE1, including its catalytic

cysteine (C4341), and only reacts with HUWE1 HECT domain in its native folded state (Love, Pandya et al. 2009). Incubation of linear and circular HUWE1 with HA-UbVME produced a nearly identical pattern of covalently labeled species (Figure 3a), suggesting that the overall fold of the circular protein is intact. To determine the biochemical consequences of ligation of the HUWE1 termini, we examined the autoubiquitination activity of wild-type HUWE1 HECT domain, a control version of the HECT domain that contains the three N-terminal glycines and a C-terminal LPET sequence, and the circular protein. The control protein was added for comparison because it has been shown that minor extensions to or deletions from the C-terminus of HECT domains impair activity (Salvat, Wang et al. 2004). Incubation of wild-type HUWE1 HECT domain with Ube1, the E2 UBE3L3, ATP, and Ub, results in robust autoubiquitination of HUWE1, as determined by anti-Ub immunoblot (Figure 3b). The control HUWE1 HECT domain with the C-terminal LPET sequence exhibits reduced activity, as expected, but still retains the ability to add up to two ubiquitin moieties to itself. In contrast, the circular protein is inactive in this assay (Figure 3b). Taken together, these results suggest that although the circular HUWE1-sortag1 retains its proper fold in solution, it is unable to catalyze isopeptide bond formation between Ub and target lysines in itself.

Catalysis by HECT domain Ub ligases involves multiple steps. The E3 enzyme binds Ub-loaded E2 and substrate followed by Ub transfer between the E2 and E3 catalytic cysteines. The E3 then catalyzes isopeptide bond formation between Ub and a lysine residue on the substrate, which may be the E3 itself, Ub, or another protein. We asked whether the lack of autoubiquitination activity in circular HUWE1 was due to impairment in the immediate upstream step, in which the catalytic cysteine of the E3 enzyme forms a thioester bond with ubiquitin. We examined HECT domain activity in a single-turnover reaction to monitor the ability of the HECT

domain to accept Ub from the E2. This assay encompasses two steps. In the first step, E2 ~ Ub

thioester is generated by incubating E1, E2, an ATP regenerating system, and Ub. After the E2 ~

Ub thioester has formed, this reaction is quenched by the addition of EDTA to prevent further

E1-catalyzed activation of Ub. In the second step, the HUWE1 HECT domain is added, and Ub

is chased from the E2~thioester onto the HECT domain (Eletr, Huang et al. 2005). The use of a

mutant version of Ub, in which all lysines are mutated to arginine (K0 Ub), prevents

polyubiquitin chain formation on the HECT domain. Ub-conjugated HECT domain is visualized

using anti-Ub immunoblot (Figure 3c). The wild-type enzyme rapidly catalyzes isopeptide bond

formation, preventing detection of a Ub-thioester intermediate on the E3, as previously observed

(Figure 3c, lower panel; (Pandya, Partridge et al.). The control (C-terminally LPET modified)

HUWE1, which exhibits reduced autoubiquitination activity, forms E3~Ub thioester

intermediates readily detected within three minutes, indicating that this version of the protein is

still able to accept Ub from UBE2L3 (Figure 3c, middle panel). Circular HUWE1, however, is

unable to accept Ub from UBE2L3 (Figure 3c, upper panel). Although we must verify that the

circular protein binds the E2 enzyme with similar affinity as the wild-type HUWE1 (for

example, by isothermal titration calorimetry), these results suggest that ligation of the termini of

HUWE1 may restrain the dynamic motion of the N- and C-lobes during catalysis, preventing the

catalytic cysteine of circular HUWE1-sortag1 from accepting Ub from UBE2L3.

If our hypothesis that circularization of HUWE1 restricts the motion of the N- and C-

lobes is true, we should be able to restore conformational flexibility to circular HUWE1 by

increasing the length of the linker between the N- and C-termini and observe a corresponding

restoration of autoubiquitination activity to control levels. We therefore cloned and expressed

recombinant HUWE1 in which we appended an additional four residues (GGGS) to the N-

terminus alongside the existing three glycines (GGGSGGG-HUWE1-LPETGGGSHis$_6$; termed HUWE1-sortag2). We may find that this circularized version of HUWE1 fails to regain autoubiquitination activity, in which case we will continue to extend the number of residues at the N-terminus of HUWE1 to determine if a sufficiently long linker will restore activity to the circularized HUWE1.

An additional property of sortase-catalyzed circularization of HUWE1 that remains to be verified is its reversibility (Antos, Popp et al. 2009). The LPETG recognition sequence is intact in the circular protein and therefore should be available for sortase-catalyzed cleavage and transpeptidation upon inclusion of an oligoglycine nucleophile and sortase in the reaction. Although incorporation of a high concentration (>100 mM) soluble Gly$_3$ peptide in the reaction mixture with linear HUWE1-sortag1 allows quantitative sortase-catalyzed transacylation of Gly$_3$ onto HUWE1's C-terminus, this re-opening reaction proceeds inefficiently, if at all, with circular HUWE1-sortag1 (data not shown). It has been shown that sortase is capable of cleaving at LPETG motifs outside of the target protein's C-terminus if they are placed within flexible, surface-exposed loops (Antos, Popp et al. 2009). Given that the overall stability of circular HUWE1 is similar to linear HUWE1 (Figure 2d), we hypothesize that the LPETG motif in circular HUWE1 is locked in a conformation inaccessible to sortase. It is possible that use of a stronger nucleophile, such as hydroxylamine (NH$_2$OH), will allow the re-opening reaction to proceed to a further extent.

Structural studies have revealed mechanistic information on the enzymatic activation and conjugation of Ub (Dye and Schulman 2007). A major theme that has emerged from these studies is that a considerable conformational change is required to juxtapose enzyme active sites to achieve Ub transfer. This is particularly true for the HECT class of E3 Ub ligases. A

comparison of the WWP1 and E6AP structures revealed that two major motions of the WWP1 C-lobe distinguish the different conformations of the HECT domain in these structures: a 100º rotation of the C-lobe about an imaginary y-axis running through the hinge loop connecting N- and C-lobes, and an approximately 30º tilt of the C lobe toward the N lobe (Verdecia, Joazeiro et al. 2003). Mutational analysis of the WWP1 flexible hinge loop (extensions and deletions) was conducted to determine the functional relevance of the observed conformational differences to HECT domain autoubiquitination activity and suggested that the ability of the C-lobe to rotate with respect to the N-lobe is critical for HECT E3 Ub ligase activity. We present here a novel method of examining conformational flexibility of HECT domain E3 Ub ligases.

We hypothesized that sortase-mediated circularization of the HECT domain could be used to probe the role of conformational flexibility in HECT domain function. Examination of existing HECT domain structures shows that the distance between N- and C-termini varies substantially (13 Å for HUWE1; 41 Å for Smurf2) and does not correlate with the distance between E2 and E3 active sites (for example, in the structure of the UbcH5B~Ub-HECT[NEDD4L] complex, E2 and E3 active sites are separated by 8 Å, while the Nedd4L HECT domain termini are 26 Å apart). We reasoned that, at least in the case of HUWE1, ligation of the N- and C-termini may restrain the dynamic movement of the HECT N- and C-lobes, and consequently reduce or abolish activity of the HECT domain. We therefore designed a construct containing a minimal number of residues required to achieve circularization (seven residues, predicted to span approximately 25 Å), and we indeed find that this circularized protein loses activity (Figure 3b, c). A prediction of our hypothesis is that a sufficiently long linker joining the N- and C-termini of HUWE1 will permit a normal range of rotation between N- and C-lobes, and hence restore activity to control levels. We have therefore designed a construct containing an additional four

residues at the N-terminus to generate an eleven-residue long linker, and we eagerly anticipate

testing the autoubiquitination activity of a circular HUWE1 containing this extended linker.

Circularization of the HUWE1 HECT domain represents a novel method to probe the role

of conformational flexibility in E3 Ub ligase function. Previously, conformational dynamics of

Ub pathway enzymes have been explored through a variety of methods. Duda *et. al*. used a

combination of structure determination, small-angle X-ray scattering (SAXS) analysis, and

proteolytic mapping to obtain insights into how covalent attachment of the ubiquitin-like

modifier Nedd8 to Cullin-RING ligases (CRLs) affords conformational control of CRL activity

(Duda, Borg et al. 2008).   NMR (Hamilton, Ellison et al. 2001; Wang, Lee et al. 2009) and

amide hydrogen exchange mass spectrometry (HX-MS) (Graf, Stankiewicz et al.) have also been

used to gain insight into E2 and E3 enzyme function and conformation. We now add sortase-

mediated engineering of HECT domain E3 Ub ligases to the list of methodology that can be used

to obtain mechanistic information on Ub transfer in the E1-E2-E3 enzymatic cascade.

Experimental Procedures

Cloning and Protein Expression

Sortase A (residues 26-206) was cloned into pQE30 (Qiagen) containing an N-terminal His$_6$ tag

for use in purification. HUWE1 HECT domain (residues 3993-4374) was cloned into a modified

pET-28a plasmid (Novagen) containing a human rhinovirus 3C (HRV3C) protease site. Two

constructs were generated to circularize the HUWE1 HECT domain (termed HUWE1-sortag1

and HUWE1-sortag2). The N-terminus of both constructs contained three glycines followed by

either no spacer (HUWE1-sortag1) or a short spacer, SGGG (HUWE1-sortag2). The C-terminus

of both constructs contains the sortase A recognition site, followed by a short spacer and a

hexahistidine tag (GGG-HECT-LPETGGGSHHHHHH or GGGSGGG-HECT-

LPETGGGSHHHHHH, respectively). UBE2L3 was cloned into the pET-28a plasmid to

generate an untagged protein for bacterial protein expression.

Bacterial Protein Expression and Purification

UBE2L3 and both version of HUWE1 HECT domain were purified as previously described

(Pandya, Partridge et al.). Sortase A was purified as described (Popp, Antos et al. 2009), and

eluted protein was further purified by gel filtration (Superdex 75 PC 3.2/30, GE Healthcare) in

50 mM Tris pH 8.0, 150 mM NaCl with 10% (w/v) glycerol.

MS/MS sequencing of Proteolytic Fragments from Circular Proteins

Protein was excised for analysis from a coomassie-stained SDS-PAGE gel and digested with

AspN at 37 ºC overnight. The proteolysed peptides were extracted, concentrated, and injected

onto a Waters NanoAcquity HPLC equipped with a self-packed Jupiter 3 uM C18 analytical

column (0.075 mm X 10 cm, Phenomenex). Peptides were eluted using standard reverse-phase gradients. The effluent from the column was analyzed using a Thermo LQT linear ion trap mass spectrometer in a nanospray configuration operated in a data-dependent manner. The resulting fragmentation spectra were correlated against the known database using SEQUEST.

ESI-MS analysis of linear and circular HUWE1 proteins

Intact Molecular weight was determined by RP-HPLC/ MS (Reversed Phase High Performance Liquid Chromatography Mass Spectrometry). A 2.1 x 50 mm Waters Symmetry C18 column was used with a Michrom Bioresources Paradigm4 HPLC. Buffer A consisted of 0.1% Formic Acid in water and buffer B was acetonitrile. The flow was set to 150 ul / min. with a gradient of 5% to 45% B in 10 min. The column effluent was coupled directly to the ESI (electrospray ionization) source on a Waters (Micromass) LCT Time-of-Flight Mass Spectrometer operated at a resolution of 5000 (FWHM). Data was acquired over the range of 400 – 1800 m/z. Data acquisition used Water's MassLynx software and deconvolution was performed using Waters MaxEnt1 software add-on.

Melting temperature assay

The melting temperature of HUWE1 was measured in a Roche LightCycler 480 assay. 4.4 μm HUWE1 in 50 mM Tris pH 7.5, 150 mM NaCl, 10 mM $CaCl_2$, 2 mM DTT, and 10% glycerol was mixed with 5 μL 100x Sypro Orange dye (Molecular Probes/Invitrogen) in 25 μL total volume per well of a 96-well plate. Melting curves were recorded on the LightCycler 480 instrument using 465/580 nm filters with continuous heating from ambient temperature to 95ºC. Data were exported in text format and analyzed using Microsoft Excel. Melting points are

defined as half maximal value of the unfolding curve, corresponding to the curve's inflection point as determined by the minimal value of the –(dFluoresence/dT) plot. Shown are the average and standard deviation of three replicates.

Sortase-catalyzed circularization reactions

To circularize the HUWE1 HECT domain, 50 μM HECT domain was incubated with 50 μM sortase A in sortase reaction buffer (50 mM Tris pH 7.5, 150 mM NaCl, 10 mM $CaCl_2$) with 10% (w/v) glycerol and 2 mM DTT for 7.25 hours at 24 ℃. Sortase A and unreacted HECT domain were removed by incubation of the reaction with NiNTA (GE Healthcare) for 1 hour at 4 ℃. Unbound protein was concentrated (Amicon, 10 kD cutoff) and further purified by gel filtration (Superdex 75 PC 3.2/30, GE Healthcare) in 50 mM Tris pH 7.5, 150 mM NaCl, 5 mM $MgCl_2$, 2 mM DTT, 10% (w/v) glycerol.

Reaction of HUWE1 with HAUbVME probe

11 μM HUWE1 (linear or circularized) was incubated with 0.5 μg HAUbVME in 50 mM Tris pH 8.0, 150 mM NaCl in a 10 μl reaction volume for 3 hours at 24 °C. The reaction was quenched with reducing sample buffer, boiled 10 minutes, and separated on 10% SDS-PAGE. Proteins were visualized by coomassie blue staining.

Biochemical Assays

Autoubiquitination assay

Reaction mixtures (10 μl) for HUWE1 autoubiquitination assay contained 100 nM human E1 (Ube1, Boston Biochem), 5.6 μM E2 (UBE2L3), 2.8 μM HECT domain, and 60 μM Ub (Sigma)

with an ATP-regenerating system (50 mM Tris pH 7.6, 5 mM $MgCl_2$, 5 mM ATP, 10 mM creatine phosphate, 3.5 units/mL creatine kinase). Reactions were incubated at room temperature, and aliquots were removed after the indicated amount of time and terminated in reducing SDS-PAGE sample buffer. Samples were boiled for 10 min, separated on 10% Tris-glycine SDS-PAGE, and analyzed by immunoblot using anti-Ub antibody (Sigma).

Single-turnover Assay

For the single-turnover assay, the E2~Ub thioester was generated in a 20-μl reaction containing 200 nM E1 (Boston Biochem), 8 μM E2, the ATP regenerating system described above, 60 μM mutant Ub in which all lysines were mutated to arginine (K0 Ub) (Boston Biochem), and 1 μg/μL bovine serum albumin incubated for 25 min at room temperature. Formation of the E2~Ub thioester was quenched with 50 mM EDTA on ice for 5 min. The E2~Ub thioester was diluted into a chase mixture containing 4 μM HECT domain, 100 mM NaCl, 50 mM EDTA, and 1 μg/μL bovine serum albumin. Reactions were incubated at room temperature, and aliquots were removed after the indicated amount of time and terminated in either 4 M urea and incubated for 15 min at 30 °C or in reducing SDS-PAGE sample buffer. Samples were boiled for 10 min, separated on 10% Tris-glycine SDS-PAGE, and analyzed by immunoblot using anti-Ub antibody (Sigma).

References

Adhikary, S., F. Marinoni, et al. (2005). "The ubiquitin ligase HectH9 regulates transcriptional activation by Myc and is essential for tumor cell proliferation." <u>Cell</u> **123**(3): 409-21.

Antos, J. M., M. W. Popp, et al. (2009). "A straight path to circular proteins." <u>J Biol Chem</u> **284**(23): 16028-36.

Bergink, S. and S. Jentsch (2009). "Principles of ubiquitin and SUMO modifications in DNA repair." <u>Nature</u> **458**(7237): 461-7.

Bernassola, F., M. Karin, et al. (2008). "The HECT family of E3 ubiquitin ligases: multiple players in cancer development." <u>Cancer Cell</u> **14**(1): 10-21.

Broemer, M. and P. Meier (2009). "Ubiquitin-mediated regulation of apoptosis." <u>Trends Cell Biol</u> **19**(3): 130-40.

Chen, D., N. Kon, et al. (2005). "ARF-BP1/Mule is a critical mediator of the ARF tumor suppressor." <u>Cell</u> **121**(7): 1071-83.

Duda, D. M., L. A. Borg, et al. (2008). "Structural insights into NEDD8 activation of cullin-RING ligases: conformational control of conjugation." <u>Cell</u> **134**(6): 995-1006.

Dye, B. T. and B. A. Schulman (2007). "Structural mechanisms underlying posttranslational modification by ubiquitin-like proteins." <u>Annu Rev Biophys Biomol Struct</u> **36**: 131-50.

Eletr, Z. M., D. T. Huang, et al. (2005). "E2 conjugating enzymes must disengage from their E1 enzymes before E3-dependent ubiquitin and ubiquitin-like transfer." <u>Nat Struct Mol Biol</u> **12**(10): 933-4.

Graf, C., M. Stankiewicz, et al. "Insights into the conformational dynamics of the E3 ubiquitin ligase CHIP in complex with chaperones and E2 enzymes." <u>Biochemistry</u> **49**(10): 2121-9.

Hall, J. R., E. Kow, et al. (2007). "Cdc6 stability is regulated by the Huwe1 ubiquitin ligase after DNA damage." <u>Mol Biol Cell</u> **18**(9): 3340-50.

Hamilton, K. S., M. J. Ellison, et al. (2001). "Structure of a conjugating enzyme-ubiquitin thiolester intermediate reveals a novel role for the ubiquitin tail." <u>Structure</u> **9**(10): 897-904.

Herold, S., A. Hock, et al. (2008). "Miz1 and HectH9 regulate the stability of the checkpoint protein, TopBP1." <u>EMBO J</u> **27**(21): 2851-61.

Hershko, A. (2005). "The ubiquitin system for protein degradation and some of its roles in the control of the cell division cycle." <u>Cell Death Differ</u> **12**(9): 1191-7.

Huang, L., E. Kinnucan, et al. (1999). "Structure of an E6AP-UbcH7 complex: insights into ubiquitination by the E2-E3 enzyme cascade." <u>Science</u> **286**(5443): 1321-6.

Iwai, H., A. Lingel, et al. (2001). "Cyclic green fluorescent protein produced in vivo using an artificially split PI-PfuI intein from Pyrococcus furiosus." <u>J Biol Chem</u> **276**(19): 16548-54.

Iwai, H. and A. Pluckthun (1999). "Circular beta-lactamase: stability enhancement by cyclizing the backbone." <u>FEBS Lett</u> **459**(2): 166-72.

Kamadurai, H. B., J. Souphron, et al. (2009). "Insights into ubiquitin transfer cascades from a structure of a UbcH5B approximately ubiquitin-HECT(NEDD4L) complex." <u>Mol Cell</u> **36**(6): 1095-102.

Kerscher, O., R. Felberbaum, et al. (2006). "Modification of proteins by ubiquitin and ubiquitin-like proteins." <u>Annu Rev Cell Dev Biol</u> **22**: 159-80.

Lee, I. and H. Schindelin (2008). "Structural insights into E1-catalyzed ubiquitin activation and transfer to conjugating enzymes." <u>Cell</u> **134**(2): 268-78.

Li, W., M. H. Bengtson, et al. (2008). "Genome-wide and functional annotation of human E3 ubiquitin ligases identifies MULAN, a mitochondrial E3 that regulates the organelle's dynamics and signaling." <u>PLoS One</u> **3**(1): e1487.

Love, K. R., R. K. Pandya, et al. (2009). "Ubiquitin C-terminal electrophiles are activity-based probes for identification and mechanistic study of ubiquitin conjugating machinery." <u>ACS Chem Biol</u> **4**(4): 275-87.

Pandya, R. K., J. R. Partridge, et al. "A structural element within the HUWE1 HECT domain modulates self-ubiquitination and substrate ubiquitination activities." <u>J Biol Chem</u> **285**(8): 5664-73.

Parsons, J. L., P. S. Tait, et al. (2009). "Ubiquitin ligase ARF-BP1/Mule modulates base excision repair." <u>EMBO J</u> **28**(20): 3207-15.

Pickart, C. M. (2001). "Mechanisms underlying ubiquitination." <u>Annu Rev Biochem</u> **70**: 503-33.

Popp, M. W., J. M. Antos, et al. (2007). "Sortagging: a versatile method for protein labeling." <u>Nat Chem Biol</u> **3**(11): 707-8.

Popp, M. W., J. M. Antos, et al. (2009). "Site-specific protein labeling via sortase-mediated transpeptidation." <u>Curr Protoc Protein Sci</u> **Chapter 15**: Unit 15 3.

Salvat, C., G. Wang, et al. (2004). "The -4 phenylalanine is required for substrate ubiquitination catalyzed by HECT ubiquitin ligases." <u>J Biol Chem</u> **279**(18): 18935-43.

Scheffner, M. and O. Staub (2007). "HECT E3s and human disease." <u>BMC Biochem</u> **8 Suppl 1**: S6.

Scott, C. P., E. Abel-Santos, et al. (1999). "Production of cyclic peptides and proteins in vivo." <u>Proc Natl Acad Sci U S A</u> **96**(24): 13638-43.

Verdecia, M. A., C. A. Joazeiro, et al. (2003). "Conformational flexibility underlies ubiquitin ligation mediated by the WWP1 HECT domain E3 ligase." <u>Mol Cell</u> **11**(1): 249-59.

Wang, J., B. Lee, et al. (2009). "Conformational transition associated with E1-E2 interaction in small ubiquitin-like modifications." <u>J Biol Chem</u> **284**(30): 20340-8.

Zhao, X., J. I. Heng, et al. (2008). "The HECT-domain ubiquitin ligase Huwe1 controls neural differentiation and proliferation by destabilizing the N-Myc oncoprotein." <u>Nat Cell Biol</u> **10**(6): 643-53.

Zhong, Q., W. Gao, et al. (2005). "Mule/ARF-BP1, a BH3-only E3 ubiquitin ligase, catalyzes the polyubiquitination of Mcl-1 and regulates apoptosis." <u>Cell</u> **121**(7): 1085-95.

Figure Legends

Figure 1. Sortase-catalyzed circularization of the HUWE1 HECT domain.

(a) Site-specific labeling of target protein C-termini through sortase-catalyzed transpeptidation. Sortase A recognizes the LPXTG motif at the C-terminus of the target protein and cleaves between the threonine and glycine to generate an acyl-enzyme intermediate. This covalent intermediate is resolved by the nucleophilic attack of the amino-group of a modified oligoglycine-based probe to form the transpeptidation product with the probe installed at the target protein C-terminus. Figure adopted from (Popp, Antos et al. 2009).

(b) Sortase A catalyzes intermolecular transpeptidation as described in (a) when the oligoglycine nucleophile is provided exogenously. If one or more glycines is instead appended to the target protein's N-terminus, sortase will catalyze an intramolecular reaction to generate a circular protein. Figure adapted from (Antos, Popp et al. 2009).

C) Structures of the HECT domains of Smurf 2 (PDB entry 1ZVD), Huwe1 (PDB entry 3H1D), and UbcH5B~Ub-HECT^{NEDD4L} (PDB entry 3JW0) with the E3 catalytic cysteine highlighted in yellow and the distance between N- and C-termini indicated.

Figure 2. Circularization of HUWE1-sortag1.

(a) Input HUWE1-sortag 1 (50 μM) (lane 1) was incubated with sortase A (50 μM) for 7 hr at room temperature in sortase reaction buffer as described (lane 2). Unreacted HUWE1-sortag1

and Sortase A were depleted by incubation with NiNTA to purify circular HUWE1 (lane 3). Proteins were separated by SDS-PAGE and visualized by coomassie blue staining.

(b) ESI-MS characterization of input (left) and circular (right) HUWE1 molecular weight revealed the expected change in mass after circularization results in loss of the C-terminal ten residues as well as a water molecule.

(c) MS/MS spectrum of an AspN fragment of circular HUWE1-sortag1 showing the ligation of the N-terminal residues to the C-terminal LPET motif. Expected masses for y and b ions are listed above and below the peptide sequence. Ions that were positively highlighted in the MS/MS spectrum are highlighted in blue and red.

(d) Thermal stability of linear and circular HUWE1. Protein is incubated with a fluorescent dye that binds exposed hydrophobic regions of unfolded protein. Normalized fluorescence is measured as a function of temperature as the protein is heated from 25ºC to 95ºC. Shown is the plot of the first derivative of the unfolding curve against temperature, used to calculate the curve's inflection point.

Figure 3. Biochemical characterization of HUWE1-sortag1.

(a) 11.0 μM HUWE1-sortag1 (linear or circular) was incubated with 0.5μg HA-UbVME for 3 hr at room temperature. The reaction was quenched with reducing sample buffer and separated by

SDS-PAGE. Proteins were visualized by coomassie-blue staining.   Covalently bound, probe-labeled species are indicated.

(b) Autoubiquitination activity of wild-type, control (LPET), and circular HUWE1-sortag1 was tested using 60 μM Ub as substrate and 2.8 μM HECT domains incubated with UBE1, UBE2L3, and an ATP regenerating system. Ubiquitinated proteins were visualized by anti-Ub immunoblot.

(c) Thioester formation of wild-type, control (LPET), and circular HUWE1-sortag1 was tested in a single-turnover pulse-chase assay monitoring transfer of Ub from the UBE2L3~Ub thioester to the catalytic cysteine in the HECT domain. The UBE2L3~Ub thioester is generated in a pulse reaction containing E1, UBE2L3, ATP regenerating system, and a Ub mutant in which all lysines are mutated to arginine (K0 Ub). Ub is chased from the E2 enzyme to the HECT domain added to the reaction. Ub-conjugated HECT domain is visualized by anti-Ub immunoblot. Samples were terminated in reducing or non-reducing sample buffer as indicated. The wild-type HECT domain transfers Ub to one or more lysines in the time scale of the reaction, obscuring detection of the HECT~Ub intermediate.
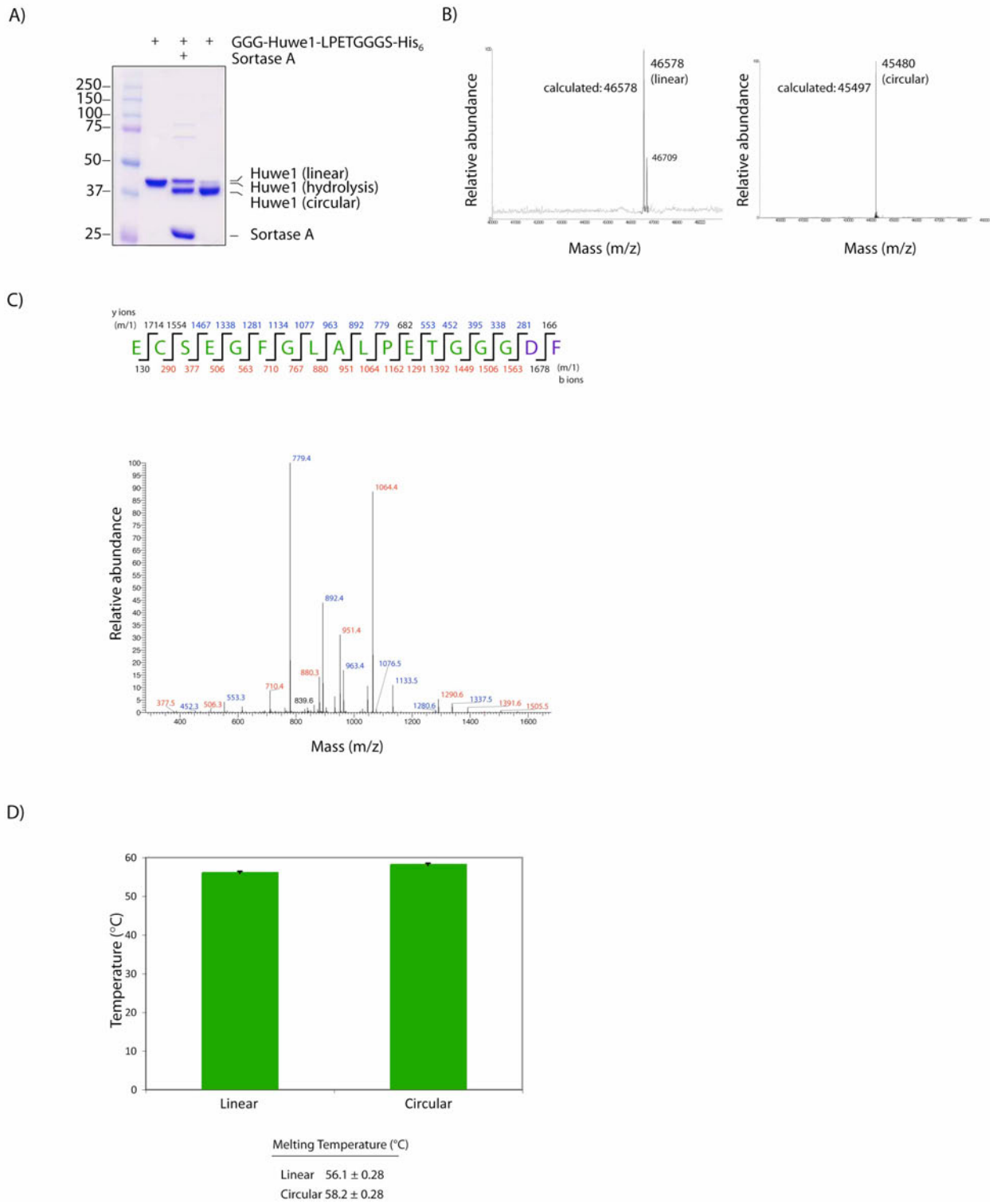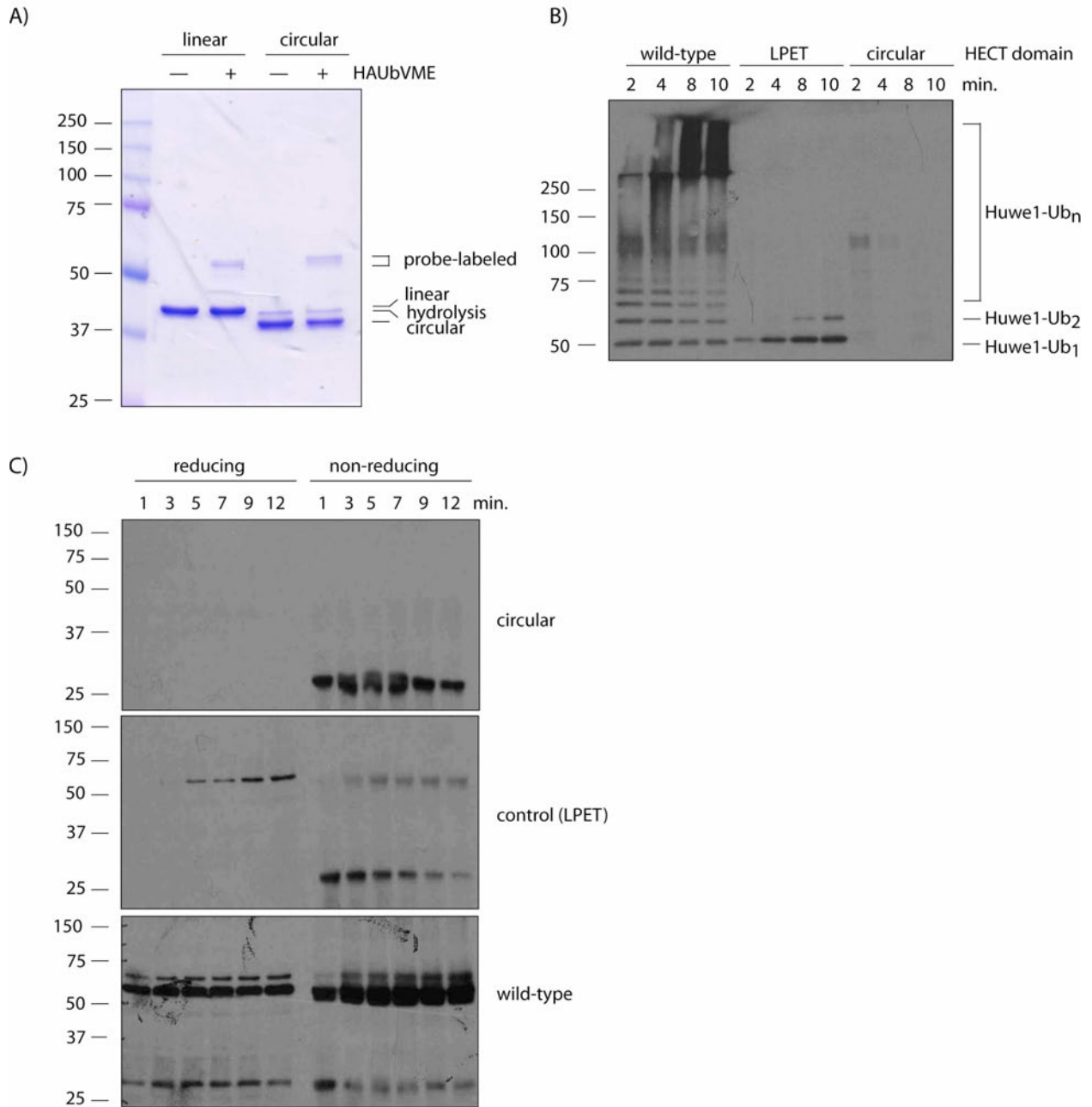
Figure 1

Figure 2

A)

B)

C)

D)

Melting Temperature (°C)

Linear   56.1 ± 0.28
Circular 58.2 ± 0.28

Figure 3

A)

B)

C)
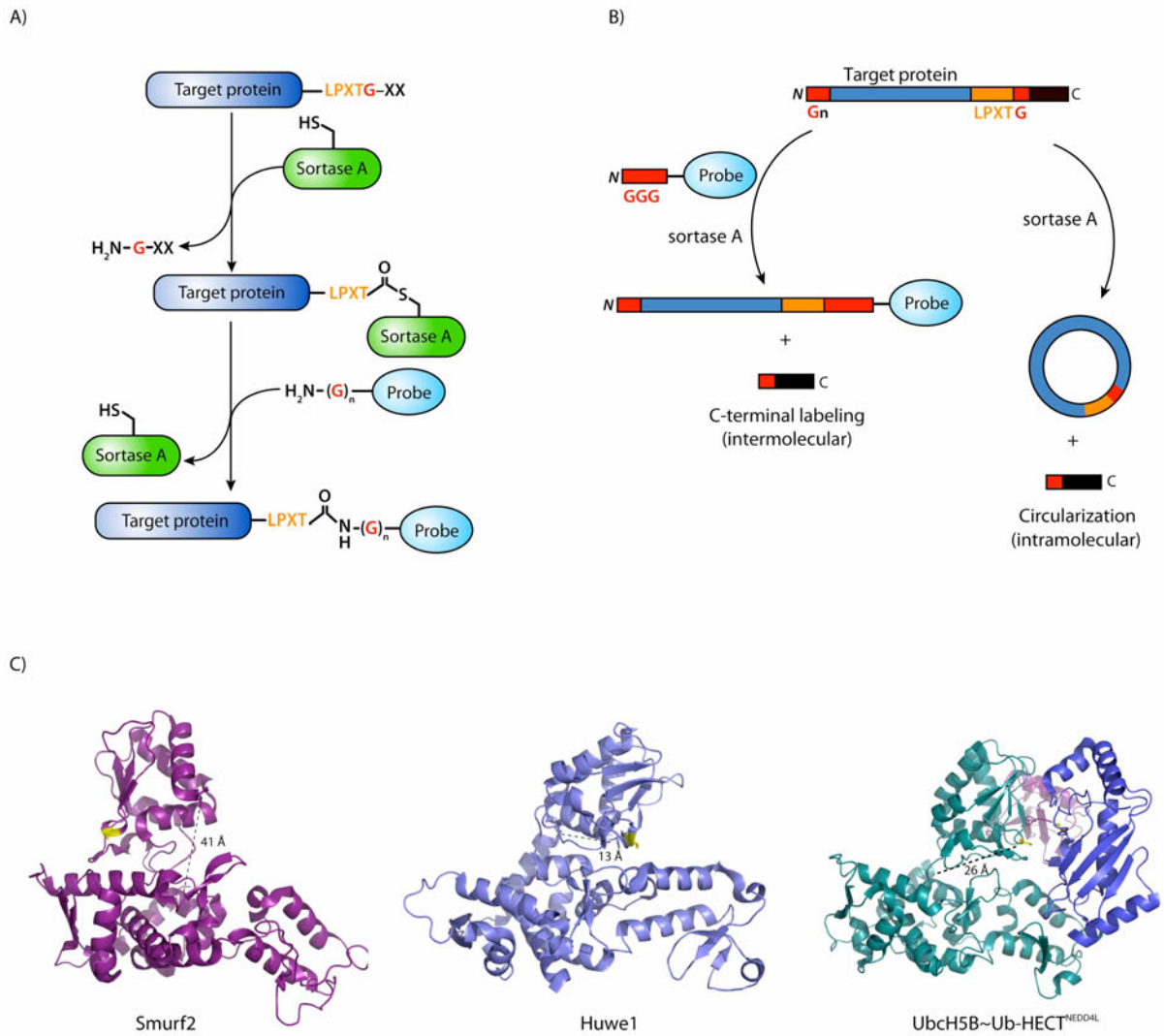
CHAPTER 5: FUTURE DIRECTIONS

Summary

Covalent attachment of the small, highly conserved protein ubiquitin (Ub) to target proteins is an important means of regulating eukaryotic protein function. Ub conjugation can alter a protein's half-life, subcellular localization, enzymatic activity, or its ability to interact with other proteins. A sequential cascade of enzymatic reactions catalyzed by Ub activating (E1), Ub conjugating (E2), and Ub ligase (E3) enzymes is required to achieve Ub conjugation. In general, Ub is covalently attached via its C-terminal glycine residue to a lysine residue in a target protein in an isopeptide linkage. The human genome encodes two Ub E1 activating, ~30 Ub E2 conjugating, and over 300 Ub E3 ligase enzymes (Li, Bengtson et al. 2008). The identification and biochemical characterization of these enzymes and their substrates has provided insight into the mechanism of Ub conjugation and its cellular function, although important questions remain to be answered. In this thesis, we describe the design of Ub-based electrophilic probes and their use to identify Ub conjugation machinery from cell extracts. Incubation of Ub-electrophilic probes with cell lysates from either a human mammary epithelial cell line or a murine thymoma cell line covalently labeled the active sites of representative members of the Ub protease family, as well as E2 and E3 enzymes, allowing for their retrieval and identification by tandem mass spectrometry. This work shows that Ub-based probes can be useful not only for the identification of Ub proteases from cell lysates, as previously shown, but also for enzymes responsible for Ub conjugation. Following our recovery of the E3 Ub ligase HUWE1, we undertook a biochemical and structural analysis of this enzyme. Our results provide a definition of the HECT domain boundary and show how minor extensions of what was

once considered the core HECT domain have important consequences for HECT domain activity. In the following section, we discuss additional areas to be explored following our work.

Activity-based inhibitors of Ub conjugation enzymes

Development of activity-based protein probes for Ub conjugation machinery

The use of active site-directed covalent probes is a powerful chemical strategy to query the functional state of enzyme families in proteomes. The architecture of a typical activity-based probe consists of a reactive group that covalently binds to the active site of a subset of enzymes in the proteome with shared catalytic features; a binding group to direct the probe to this specific subset of enzymes; and an analytic handle to facilitate detection and retrieval of probe-labeled enzyme complexes (Evans and Cravatt 2006). Our work describes an expanded class of Ub C-terminal electrophilic probes that were designed to bind active site thiol-containing enzymes that also bind ubiquitin. Using these probes, we recovered members of the Ub protease family, including novel enzymes not previously identified using a chemical biology approach (OTUD-7A, OTUD4, OTUD5, U2afl-rs1, JOS1, JOS2). We recovered, in addition, representative members of the Ub conjugation families – E1, E2, and E3 enzymes – the first time these enzymes were recovered from a complex proteome using a chemical biology approach.

Surprisingly, we recovered Ub conjugation enzymes that do not contain relevant active site residues for labeling – members of the RING domain family of E3 Ub ligases, as well as two ubiquitin E2-variant (UEV) enzymes. This latter class of E2 enzymes possesses the core UBC domain, but lack the active site-cysteine required to become charged with Ub. UEV enzymes associate with canonical E2 enzymes to enhance Ub transfer. We hypothesize that these enzymes were recovered as part of a complex of associated proteins containing a single probe-

labeled species, as our IPs were performed under non-denaturing conditions, but did not explicitly test this assumption.

An additional unexpected feature of our Ub C-terminal electrophilic probes is that they covalently label, in addition to the conserved, catalytic cysteine residue, at least three cysteines in the HECT domain E3 Ub ligase HUWE1 (Chapter 2), as well as the E2 UBE2L3 (data not shown) in vitro. These additional cysteine residues are partially surface-exposed, providing a likely explanation for the ability of HAUbVME to react with them. If it is a completely non-specific reaction of probe with surface-exposed cysteines, however, this reaction only occurs in the context of properly folded HUWE1 (Chapter 2, Figure 3a). This behavior is not observed with Ub proteases, for which the probe invariably reacts with the single, active site cysteine residue (Kattenhorn, Korbel et al. 2005). These properties of our expanded set of Ub electrophilic probes – that they behave more like affinity-based probes – limit their utility as mechanism-based inhibitors. For example, our attempts at purification of a complex between HUWE1 singly bound at its catalytic cysteine with HAUbVME proved challenging due to the formation of a complex mixture of probe-labeled species. Furthermore, a mutant HUWE1 in which all surface exposed Cys were mutated to Ala, leaving intact only the catalytic cysteine, reacted inefficiently (5-10%) with probe (data not shown).

Recently, two activity based-inhibitors were developed for the SUMO E1 activating enzyme (Lu, Olsen et al.) that trap the SUMO E1 as if bound to intermediates. SUMO was synthesized with one of two non-hydrolysable synthetic analogs of AMP (AMSN and AVSN) attached to its C-terminus. As explained in the Introduction, the E1~SUMO~AMSN complex mimics the enzyme bound to the SUMO~AMP intermediate in the first half-reaction, and the E1~SUMO~AVSN complex mimics the E1~SUMO~AMP transition state after thioesterification

has occurred, but prior to AMP release (Lu, Olsen et al.). For the SUMO and Ub E1s, inhibitors based on the second half-reaction, in which the Ub/Ubl-adenylate is transferred to the active site-cysteine in thioester linkage (Ub/Ubl containing a C-terminal vinyl sulfonamide electrophile), were developed. Interestingly, though our Ub C-terminal electrophilic probes lack the adenylate in Lu *et al*'s probes, they nevertheless label and permit recovery of Ub E1 from cell lysates.

Structural insights into Ub conjugation using activity-based inhibitors

An important question to understand the mechanism of the E1-E2-E3 Ub conjugation cascade is how Ub is transferred between juxtaposed active sites – either different active sites within the same enzyme, or active sites in two different enzymes. A common theme observed repeatedly in the Ub/Ubl enzymatic cascade is that these distances are in the tens of angstroms: for example, between the adenylate domain and catalytic cysteine in E1 activating enzyme, between the E1 and E2 catalytic cysteines, and E2 and HECT E3 catalytic cysteines. One approach to understand Ub transfer is through structures of enzyme reaction intermediates – for example, enzyme~Ub thioester intermediates. A significant challenge in the purification of reaction intermediates is, of course, that they are labile. After adenylation of the Ub/Ubl C-terminus, the E1 active site cysteine immediately attacks Ub/Ubl-AMP to form the Ub/Ubl-thioester intermediate, thus preventing the non-productive hydrolysis of the activated Ub/Ubl-AMP. The E1~Ub/Ubl thioester intermediate is also subject to hydrolysis during purification. The use of active site-directed probes can help to overcome these challenges by permitting purification of stable reaction intermediate analogs. Numerous examples of structures of Ub proteases in complex with activity-based inhibitors exist in the literature (Hu, Li et al. 2002;

Misaghi, Galardy et al. 2005; Schlieker, Weihofen et al. 2007); however, the examples for

conjugating enzymes are elegant but few (Brownell, Sintchak et al. ; Olsen, Capili et al.).

The development of a mechanism-based inhibitor would aid the study of HECT E3

ligases. Two avenues could be employed to attempt purification of a stable reaction intermediate

(HECT~Ub): One would be to mutate the HECT domain catalytic cysteine to a serine, and purify

a HECT~Ub oxyester intermediate, rather than an Ub thioester intermediate (Kamadurai,

Souphron et al. 2009). A second approach would be to utilize a Ub activity-based inhibitor.

This strategy would prevent the rapid nucleophilic attack on the Ub~thioester intermediate by a

lysine in the HECT domain, as observed during autoubiquitination, and hydrolysis of the

HECT~Ub thioester during purification. The HECT~Ub intermediate represents a part of the E3

Ub ligase reaction cycle that has so far not been examined structurally, and would provide

insight into numerous questions: Is there a structural rearrangement in the E2 binding region on

the HECT domain that promotes dissociation of the newly-unloaded E2 enzyme after Ub

transfer? How is Ub positioned on the HECT active site Cys? Does its orientation reveal

information about the assembly of polyubiquitin chains? How does the E3 active site

accommodate Ub, and does this reveal information about Ub/Ubl selectivity? A comparison of

structures of complexes between an E2~Ub and HECT E3 and a HECT~Ub intermediate, would

greatly aid in answering these questions, and require the development of a true mechanism-based

inhibitor of HECT E3 enzymes.

Improvements to Ub C-terminal electrophilic probes

Activity-based probes are becoming increasingly sophisticated and promise to provide a

greater level of insight into enzyme function in cells, tissues, and even in whole-body animal

experiments. One area of design improvement lies in the method of elution of immunoprecipitated probe-enzyme complexes. Elution has been performed using SDS-PAGE sample buffer for the HA-Ub electrophilic probes, which releases all bead-bound proteins, including non-specifically bound complexes. The use of biotin-labeled probes requires harsh elution conditions. The incorporation of a chemically cleavable diazobenzene linker joining the binding group and electrophilic moiety allows for chemoselective release of probe-bound proteins under mild elution conditions (Fonovic, Verhelst et al. 2007). A second development in ABPP technology is the development of quenched fluorescent activity-based probes targeting the papain-family cysteine proteases. These qABPs only fluoresce upon covalent binding to target proteins. Furthermore, they are stable in vivo, allowing non-invasive, whole-body imaging of cysteine protease activity (Fonovic, Verhelst et al. 2007). The development of cell-permeable ABPP opens an avenue of research for *in vivo* studies of enzyme activity (Blum, Mullins et al. 2005; Yee, Fas et al. 2005). Cell-permeable ABPs are enabled in a two-step reaction in which proteins are first labeled *in vivo* with a small molecule specific for the enzymatic class of interest, and the visualization or affinity tag is appended in a second step using, for example, the Staudinger ligation (Saxon and Bertozzi 2000) or Huisgen [3 + 2] cycloaddition ("click chemistry") (Wang, Chan et al. 2003). The development of these bioorthogonal labeling reactions permits the labeling of enzymes *in vivo*, and ABPs incorporating click chemistry was used to visualize Cathepsin cysteine protease activity in living cells during microbial infection (Hang, Loureiro et al. 2006).

Identification of Ubl conjugation enzymes using activity-based inhibitors

The discovery of ubiquitin over three decades ago has been followed by the identification

of numerous, structurally related small proteins (called ubiquitin-like modifiers, or Ubls) in

eukaryotes. These Ubls do not necessarily share high sequence homology with Ub but all

possess the β-grasp fold characteristic of ubiquitin's three-dimensional structure. Ubls that have

been demonstrated to become conjugated to target proteins contain the di-glycine motif at their C

terminus, similar to Ub (Hochstrasser 2006). Dedicated Ubl-E1, E2, and E3 enzymes have been

identified through bioinformatics and biochemical approaches for several of these modifiers,

such as SUMO, Nedd8, and ISG15. Enzymes responsible for the conjugation of other Ubls,

however, are unknown. Furthermore, the recent discovery of a Ubl in prokaryotes (Prokaryotic

ubiquitin-like protein, or Pup) and in archaeon *Haloferax volcanii* (SAMP1, SAMP2) suggests

that ubiquitin-like modification systems exist in the other two major evolutionary lineages of life

besides eukaryotes (Humbard, Miranda et al.; Pearce, Mintseris et al. 2008). Sequence profile

searches combined with structural analysis have identified E1-like adenylating enzymes and Ub-

conjugating enzyme related proteins in prokaryotes (Iyer, Burroughs et al. 2006). The discovery

of these Ubls leads to the question of how these modifiers are attached to target proteins, a

question that could be addressed through the use of active site-directed probes. Only one protein

(PafA) is known to be required for pupylation in prokaryotes; a putative SAMP E1 enzyme was

identified, but not functionally characterized (Humbard, Miranda et al.). A functional

proteomics approach conceptually similar to ours, using either a broadly reactive probe

(HAUbVME) or probes with increased electrophilicity (HAUbLactone, HAUbTF$_3$Bok, and

HAUbOEtVS) for extended incubation times could be applied to the identification of candidate

Ubl-conjugation machinery for eukaryotic Ubls with unknown conjugation enzymes as well as

newly discovered prokaryotic and archaeal Ubls. Although it is not known what type of conjugation machinery (if any) these modifiers are expected to use, it is not an unreasonable hypothesis that they use thiol-containing catalytic residues. If not, a non-directed approach in which a library of Ubl-small molecule conjugates is used to interrogate the proteome may recover candidate Ubl conjugation and ligase enzymes.

Role of non-covalent interactions during Ub transfer

Recent biochemical and structural work on HECT domain E3s have shown that certain HECT domains (Smurf2, NEDD4L, and Rsp5) interact non-covalently with Ub (Ogunjimi, Wiesner et al. ; French, Kretzmann et al. 2009; Kamadurai, Souphron et al. 2009) or substrate (Lee, Oestreich et al. 2009). All three enzymes belong to the C2-WW-HECT subclass of HECT domain E3s. The location, and function, of this ubiquitin-binding site differs among the HECT domains: for NEDD4L, Ub (bound to E2 active site) interacts with the HECT C-lobe; for Rsp5 and Smurf2, the Ub interaction maps to the N-lobe, and appears to be important for the ability to catalyze polyubiquitination of itself or substrate. These observations suggest that non-covalent interactions between certain HECT domains and Ub or substrate may underlie mechanistic differences between Ub conjugation, but this observation would benefit from more complete structures of Ub-loaded HECT domains alone or in complex with substrate, in the case of Rsp5. These interactions have not been reported for the other classes of HECT domains.

Probing conformational flexibility of HECT domains using sortase-mediated protein engineering

159

Based on several crystal structures of isolated HECT domains alone or in complex with E2 enzyme, it is clear that rotation of the HECT C-lobe about a flexible linker connecting the two HECT lobes, as well as non-covalent interactions between the HECT C-lobe and Ub bound to the active site of the E2 enzyme, are critical for E2 to E3 Ub transfer (Pandya, Partridge et al. ; Huang, Kinnucan et al. 1999; Verdecia, Joazeiro et al. 2003; Ogunjimi, Briant et al. 2005; Kamadurai, Souphron et al. 2009). Are there new methods that can be used to investigate the role of conformational flexibility to HECT domain function to complement these structural approaches? We discuss a potential method (Chapter 4) using the enzyme Sortase A from the bacteria *Staphaloccus aureus* to catalyze a circularization of the HUWE1 HECT domain (Antos, Popp et al. 2009). Using this system, sortase A can be used to ligate the N- and C-terminus of the HECT domain, thereby restraining the motion of the C-lobe in a manner dependent on the length of the connecting linker. This question could also be monitored by installing a fluorescence resonance energy transfer (FRET) pair on the two lobes of the HECT domain to monitor conformational transitions occurring in solution, or occurring upon binding of unloaded or Ub-loaded E2 enzyme. A combination of approaches could yield insight into HECT domain function: the installation of a FRET pair on the N- and C-lobes of various circular versions of the HECT domain, would allow one to correlate any increase in activity of circular HECT domains containing extended linkers with the magnitude of observed FRET.

Physiological functions of E3 Ub ligases

E3 Ub ligases function in diverse processes in the cell. The biological role of many E3 Ub ligases, however, is obscure, and an important area of research centers on defining their physiological role: identifying their substrates and the E2 enzymes with which they function,

characterizing their biological role, and the phenotypic consequences to their mutation or absence. The HUWE1 E3 Ub ligase, as discussed in the introduction, has had a number of substrates ascribed to it since its identification as an E3 Ub ligase in 2005, including p53, Mcl-1, CDC6, N-myc, c-myc, TopBP1, DNA polymerase beta, and histones (Adhikary, Marinoni et al. 2005; Chen, Kon et al. 2005; Zhong, Gao et al. 2005; Hall, Kow et al. 2007; Herold, Hock et al. 2008; Zhao, Heng et al. 2008; Parsons, Tait et al. 2009). As some of these substrates suggest that HUWE1 functions in opposing pathways in the cell, more work is required to understand the physiological function of this E3 enzyme.

Identification of physiologically relevant E2-E3 pairs

E2 enzymes function centrally in the Ub cascade, as they select the correct Ub/Ubl-loaded E1 enzyme with which to interact and the proper E3 enzyme to charge with Ub/Ubl (ref). E2 enzymes also influence several aspects of Ub chain formation: length of the polyubiquitin chain, its topology, and the processivity of chain formation (Ye and Rape 2009). In the SUMO pathway, E2 also contributes to substrate selection (Sampson, Wang et al. 2001; Johnson 2004). It is therefore important when studying E3 ligase function and regulation *in vitro* to use the physiologically relevant E2 partner enzyme(s). Studies describing the ubiquitin ligase activity of HUWE1 have employed the widely used UbcH5 and UBE2L3 enzymes (Adhikary, Marinoni et al. 2005; Chen, Kon et al. 2005; Zhong, Gao et al. 2005; Hall, Kow et al. 2007; Zhao, Heng et al. 2008), and, with one exception (Parsons, Tait et al. 2009), there are no data to indicate that these E2 enzymes are the true *in vivo* partners of HUWE1. One approach to identify the relevant E2 enzyme(s) is to screen the ~30 known human E2 enzymes, for both interaction with the E3 by yeast two hybrid or NMR (Christensen, Brzovic et al. 2007), fluorescence polarization or

isothermal titration calorimetry (Eletr, Huang et al. 2005), and activity with the E3. Surprisingly,

these two properties do not always correlate – for example, the RING E3 heterodimer

BRCA1/BARD1 was shown to interact with UBE2L3 by both yeast two hybrid and NMR, but

this E2-E3 pair was not active in catalyzing BRCA1 ubiquitination (Christensen, Brzovic et al.

2007). Candidate E2 enzymes identified as interacting with and promoting E3 Ub ligase

substrate ubiquitination activities must be followed up in cellular studies, using genetic

manipulation of expression, for example, to confirm an effect on E3 function. Other factors,

such as co-localization of E2 and E3, could be used to validate functional pairs.

Identification of E3 ligase substrates

An important aspect in understanding E3 Ub ligase function is to identify the cellular

context in which they function and their physiological substrate(s). In the case of HUWE1, its

substrates have been identified through a variety of methods: yeast two-hybrid or biochemical

interaction (Chen, Kon et al. 2005; Hall, Kow et al. 2007; Zhao, Heng et al. 2008), genetic

approaches using conditional inactivation or knockout in mice (D'Arca, Zhao et al.; Zhao, D et

al. 2009), or an RNAi screen (Zahreddine, Zhang et al.). Other approaches start with a known

ubiquitin-regulated substrate and used a biochemical fractionation approach to identify the

responsible Ub ligase (Zhong, Gao et al. 2005; Parsons, Tait et al. 2009). Low affinities between

E3 and substrate, as well as low intracellular levels of substrate, can render biochemical

interaction studies challenging. Recently developed genetic approaches are promising methods

of identifying new substrates. One strategy employs a library of yeast strains in which each

strain expresses one open reading frame (ORF) tagged at its endogenous locus with green

fluorescent protein (GFP). This library is crossed to a strain deleted for a particular E3 ligase of

interest, and the resulting population is screened for proteins that accumulate as indicated by

increased GFP fluorescence (Benanti, Cheung et al. 2007). A second genetic approach uses a

high-throughout approach to measure proteome-scale protein turnover, termed global protein

stability (GPS) analysis. A reporter construct contains a single promoter that, with an internal

ribosome entry site (IRES), allows the translation of two fluorescent proteins from a single

mRNA transcript. The first fluorescent protein is *Discosoma* sp. red fluorescent protein

(DsRed), an internal control. The second fluorescent protein is a fusion between enhanced green

fluorescent protein (eGFP) and a protein of interest. After integration of this construct into cells,

the eGFP/DsRed ratio in these cells is a measure of stability of protein of interest that is not

affected by transcriptional changes. This ratio can be measured upon knockdown or inactivation

of a particular E3 ligase to identify candidate substrates (Yen and Elledge 2008; Yen, Xu et al.

2008).

Conclusions

Chemical biology and protein engineering methods have converged to provide important

mechanistic insight into the function of ubiquitin conjugation machinery. The increasing

sophistication of activity-based probes must be applied to probes for Ub conjugation enzymes to

identify new members that escape detection using bioinformatics approaches, their interacting

partners and regulators, and mechanism of catalysis. The discovery of Ub conjugation enzymes

in prokaryotes and archaea will inform the evolutionary development of Ub conjugation. Do

these branches of life contain the antecedents of E2 and E3 enzymes? Detailed structures have

been solved for representative members of Ub pathway enzymes, although more complete

structures of enzyme-substrate complexes and pathway intermediates are needed. In the case of

HECT E3s, there are no structures that include the upstream regions encompassing substrate-recruitment domains, and visualizing these regions will help dissect the mechanism of substrate ubiquitination. How is the growing ubiquitin chain accommodated in an E3-substrate complex? Is the polyubiquitin chain built up on the E3 active site, or does the position of the bound substrate favor the sequential addition of polyubiquitin chains? Finally, a large challenge is to deduce the physiological role of the hundreds of E3 Ub ligases in the cell. The answers to these questions will provide insight into the function of the ubiquitin pathway in fundamental cellular processes.

References

Adhikary, S., F. Marinoni, et al. (2005). "The ubiquitin ligase HectH9 regulates transcriptional activation by Myc and is essential for tumor cell proliferation." Cell **123**(3): 409-21.

Antos, J. M., M. W. Popp, et al. (2009). "A straight path to circular proteins." J Biol Chem **284**(23): 16028-36.

Benanti, J. A., S. K. Cheung, et al. (2007). "A proteomic screen reveals SCFGrr1 targets that regulate the glycolytic-gluconeogenic switch." Nat Cell Biol **9**(10): 1184-91.

Blum, G., S. R. Mullins, et al. (2005). "Dynamic imaging of protease activity with fluorescently quenched activity-based probes." Nat Chem Biol **1**(4): 203-9.

Chen, D., N. Kon, et al. (2005). "ARF-BP1/Mule is a critical mediator of the ARF tumor suppressor." Cell **121**(7): 1071-83.

Christensen, D. E., P. S. Brzovic, et al. (2007). "E2-BRCA1 RING interactions dictate synthesis of mono- or specific polyubiquitin chain linkages." Nat Struct Mol Biol **14**(10): 941-8.

D'Arca, D., X. Zhao, et al. "Huwe1 ubiquitin ligase is essential to synchronize neuronal and glial differentiation in the developing cerebellum." Proc Natl Acad Sci U S A **107**(13): 5875-80.

Eletr, Z. M., D. T. Huang, et al. (2005). "E2 conjugating enzymes must disengage from their E1 enzymes before E3-dependent ubiquitin and ubiquitin-like transfer." Nat Struct Mol Biol **12**(10): 933-4.

Evans, M. J. and B. F. Cravatt (2006). "Mechanism-based profiling of enzyme families." Chem Rev **106**(8): 3279-301.

Fonovic, M., S. H. Verhelst, et al. (2007). "Proteomics evaluation of chemically cleavable activity-based probes." Mol Cell Proteomics **6**(10): 1761-70.

French, M. E., B. R. Kretzmann, et al. (2009). "Regulation of the RSP5 ubiquitin ligase by an intrinsic ubiquitin-binding site." J Biol Chem **284**(18): 12071-9.

Hall, J. R., E. Kow, et al. (2007). "Cdc6 stability is regulated by the Huwe1 ubiquitin ligase after DNA damage." Mol Biol Cell **18**(9): 3340-50.

Hang, H. C., J. Loureiro, et al. (2006). "Mechanism-based probe for the analysis of cathepsin cysteine proteases in living cells." ACS Chem Biol **1**(11): 713-23.

Herold, S., A. Hock, et al. (2008). "Miz1 and HectH9 regulate the stability of the checkpoint protein, TopBP1." EMBO J **27**(21): 2851-61.

Hochstrasser, M. (2006). "Lingering mysteries of ubiquitin-chain assembly." Cell **124**(1): 27-34.

Hu, M., P. Li, et al. (2002). "Crystal structure of a UBP-family deubiquitinating enzyme in isolation and in complex with ubiquitin aldehyde." Cell **111**(7): 1041-54.

Huang, L., E. Kinnucan, et al. (1999). "Structure of an E6AP-UbcH7 complex: insights into ubiquitination by the E2-E3 enzyme cascade." Science **286**(5443): 1321-6.

Humbard, M. A., H. V. Miranda, et al. "Ubiquitin-like small archaeal modifier proteins (SAMPs) in Haloferax volcanii." Nature **463**(7277): 54-60.

Iyer, L. M., A. M. Burroughs, et al. (2006). "The prokaryotic antecedents of the ubiquitin-signaling system and the early evolution of ubiquitin-like beta-grasp domains." Genome Biol **7**(7): R60.

Johnson, E. S. (2004). "Protein modification by SUMO." Annu Rev Biochem **73**: 355-82.

Kamadurai, H. B., J. Souphron, et al. (2009). "Insights into ubiquitin transfer cascades from a structure of a UbcH5B approximately ubiquitin-HECT(NEDD4L) complex." Mol Cell **36**(6): 1095-102.

Kattenhorn, L. M., G. A. Korbel, et al. (2005). "A deubiquitinating enzyme encoded by HSV-1 belongs to a family of cysteine proteases that is conserved across the family Herpesviridae." Mol Cell **19**(4): 547-57.

Lee, J. R., A. J. Oestreich, et al. (2009). "The HECT domain of the ubiquitin ligase Rsp5 contributes to substrate recognition." J Biol Chem **284**(46): 32126-37.

Li, W., M. H. Bengtson, et al. (2008). "Genome-wide and functional annotation of human E3 ubiquitin ligases identifies MULAN, a mitochondrial E3 that regulates the organelle's dynamics and signaling." PLoS ONE **3**(1): e1487.

Lu, X., S. K. Olsen, et al. "Designed semisynthetic protein inhibitors of Ub/Ubl E1 activating enzymes." J Am Chem Soc **132**(6): 1748-9.

Misaghi, S., P. J. Galardy, et al. (2005). "Structure of the ubiquitin hydrolase UCH-L3 complexed with a suicide substrate." J Biol Chem **280**(2): 1512-20.

Ogunjimi, A. A., D. J. Briant, et al. (2005). "Regulation of Smurf2 ubiquitin ligase activity by anchoring the E2 to the HECT domain." Mol Cell **19**(3): 297-308.

Ogunjimi, A. A., S. Wiesner, et al. "The ubiquitin binding region of the Smurf HECT domain facilitates polyubiquitylation and binding of ubiquitylated substrates." J Biol Chem **285**(9): 6308-15.

Olsen, S. K., A. D. Capili, et al. "Active site remodelling accompanies thioester bond formation in the SUMO E1." Nature **463**(7283): 906-12.

Pandya, R. K., J. R. Partridge, et al. "A structural element within the HUWE1 HECT domain modulates self-ubiquitination and substrate ubiquitination activities." J Biol Chem **285**(8): 5664-73.

Parsons, J. L., P. S. Tait, et al. (2009). "Ubiquitin ligase ARF-BP1/Mule modulates base excision repair." EMBO J **28**(20): 3207-15.

Pearce, M. J., J. Mintseris, et al. (2008). "Ubiquitin-like protein involved in the proteasome pathway of Mycobacterium tuberculosis." Science **322**(5904): 1104-7.

Sampson, D. A., M. Wang, et al. (2001). "The small ubiquitin-like modifier-1 (SUMO-1) consensus sequence mediates Ubc9 binding and is essential for SUMO-1 modification." J Biol Chem **276**(24): 21664-9.

Saxon, E. and C. R. Bertozzi (2000). "Cell surface engineering by a modified Staudinger reaction." Science **287**(5460): 2007-10.

Schlieker, C., W. A. Weihofen, et al. (2007). "Structure of a herpesvirus-encoded cysteine protease reveals a unique class of deubiquitinating enzymes." Mol Cell **25**(5): 677-87.

Verdecia, M. A., C. A. Joazeiro, et al. (2003). "Conformational flexibility underlies ubiquitin ligation mediated by the WWP1 HECT domain E3 ligase." Mol Cell **11**(1): 249-59.

Wang, Q., T. R. Chan, et al. (2003). "Bioconjugation by copper(I)-catalyzed azide-alkyne [3 + 2] cycloaddition." J Am Chem Soc **125**(11): 3192-3.

Ye, Y. and M. Rape (2009). "Building ubiquitin chains: E2 enzymes at work." Nat Rev Mol Cell Biol **10**(11): 755-64.

Yee, M. C., S. C. Fas, et al. (2005). "A cell-permeable, activity-based probe for protein and lipid kinases." J Biol Chem **280**(32): 29053-9.

Yen, H. C. and S. J. Elledge (2008). "Identification of SCF ubiquitin ligase substrates by global protein stability profiling." Science **322**(5903): 923-9.

Yen, H. C., Q. Xu, et al. (2008). "Global protein stability profiling in mammalian cells." Science **322**(5903): 918-23.

Zahreddine, H., H. Zhang, et al. "CRT-1/calreticulin and the E3 ligase EEL-1/HUWE1 control hemidesmosome maturation in C. elegans development." <u>Curr Biol</u> **20**(4): 322-7.

Zhao, X., D. A. D, et al. (2009). "The N-Myc-DLL3 cascade is suppressed by the ubiquitin ligase Huwe1 to inhibit proliferation and promote neurogenesis in the developing brain." <u>Dev Cell</u> **17**(2): 210-21.

Zhao, X., J. I. Heng, et al. (2008). "The HECT-domain ubiquitin ligase Huwe1 controls neural differentiation and proliferation by destabilizing the N-Myc oncoprotein." <u>Nat Cell Biol</u> **10**(6): 643-53.

Zhong, Q., W. Gao, et al. (2005). "Mule/ARF-BP1, a BH3-only E3 ubiquitin ligase, catalyzes the polyubiquitination of Mcl-1 and regulates apoptosis." <u>Cell</u> **121**(7): 1085-95.

APPENDIX A: SUPPLEMENTARY INFORMATION FOR "UBIQUITIN C-TERMINAL ELECTROPHILES ARE ACTIVITY-BASED PROBES FOR IDENTIFICATION AND MECHANISTIC STUDY OF UBIQUITIN CONJUGATING MACHINERY"

Supporting Information and Methods

Ubiquitin C-terminal electrophiles are activity-based probes for identification and mechanistic study of ubiquitin conjugating machinery

Kerry Routenberg Love, Renuka K. Pandya, Eric Spooner, and Hidde L. Ploegh

Synthesis and Characterization of Electrophilic Glycine Analogs

General Methods. All chemicals were reagent grade and used as supplied unless otherwise noted. HPLC-grade, low moisture organic solvents (Dri Solv), including *N,N'*-dimethylformamide (DMF), dichloromethane (CH$_2$Cl$_2$), tetrahydrofuran (THF), methanol (MeOH), and diethyl ether (Et$_2$O), were purchased from EMD Chemicals. Analytical thin-layer chromatography was performed on E. Merck silica gel 60 F$_{254}$ plates (0.25 mm). Compounds were visualized by dipping the plates in a cerium sulfate-ammonium molybdate solution or a ninhydrin solution followed by heating. Liquid flash column chromatography was performed using forced flow of the indicated solvent on EMD Chemicals silica (200-400 mesh). ^{1}H NMR spectra were obtained using a 400 MHz spectrometer and are reported in parts per million (δ) relative to CDCl$_3$ (7.27 ppm) or MeOD (4.87 ppm, 3.31 ppm).
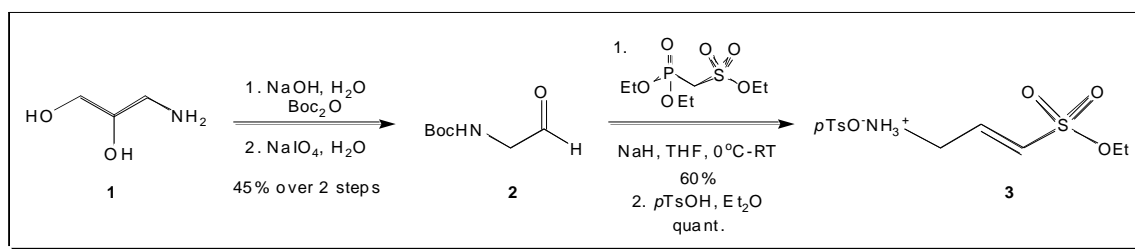

4-amino-but-1-enyl ethoxysulfonate (3). *N*-tert-butyloxycarbonyl (Boc) protected glycinal was prepared as previously reported[1] and was subjected to sodium metaperiodate-mediated oxidative cleavage[2] to obtain *N*-Boc-glycinal (**2**), which was used without further purification. A solution of sodium hydride (258 mg, 10.2 mmol) in THF (60 mL) was cooled to 0°C before the dropwise addition of triethyl α-phosphonylmethanesulfonate (2.66 g, 10.2 mmol)[3], followed by a 5 mL rinse of the phosphonate-source vessel[4]. The reaction mixture was stirred for 20 min at 0°C before adding the above prepared *N*-Boc-glycinal (**2**) as a neat solid. The reaction mixture was allowed to warm to room temperature and was stirred for 6 h before quenching with water (50 mL) and extracting with ethyl acetate (3 × 50 mL) The combined organic extracts were dried over Na$_2$SO$_4$, filtered and concentrated. The resulting crude residue was purified using flash column chromatography by elution with 25% ethyl acetate/hexanes, yielding 0.8 g (60%) pure *N*-Boc-4-amino but-1-enyl ethoxysulfonate. ^{1}H NMR: 6.78 (dt, 1H), 6.34 (d, 1H), 4.82 (br s, 1H), 4.17 (q, 2H), 3.99 (br s, 2H), 1.45 (s, 9H), 1.39 (t, 3H). Removal of the Boc group was accomplished using three equivalents dry *p*-toluenesulfonic acid as

described[5] to yield **3** as the sulfonic acid salt of the deprotected amine. ESI-MS: Calculated; $[M + H]^+ = 166.05$. Observed; $[M + H]^+ = 166.05$.
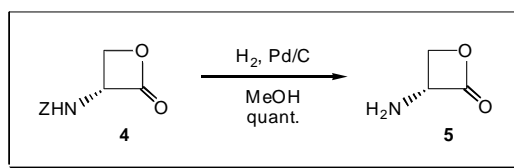
Serine-β-lactone (5). *N*-(benzyloxycarbonyl[Z])-D-serine-β-lactone (**4**) was prepared as previously reported[6]. Removal of the Z group was accomplished in quantitative yield by hydrogenation over Pd/C in methanol. ^{1}H NMR: 4.23 (m, 1H), 4.12 (m, 2H), 3.54 (m, 1H), 1.41 (appd, 1H). ESI-MS: Calculated; $[2M + H]^+ = 177.09$. Observed; $[2M + H]^+ = 177.09$.
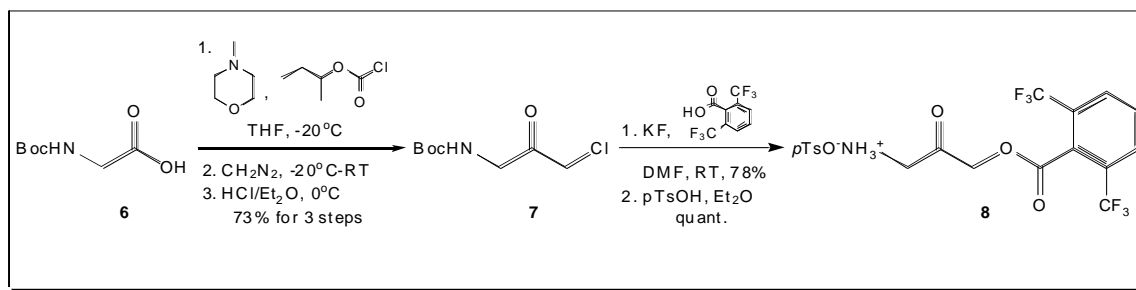
2,6-trifluoromethylbenzyloxy glycine methyl ketone (8). Boc-protected glycine (**6**) was converted to the amino acid diazomethyl ketone as previously reported[7] via addition of a cold solution of diazomethane to a mixed anhydride formed by treatment of the protected amino acid with isobutyl chloroformate in the presence of *N*-methyl morpholine. The diazomethyl ketone was easily converted to the chloromethyl ketone (**7**) by addition of a solution of HCl in Et$_2$O[8]. *N*-Boc-glycine chloromethyl ketone **7** (430 mg, 2.07 mmol) was treated with potassium fluoride (361 mg, 6.21 mmol) in DMF (20 mL), followed by 2,6-trifluorobenzoic acid (587 mg, 2.28 mmol) overnight at room temperature[9]. After 12 h the reaction was diluted with Et$_2$O and ethyl acetate (50 mL each) and washed with water, aqueous NaHCO$_3$ (sat.) and brine. The organic layer was dried over Na$_2$SO$_4$, filtered and concentrated to yield 0.69 g (78%) of compound **8**, which was used without further purification. ^{1}H NMR: 7.95 (appd, 2H), 7.76 (appt, 1H), 5.22 (br s, 1H), 4.90 (s, 1H), 4.13 (m, 2H), 1.40 (s, 9H). Removal of the Boc group was accomplished using three equivalents dry *p*-toluenesulfonic acid as described[5] to yield **8** as the sulfonic acid salt of the deprotected amine. ESI-MS: Calculated; $[M + H]^+ = 330.06$. Observed; $[M + H]^+ = 330.06$.

Synthesis and Characterization of HAUb-electrophilic Probes
HAUb-electrophilic probes were made using the electrophilic glycine analogs synthesized above as described in the Experimental Procedures. The FPLC purified HAUb-electrophilic probes were characterized by ESI-LC/MS and multi-charged species were observed for each probe. Probe yields were estimated using traces obtained during FPLC purification. HAUbOEtVS (quant. yield) ESI-MS: Calculated; $[M + 11H]^{11+} = 937$. Observed; $[M + 11H]^{11+} = 936.7266$. HAUbLac (50% yield) ESI-MS: Calculated; $[M + 11H]^{11+} = 931$. Observed; $[M + 11H]^{11+} =$

931.4602. HAUbTF$_3$BOK (80% yield) ESI-MS: Calculated; [M + 11H]$^{11+}$ = 952. Observed; [M + 11H]$^{11+}$ = 952.0001.

EL-4 Cell Lysate Labeling and Blocking of Labeling with NEM (N-ethylmaleimide)
30 μg of protein extract (see Methods section for cell culture and lysate harvesting conditions) treated with NEM (10 mM) for 30 min at room temperature. Following this treatment, 0.2 μg of HAUb-electrophilic probe (2.0 μM in each sample) was added and the reactions were incubated for 5 h at room temperature. Control reactions were run for each probe without prior addition of NEM to observe the extent of labeling in 5 h. Reactions were quenched by addition of reducing sample buffer, boiled 10 min and separated by SDS-PAGE (10%). Results were analyzed by immunoblotting with an anti-HA antibody (3F10, Roche).

EL-4 Cell Lysate labeling and Detection of RING Ligase UBAC1 Modification by Gel Shift.
30 μg EL-4 lysate was incubated with indicated quantities of probe (concentrations are 2.3μM, 4.6 μM, 9.2 μM, and 18.4 μM) in buffer containing 50mM Tris pH 8.0, 150mM NaCl for 4 hr at room temperature (24°C). Reactions were quenched by addition of reducing sample buffer, resolved by SDS-PAGE analyzed by immunoblot using either a UBAC1 antibody (Novus Biologicals) or a UCH37 antibody (polyclonal rabbit) for comparison.

Plasmid Construction
The C-terminal residues of ARF-BP1 (amino acids 4012-4374) were subcloned into vector pet28a for expression and purification as an N-terminal His$_6$ fusion protein using forward primer 5'-ccgcatatgctccggaaagaagacatgg and reverse primer 5'-ccggaattcttaggccagcccaaagcc. Single, double, and triple cysteine-to-alanine ARF-BP1 HECT domain mutants at residues C4099, C4341, C4367, were generated using site-directed mutagenesis (Stratagene). A truncated version of ARF-BP1 (ARF-BP1 Δ4) (residues 4012-4370) was cloned into pet28a for Ub-thioester assays using the forward primer listed above and the reverse primer 5'-cgcggatccttagccttcagagcactcctg.

The C-terminal residues of Trip12 (amino acids 1629-2040, KIAA0045, Kazusa DNA Research Institute) were subcloned with an N-terminal His$_6$ tag into the vector pGEX-6P-1 (GE Healthcare) for expression and purification as an N-terminal GST fusion protein using forward primer 5'-cgcggatccggacatcatcatcatcatcacagcagcggcagagttgcacctagattgg and reverse primer 5'-cgcgtcgactcaggaaagatggaacgactg.

The N-terminal residues of Mcl-1 (amino acids 1-327) were cloned with an N-terminal PKA (protein kinase A) recognition sequence into the vector pet16b for expression and purification as an N-terminal His$_{10}$ fusion protein using forward primer 5'-ccgcatatggactacaaggacgacgacgacaaggcaggacgtcgtgcatctgttggatcctttggcctcaaaagaaacgcgg and reverse primer 5'-cgcggatccctagccaccttctaggtcctctac.

Ubiquitin was cloned with an N-terminal PKA (protein kinase A) recognition sequence into the vector pet28a for expression and purification as an N-terminal His$_6$ fusion protein using forward primer 5'-ccgcatatgcgtcgtgcatctgttggatccatgcagatcttcgtcaagacg and reverse primer 5'-cgcggatcctcatcccccacgcagtc.

Protein Expression and Purification of ARF-BP1 HECT domain and PKA-Mcl-1

ARF-BP1 HECT domain and FLAG-Mcl-1 containing plasmids were transformed into Rosetta competent cells (DE3(PLysS), Novagen) and cells were plated on LB-agar supplemented with 50 μg/mL kanamycin (ARF-BP1) or 100 μg/mL ampicillin (Mcl-1) and 20 μg/mL chloramphenicol. A single colony for each protein was used to inoculate a 1.5 L liquid culture (LB, Miller) and cultures were grown to late log ($OD_{600} > 0.8$) at 37°C. Cultures were induced with 0.5 mM IPTG at 22°C overnight. Cells were pelleted and washed once with PBS before resuspending in 25 mL lysis buffer (50 mM Tris [pH 8.0], 300 mM NaCl, 10 mM imidazole). DNAse was added to a final concentration of 10 μg/mL and the cells were lysed under pressure (1500 psi) using a French press. Cell debris was pelleted and the supernatant was purified using Ni-NTA beads (Qiagen) for His-tag-based purification. Eluted proteins were further purified by gel filtration (Superdex 75 PC 3.2/30, GE Healthcare) using a buffer containing 50 mM Tris (pH 7.5), 150 mM NaCl, 2 mM EDTA, 5 mM $MgCl_2$, 2 mM DTT, and 5% glycerol.

Protein Expression and Purification of Trip12 HECT domain

Trip 12 HECT domain-containing plasmid was transformed into Rosetta competent cells (DE3(PLysS), Novagen) and cells were plated on LB-agar supplemented with 100 μg/mL ampicillin and 20 μg/mL chloramphenicol. A single colony for each protein was used to inoculate a 1.5 L liquid culture (LB, Miller) and cultures were grown to late log ($OD_{600} > 0.8$) at 37°C. Cultures were induced with 0.5 mM IPTG at 22°C overnight. Cells were pelleted and washed once with PBS before resuspending in 25 mL PBS supplemented with DNAse (final concentration of 10 μg/mL) and 1 mM $MgCl_2$. Cells were lysed under pressure (1500 psi) using a French press. Cell debris was pelleted and the supernatant was purified using Glutathione Separose 4B beads (GE Healthcare) for GST-tag-based purification. Eluted proteins were used without further purification.

Protein Expression and Purification of PKA-Ub

PKA-Ub-containing plasmid was transformed into Rosetta competent cells (DE3(PLysS), Novagen) and cells were plated on LB-agar supplemented with 50ug/mL kanamycin and 20ug/mL chloramphenicol. A single colony was used to inoculate 6L liquid culture (LB, Miller) and cultures were growth to late log ($OD_{600} > 0.8$) at 37°C. Cultures were induced with 0.5 mM IPTG at 30°C for 3.5hr. Cells were pelleted and washed once with PBS before resuspending in lysis buffer (50mM Tris pH 8.0, 500mM NaCl, 20mM imidazole, 10ug/mL DNase). Cells were lysed under pressure (1500 psi) using a French press. Cell debris was pelleted and the supernatant purified using Ni-Sepharose (High Performance, GE Healthcare) for His-tag-based purification. Eluted proteins were further purified by gel filtration (Superdex 75 PC 3.2/30, GE Healthcare) using a buffer containing 50mM Tris pH 7.5, 150mM NaCl, and 5% glycerol.

Synthesis of [^{32}P]-labeled proteins

Recombinant proteins (1 mg Ub or 120 ug Mcl-1) bound to Ni-sepharose (High Performance, GE Healthcare) were washed once in HMK buffer (20mM Tris pH 7.5, 100mM NaCl, 12mM $MgCl_2$) and incubated with the catalytic subunit of cAMP-dependent Protein Kinase (PKA, New England Biolabs; 50,000 U for Ub or 25,000 U for Mcl-1), and a 10-fold molar excess of ATP in

a ratio of 1:100 (Ub) or 1:10 (Mcl-1) γ-[^{32}P]-ATP (6000 Ci/mmol, 10mCi/mL, PerkinElmer) to unlabeled ATP, in HMK buffer containing 1 mM DTT in a final volume of either 200 ul (Ub) or 100 ul (Mcl-1) for 3 hours at 25°C. The phosphorylation reaction was terminated by incubation of proteins with HMK stop buffer (10mM sodium phosphate pH 8.0, 10mM sodium pyrophosphate, 10mM EDTA, 1mg/ml bovine serum albumin) for 5 min at 25°C. Proteins were washed 5 times with NET buffer and eluted in 50mM Tris pH 8.0, 250mM NaCl, 250mM imidazole.

Autoubiquitination Assay with GST-Trip12 HECT Domain
Recombinantly expressed and purified GST-Trip12 HECT domain (10 µg) (see above for plasmid construction, protein expression and purification conditions) was incubated with 100 ng human E1 (Ube1, Boston Biochem), 1 µg UbcH7, and 10 µg Ub with an ATP regenerating system (50 mM Tris [pH 7.6], 5 mM MgCl$_2$, 5 mM ATP, 10 mM creatine phosphate, 3.5 U/mL creatine kinase) for 10 min at room temperature. After terminating the reactions with reducing SDS-PAGE sample buffer and boiling 10 min, reaction mixtures were separated by SDS-PAGE (8%) and analyzed by immunoblotting using an anti-Ub antibody (Sigma). Control reactions were run without either E1 or E2.

References
1. Liu, S., and Hanzlik, R.P. (1992). Structure-Activity-Relationships For Inhibition Of Papain By Peptide Michael Acceptors. J. Med. Chem. *35*, 1067-1075.
2. Dilek, I., Madrid, M., Singh, R., Urrea, C.P., and Armitage, B.A. (2005). Effect of PNA Backbone Modifications on Cyanine Dye Binding to PNA-DNA Duplexes Investigated by Optical Spectroscopy and Molecular Dynamics Simulations. J. Am. Chem. Soc. *127*, 3339-3345.
3. Carretero, J.C., Demillequand, M., and Ghosez, L. (1987). Synthesis Of Alpha,Beta-Unsaturated Sulfonates Via The Wittig-Horner Reaction. Tet. *43*, 5125-5134.
4. Reddick, J.J., Cheng, J.M., and Roush, W.R. (2003). Relative rates of Michael reactions of 2 '-(phenethyl)thiol with vinyl sulfones, vinyl sulfonate esters, and vinyl sulfonamides relevant to vinyl sulfonyl cysteine protease inhibitors. Org. Lett. *5*, 1967-1970.
5. Borodovsky, A., Ovaa, H., Kolli, N., Gan-Erdene, T., Wilkinson, K.D., Ploegh, H.L., and Kessler, B.M. (2002). Chemistry-based functional proteomics reveals novel members of the deubiquitinating enzyme. Chem. Biol. *9*, 1149-1159.
6. Lall, M.S., Ramtohul, Y.K., James, M.N.G., and Vederas, J.C. (2002). Serine and threonine beta-lactones: A new class of hepatitis a virus 3C cysteine proteinase inhibitors. J. Org. Chem. *67*, 1536-1547.
7. Green, G.D.J., and Shaw, E. (1981). Peptidyl Diazomethyl Ketones Are Specific Inactivators Of Thiol Proteinases. J. Biol. Chem. *256*, 1923-1928.
8. Sajadi, Z., Kashani, M., Loeffler, L.J., and Hall, I.H. (1980). Anti-Tumor Agents - Diazomethyl Ketone And Chloromethyl Ketone Analogs Prepared From N-Tosyl Amino-Acids. J. Med. Chem. *23*, 275-278.
9. Krantz, A., Copp, L.J., Coles, P.J., Smith, R.A., and Heard, S.B. (1991). Peptidyl (Acyloxy)Methyl Ketones And The Quiescent Affinity Label Concept - The Departing Group As A Variable Structural Element In The Design Of Inactivators Of Cysteine Proteinases. Biochemistry *30*, 4678-4687.

080607_KRL_HAUbTF3BOK — TOF MS ES+ TIC 9.63e5

080607_KRL_HAUbLactone — TOF MS ES+ TIC 5.15e5

080607_KRL_HAUbOEtVS — TOF MS ES+ TIC 9.08e5

080607_KRL_HAUbVME — TOF MS ES+ TIC 8.74e5

* This peak corresponds to the loss of the electrophilic warhead from the peptide during LC/MS analysis (Calculated: $[M + 11H]^{11+} = 921$; Observed: $[M + 11H]^{11+} = 921.6114$).

Supplementary Figure 1. Labeling of EL-4 cell lysate with Ub electrophilic probes is efficiently blocked by preincubation with NEM (10 mM).

Supplementary Figure 2. Autoubiquitination activity of recombant HECT domain of GST-Trip12. Ubiquitinated Trip 12 HECT domain was resolved by SDS-PAGE (8%) and visualized by immunoblotting with an anti-Ub antibody.

Supplementary Figure 3. (a) RING ligase UBAC1, present in EL-4 cell lysate, is not directly modified by HAUbVME, suggesting that RING E3s are retrieved in immunoprecipitations of probe-labeled lysate as part of multi-subunit complexes where 1 or more members binds probe directly. (b) UCH37 (UCH-L5), by comparison, is efficiently and quantitatively labeled when lysate containing this DUB is treated with HAUbVME as seen by a ~10 kD increase in its apparent molecular weight.

Supplementary Table 1.
Supplementary Table 1.

A. Proteins identified from EL-4 cell lysates.

Protein identified	Protein activity	Accession number (NCBI)	Predicted MW (kDa)	HAUb probe used for retrieval (number of peptide matches / sequence coverage)
USP4	DUB	2851531	108	VME (52/59.8%), OEtVS (2/5%), Lac (4/7%), TF$_3$BOK (26/31.9%)
USP5 (IsoT)	DUB	3024764	96	VME, TF$_3$BOK (6/7.9%)
USP7 (HAUSP)	DUB	51491860	128	TF$_3$BOK (2/1.5%)
USP8	DUB	122890054	122.5	VME (26/26.4%)
USP9X	DUB	123296796	290	VME (21/9.9%), TF$_3$BOK (3/1.5%)
USP10	DUB	6678493	87	VME (6/9.1%)
USP11	DUB	123229791	105	VME (16/25.6%), TF$_3$BOK (7/12.6%)
USP 14	DUB	20178168	56	VME (2/7.1%)
USP14 (isoform2)	DUB	84452155	52	VME (24/57.4%), TF$_3$BOK (8/19.9%)
USP15	DUB	28558361	112	VME (42/34%), OEtVS (5/4.8%), Lac (6/8.9%), TF$_3$BOK (15/20.4%)
USP19	DUB	123791392	150	VME (12/13%), TF$_3$BOK (3/5.1%)
USP24	DUB	123858181	294	VME (2/1.5%)
USP25	DUB	31980712	121	VME (18/21.2%)
USP28	DUB	78103330	119	VME (3/2.9%)
USP29	DUB	114145573	98	VME (2/3.3%)
USP38	DUB	34328301	116	VME (8/9.8%)
USP47	DUB	48928014	157	VME (14/15.5%)
CYLD1	DUB	27734060	106.5	VME (7/12.4%)
UCH-L1	DUB	6755929	25	VME (32/62.3%), OEtVS (13/59.6%), Lac

				(20/58.3%), TF$_3$BOK (24/60.1%)
UCH-L3	DUB	17380334	26	VME (9/27%), OEtVS (5/23.5%), Lac (9/28.7%), TF$_3$BOK (18/37.4%)
UCH-L4	DUB	19924308	26	VME (24/47.6%), OEtVS (9/32.6%), Lac (13/43.3%), TF$_3$BOK (27/47.6%)
UCH-L5 (UCH37)	DUB	9625047	37.5	VME (9/34.3%), OEtVS (2/5.8%)
OTUB1	DUB	44888264	31	VME (5/23.6), Lac (7/24%), TF$_3$BOK (4/19.2%)
OTUB2	DUB	44888287	27	VME (2/9.8%)
OTUD-6B	DUB	22779903	34	VME (6/21.1%)
OTUD-7A (Cezanne 2)	DUB	51701338	100	VME (2/1.9%)
OTUD-7B (Cezanne)	DUB	71043959	92	VME (9/19.2%), TF$_3$BOK (2/3.7%)
VCIP135	DUB	42559967	134	VME (2/3.3%)
U2afl-rs1	DUB	151357946	409.5	Lac (2/0.8%)
UBE1	E1 Ub-activating enzyme	267190	118	TF$_3$BOK (10/12.3%)
UBE1-L2	E1 Ub-activating enzyme	27370032	118	TF$_3$BOK (7/12.7%)
UBE1 (Chromosome X)	E1 Ub-activating enzyme	148878383	118	TF$_3$BOK (52/53.5%)
UBA2	E1 Ubl-activating enzyme	32493410	70.5	TF$_3$BOK (4/8.5%)
Aos1	E1 Ubl-activating enzyme	18490720	38.5	TF$_3$BOK (5/12.6%)
UBC9	E2 Ubl-conjugating enzyme	54039792	18	TF$_3$BOK (2/16.5%)
UBC12	E2 Ubl-conjugating enzyme	46577656	21	TF$_3$BOK (5/31.1%)
UBC13	E2 Ub-conjugating enzyme	18017605	17	TF$_3$BOK (3/26.3%)

UB2V1	E2 Ub-conjugating enzyme	51702141	16	TF$_3$BOK (2/21.1%)
UB2V2	E2 Ub-conjugating enzyme	51702142	16	TF$_3$BOK (2/17.2%)
UBE2-L3 (UbcM4)	E2 Ub-conjugating enzyme	54039806	18	TF$_3$BOK (2/7.1%)
UBE2S	E2 Ub-conjugating enzyme	53734650	24	TF$_3$BOK (4/21.5%)
UBE2O	E2 Ub-conjugating enzyme	50234896	141	TF$_3$BOK (3/2.7%)
E6-AP (Ube3A)	HECT E3 Ub ligase	76880500	97.5	VME (3/4.7%)
Nedd4 (Rsp5)	HECT E3 Ub ligase	32172436	103	OEtVS (2/3%), TF$_3$BOK (2/2%)
ARF-BP1 (Mule)	HECT E3 Ub ligase	73915354	482	VME (6/2.7%), Lac (4/0.9%), TF$_3$BOK (4/1.4%)
Trip12	Putative HECT E3 Ub ligase	91932791	224	VME (2/0.9%), TF$_3$BOK (2/1.2%)
UBAC1 (KPC2)	RING E3 Ub ligase	19527050	45	VME (2/4.9%)
UBR2	RING E3 Ub ligase	73622074	199	TF$_3$BOK (3/2.5%)
CUL-4A	RING E3 Ub ligase	108936014	88	OEtVS (3/5.1%)
TRAF2	RING E3 Ub ligase	83921633	56	OEtVS (2/4.2%)

B. Proteins identified from HMEC cell lysates.

| Protein Identified	Protein Activity	Accession Number (NCBI)	Predicted MW (kDa)	HAUb probe used for retrieval (number of peptide matches / sequence coverage)
USP4	DUB	116242839	20.6	VME (14, 20.6%)
USP5 (isoform 2)	DUB	148727247	93.2	TF$_3$BOK (2, 2.9%)

Appendix A: Supplementary Information for "Ubiquitin C-terminal electrophiles are activity-based probes for identification and mechanistic study of ubiquitin conjugating machinery"

USP7	DUB	150378533	128.2	VME (2, 2.7%), Lac (2, 1.9%)
USP8	DUB	731046	127.4	VME (8, 9.5%)
USP14 (isoform 2)	DUB	82880645	52.3	VME (14, 31.8%)
USP15	DUB	28381406	112.3	VME (27, 30.5%)
USP22	DUB	78103328	59.9	VME (4, 11.4%)
USP24	DUB	149192845	27.7	VME (3, 2%)
USP25	DUB	20141973	125.7	VME (17, 20.5%)
USP28	DUB	20140700	122.4	VME (8, 9.5%)
CYLD1	DUB	14165258	107.2	VME (2, 2.4%)
UCH-L1	DUB	136681	24.8	VME (7, 28.7%)
UCH-L3	DUB	5174741	26.2	VME (27, 64.8%), OEtVS (8, 31.7%), TF$_3$BOK (13, 54.8%), Lac (14, 56.1%)
UCH-L5 (UCH37)	DUB	108936023	37.6	VME (5, 14%), OEtVS (3, 9.7%,), TF$_3$BOK (12, 43.2%), Lac (3, 14%,)
OTUB1	DUB	44888286	31.3	VME (9, 35.4%), OEtVS (9, 31.7%), TF$_3$BOK (7, 31.7%), Lac (8, 26.9%)
OTUB2	DUB	44888285	27.2	VME (3, 15.8%)
OTUD4 (isoform 3)	DUB	156630992	117	VME (3, 7.2%)
OTUD5	DUB	74731791	60.6	VME (2, 7.7%)
OTUD-6B	DUB	74729149	33.8	VME (4, 20.1%)
OTUD-7B (Cezanne)	DUB	118026942	92.5	VME (2, 5.5%)
VCIP135	DUB	42560002	134.2	VME (13, 13.6%)
JOS1	DUB	3123051	23.2	VME (2, 13.4%)
JOS2	DUB	29840785	20.7	VME (3, 13.8%)
SENP8	NEDD8 protease	26006881	24.1	VME (2, 5.2%)
UBE1	E1 Ub-activating enzyme	24418865	117.8	VME (6, 10.2%), OEtVS (5, 10.2%), TF$_3$BOK (7, 12.1%)
UBC1	E2 Ub-conjugating enzyme	46577658	22.4	VME (3, 22.5%), TF$_3$BOK (3, 24%), Lac (5, 47%)
UB2E2	E2 Ub-conjugating	47606201	22.2	VME (2, 9.5%),

|				
	enzyme			TF$_3$BOK (2, 9.5%)
UBE2N	E2 Ub-conjugating enzyme	46577660	17.1	VME (2, 20.4%), TF$_3$BOK (6, 42.8%), Lac (4, 29.6%)
UBE2S	E2 Ub-conjugating enzyme	23829978	23.8	TF$_3$BOK (2, 14.9%)
UBE2C (isoform 4)	E2 Ub-conjugating enzyme	32967289	46.4	TF$_3$BOK (6, 46.4%)
UBE2T	E2 Ub-conjugating enzyme	73622065	22.5	TF$_3$BOK (2, 11.7%)
E6-AP (isoform 3, Ube3A)	HECT E3 Ub ligase	19718764	100	VME (8, 11.8%)
ARF-BP1	HECT E3 Ub ligase	73915353	481.6	VME (43, 13.9%), TF$_3$BOK (22, 6.6%)
Trip12	Putative HECT E3 Ub ligase	2499839	220.3	TF$_3$BOK (3, 1.8%)
RN138	RING E3 Ub ligase	74733576	28.2	Lac (2, 13.9%)
CUL-4A	RING E3 Ub ligase	108936013	87.6	Lac (2, 3%)
CUL-4B (isoform 2)	RING E3 Ub ligase	121114302	102.2	VME (2, 3.4%), Lac (2, 2.7%)
SH3R2	Putative RING E3 Ub ligase	122070123	79.2	TF$_3$BOK (6, 10.3%), Lac (4, 8.5%)

Supplementary Figure 1
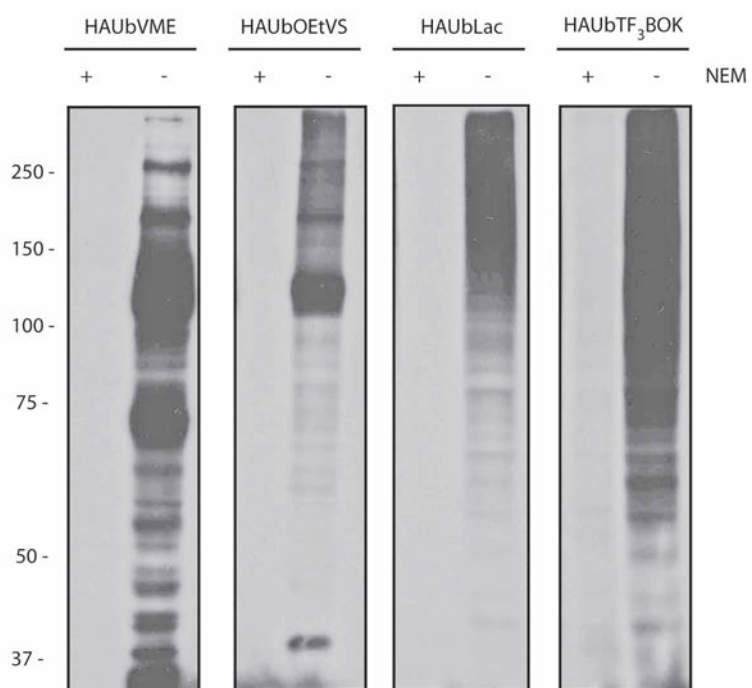
Supplementary Figure 2
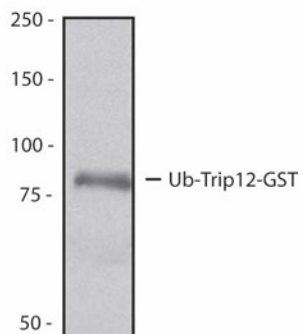
Supplementary Figure 3
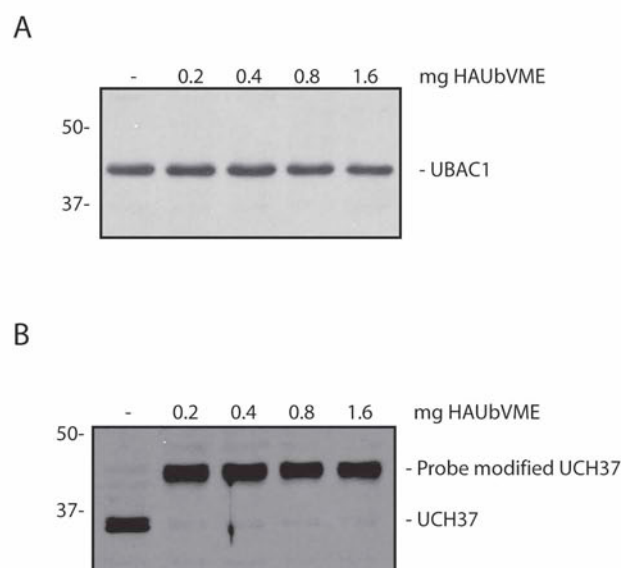
APPENDIX B: SUPPLEMENTARY INFORMATION FOR "A STRUCTURAL ELEMENT WITHIN THE HUWE1 HECT DOMAIN MODULATES SELF-UBIQUITINATION AND SUBSTRATE UBIQUITINATION ACTIVITIES"

Supplementary Information for "A structural element within the HUWE1 HECT domain modulates self-ubiquitination and substrate ubiquitination activities"

Supplementary Figure 1. Both HUWE1 Δα1 and HUWE1 +α1 HECT domains maintain the ⊥ conformation.

(a) Overlay of the C_α backbone of the HUWE1 + α1 HECT domain (orange) and HUWE1 Δ α1 HECT domain (blue).

(b) The C_α backbone of the HUWE1 + α1 HECT domain fit into electron density of the HUWE1 Δ α1 structure demonstrates the similarity of these structures.

Supplementary Figure 2. Mutation of the catalytic cysteine (C4341) to alanine abolishes activity of the HECT domain.
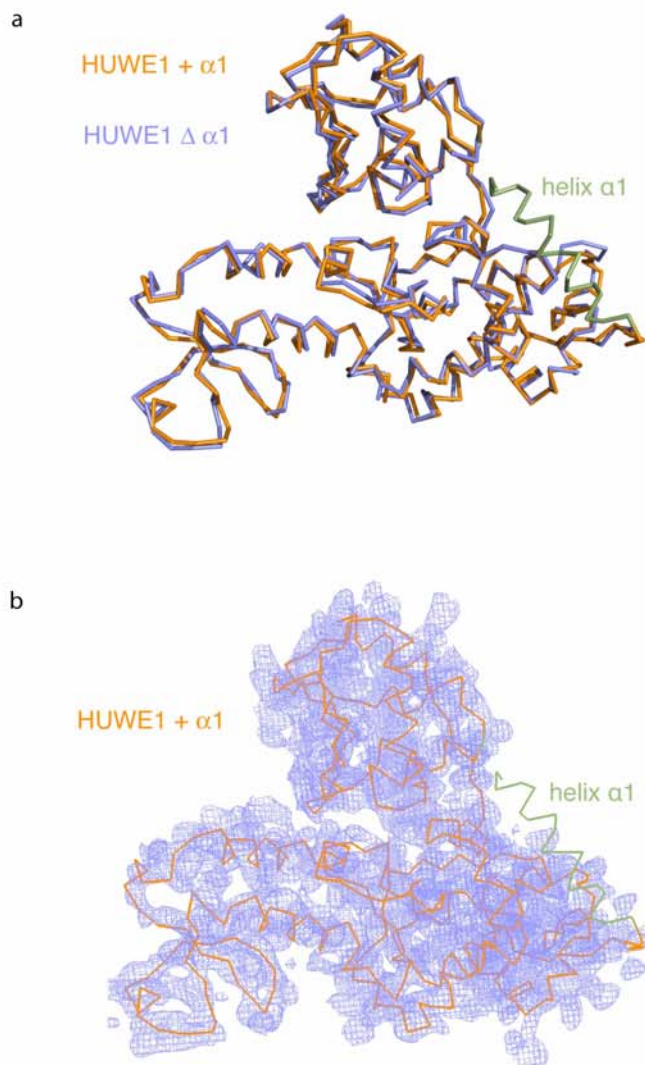
(a, b) The autoubiquitination activity of C4341A HECT domain was tested using 60 μM [^{32}P]-Ub as substrate and (a) 11.6 μM C4341A Δ α1 or (b) 12.1 μM C4341A + α1 HECT domains incubated with UBE1, UBE2L3, and an ATP regenerating system. Aliquots of the reaction mix were removed after the indicated amount of time, quenched in reducing SDS sample buffer, and separated on SDS-PAGE. HECT domain is omitted in the lane marked "N". Asterisk denotes a likely ubiquitin polymer.

(c, d) Substrate ubiquitination activity was measured using 5 μM [^{32}P]-Mcl-1 as substrate and (a) 11.6 μM C4341A Δ α1 or (b) 12.1 μM C4341A + α1 HECT domains incubated with UBE1, UBE2L3, Ub, and an ATP regenerating system. HECT domain is omitted in the lane marked "N".

(e, f) Ligation activity of the HECT domains in the (e) autoubiquitination or (f) Mcl-1 ubiquitination assay. Activity is given as the ratio between initial velocity (pmol total [^{32}P]-Ub
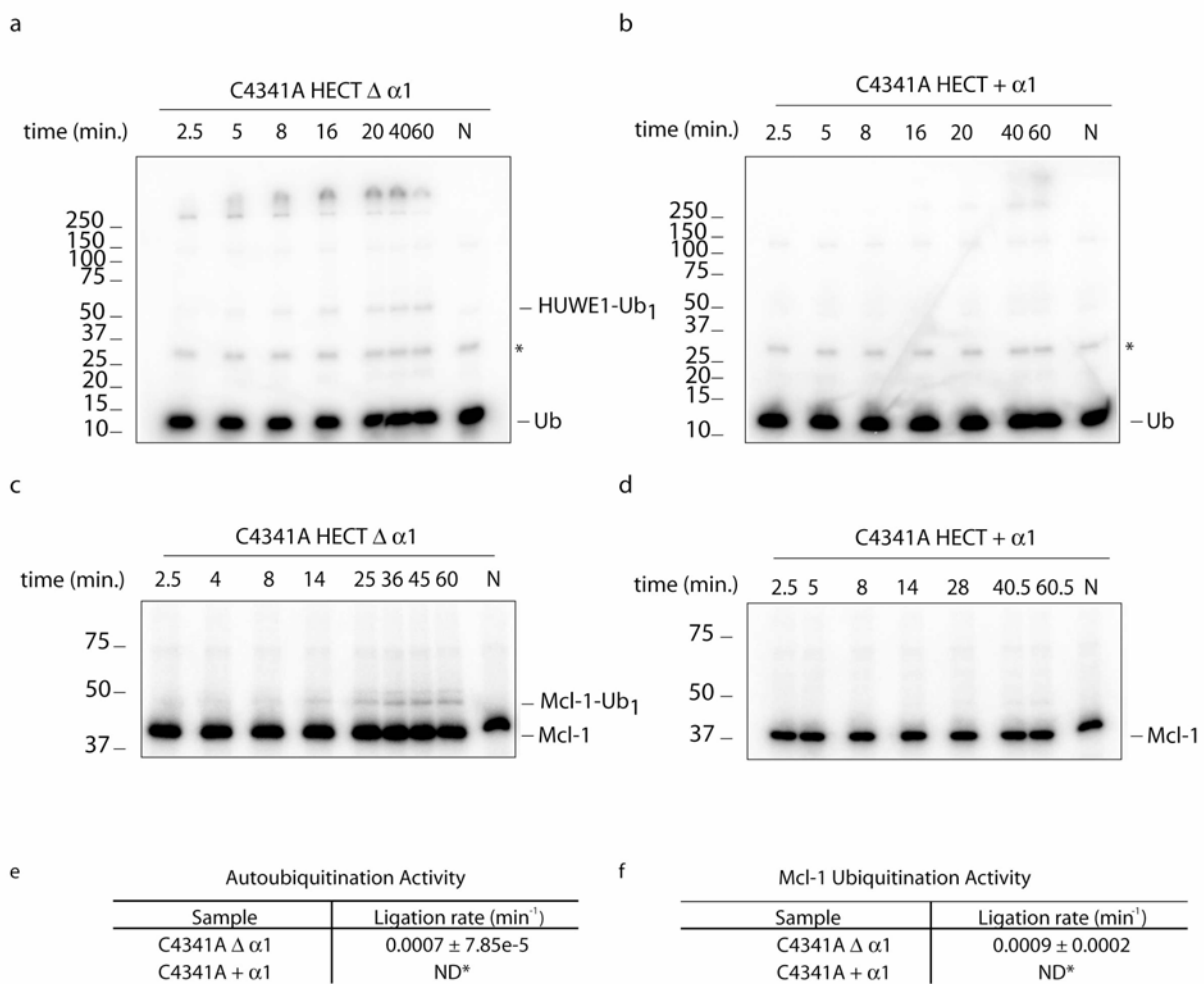
product/min) and total enzyme concentration E (pmol). Errors are the standard deviations

calculated from three independent experiments, shown in parenthesis.

Supplementary Figure 1

a

b

Supplementary Figure 2

e Autoubiquitination Activity

Sample	Ligation rate (min^{-1})
C4341A Δ α1	0.0007 ± 7.85e-5
C4341A + α1	ND*

f Mcl-1 Ubiquitination Activity

Sample	Ligation rate (min^{-1})
C4341A Δ α1	0.0009 ± 0.0002
C4341A + α1	ND*

*Product formation above background not detected.